THESIS FOR THE DEGREE OF DOCTOR OF PHILOSOPHY (Ph.D.)

Molecular interactions of ErbB receptor tyrosine kinases and integrin β1: implications for tumor therapy

by Miklós Petrás

Supervisor: Prof. János Szöllősi, D.Sc.
Álmos Klekner, Ph.D.

UNIVERSITY OF DEBRECEN
DOCTORAL SCHOOL OF MOLECULAR MEDICINE

DEBRECEN, 2013

Molecular interactions of ErbB receptor tyrosine kinases and integrin β1: implications for tumor therapy

Miklós Petrás

Ph.D. Thesis

UNIVERSITY OF DEBRECEN
MEDICAL AND HEALTH SCIENCE CENTER

DEPARTMENT OF BIOPHYSICS AND CELL BIOLOGY
DEPARTMENT OF NEUROSURGERY

DEBRECEN, 2013.

Ph. D. thesis data

Title: Molecular interactions of ErbB receptor tyrosine kinases and integrin β1: implications for tumor therapy

Author: Miklós Petrás, M.D.

Supervisors: Prof. János Szöllősi, D.Sc.
Álmos Klekner, M.D., Ph.D.

Doctoral School: "Molecular Medicine" at the University of Debrecen
Head of Doctoral School: Prof. László Csernoch, D.Sc.

Doctoral examination committee:
Chairman: Prof. László Csernoch, D.Sc.
Members: Prof. Ferenc Erdődi, D.Sc.
Beáta Bugyi, Ph.D.

Place and time of doctoral examination: Debrecen, 3 May 2013

Doctoral thesis committee:
Chairman: Prof. László Csernoch, D.Sc.
Reviewers: Prof. István Jóna, D.Sc.
József Tóvári, Ph.D.
Members: Prof. Ferenc Erdődi, D.Sc.
Beáta Bugyi, Ph.D.

Place and time of thesis defence: Debrecen, 3 May 2013

Key words: ErbB (EGFR), integrin, tyrosine kinase, FRET, trastuzumab, PI-3K/Akt, breast cancer, astrocytoma (glioblastoma)

"Because strait is the gate, and narrow is the way, which leadeth unto life, and few there be that find it."

Matthew 7:14
Bible - King James Version, 1611

Oxford King James Bible (Authorized Version), 1769

CONTENTS

ABBREVIATIONS

abFRET	- Acceptor Photobleaching FRET
ADCC	- Antibody Dependent Cellular Cytotoxicity
ADMIDAS	- Adjacent Region to MIDAS
AR	- Amphiregulin
ASR	- Age-Standardized Incidence Rate
BAD	- Bcl-2 Associated Death Promoter
BCNU	- Carmustine
BRCA1/2	- Breast Cancer Susceptibility Gene 1/2
Brk/PTK6	- Breast Cancer Protein Tyrosine Kinase 6
BSA	- Bovine Serum Albumin
DAG	- 1,2-Diacylglycerol
dbFRET	- Donor Photobleaching FRET
CCNU	- Lomustine
cDNA	- Complementary DNA
Chr7	- Chromosome 7
CISH	- Chromogenic *in situ* Hybridization
CSF-1R	- Colony Stimulating Factor 1 Receptor
CTC	- Circulating Tumor Cell
CTX-B	- Subunit B of Cholera Toxin
DMEM	- Dulbecco's Modified Eagle Medium
DNA	- Deoxyribonucleic Acid
DTC	- Disseminated Tumor Cell
ECL	- Enhanced Chemiluminescence
EBSS	- Earle's Balanced Salt Solution
ECM	- Extracellular Matrix
EGF	- Epidermal Growth Factor
EGFR	- EGF Receptor (ErbB1)
ER	- Estrogen Receptor
ERK	- Extracellular Signal Regulated Kinase
FAK	- Focal Adhesion Kinase
FAM126A	- Family with Sequence Similarity 126, Member A
FCET	- Flow Cytometric FRET
FCGR3A	- Immunoglobulin G Fragment-C Receptor 3A
FCS	- Fetal Calf Serum
FISH	- Fluorescent *in situ* Hybridization
FLT-3	- Fms-like Tyrosine Kinase 3
FRET	- Fluorescence Resonance Energy Transfer
GEF	- Guanine Nucleotide Exchange Factor
GFOGER	- Glycine - Phenylalanine - Hydroxiproline - Glycine - Glutamic acid - Arginine
GM1	- Mono-Sialogangliosid-1
GPI	- Glycosyl-Phosphatidyl-Inositol
GSK-3β	- Glycogen Synthase Kinase-3β
HB-EGF	- Heparin-Binding EGF
HSP90	- Heat Shock Protein 90
HRGα/β	- Heregulin α/β
ICAM	- Intercellular Adhesion Molecule
IDAP	- Isoleucine - Aspartic acid - Alanine - Proline
IDH	- Isocitrate Dehydrogenase
IDSP	- Isoleucine - Aspartic acid - Alanine - Proline
IGF-I	- Insulin-Like Growth Factor I
IGF-IR	- IGF-I Receptor
IHC	- Immunohistochemistry
ILK	- Integrin-Linked Kinase
IP_3	- Inositol-1,4,5-Trisphosphate
JAK	- Janus Kinase
LDV	- Leucine - Aspartic acid - Valine
LN	- Laminin

LOH	- Loss of Heterozygosity
MAD1	- Mitotic Arrest Deficient-like 1
MadCAM	- Mucosal Vascular Addressin Cell Adhesion Molecule
MAPK	- Mitogen-Activated Protein Kinase
MEK	- MAPK and ERK Kinase
MEM	- Minimum Essential Medium Eagle
MGMT	- Methyl-Guanine Methyl Transferase
MIDAS	- Metal Ion Dependent Adhesion Site
MR	- Magnetic Resonance
mTOR	- Mammalian Target of Rapamycin
Nck2	- Non-Catalytic Tyrosine Kinase 2
NK	- Natural Killer
NRG 1-4	- Neuregulin 1-4
PBS	- Phosphate Buffered Saline
PDGF	- Platelet-Derived Growth Factor
PDGFR	- PDGF Receptor
PgR	- Progesterone Receptor
PI-3K	- Phosphatidylinositol 3'-Kinase
PIK3CA	- Phosphatidylinositol-4,5-bisphosphate 3-Kinase, Catalytic Subunit Alpha
PINCH	- Particularly Interesting New Cysteine-Histidine Rich Protein
PIP_2	- Phosphatidylinositol 4,5-Bisphosphate
PKB	- Protein Kinase B
PKC	- Protein Kinase C
PLC	- Phospholipase C
PMS2	- Postmeiotic Segregation Increased 2
PTEN	- Phosphatase and Tensin Homolog Deleted on Chromosome TEN
Rb	- Retinoblastoma gene
RET	- Rearranged During Transfection (member of the cadherin superfamily)
RGD	- Arginine - Glycine - Aspartic acid
RNA	- Ribonucleic Acid
SD	- Standard Deviation
SDS-PAGE	- Sodium Dodecyl Sulphate - Polyacrylamide Gel Electrophoresis
SEM	- Standard Error of the Mean
SFM	- Serum Free Medium
SH2	- SRC Homology 2
Src	- Src Protein Tyrosine Kinase ("sarcoma")
SRE	- Serum Response Element
SRF	- Serum Response Factor
STAT	- Signal Transducers and Activators of Transcription
TCF	- Ternary Complex Factor
TGFα	- Transforming Growth Factor alpha
TNM	- Tumor - Node - Metastasis
tsFRET	- Two-Sided FRET
UN	- United Nations
US	- United States
NCI	- National Cancer Institute (US)
VCAM	- Vascular Cell Adhesion Molecule
VEGF	- Vascular Endothelial Growth Factor
VEGFR	- VEGF Receptor
WHO	- World Health Organization

1. INTRODUCTION

Treatment of malignant tumors does still often meet insurmountable difficulties despite ever-broadening diagnostic and therapeutic modalities. In the year 2008, 12.7 million new cases of cancers were diagnosed worldwide (latest GLOBOCAN survey of IARC) [1, 2], which is predicted to be increased by ~ 68 % - up to over 21 million - until 2030, taking into consideration recent time trends as well as the expected world population growth (UN, World Population Prospects, 2008) [3]. Of all types of tumors, lung cancers in males and breast cancers in females showed the highest age-standardized incidence (33.8 and 38.9 / 100.000, respectively) and mortality rate (29.2 and 12.4 / 100.000, respectively). These tumors could be accounted for the deaths of almost 1 million men and 0.5 million women worldwide in 2008. Additionally, tumors of the central nervous system stand now as the second most frequent cause of cancer mortality under age 35, showing a dramatically increased incidence (up to 300%) over the past decades [4, 5]. Indeed, despite expanding medical and health services in developed countries, incidence of tumors - all together - were two times higher.

In the background of these distressful data, therapy resistance and even in-treatment evolving metastatic ability of the tumors define themselves as attributable factors to treatment failures. In this line, the decreased chemo- or radiosensitivity and the developing uncontrollable metastasizing ability of the tumor cells frequently hamper the therapeutic break-through, even though significant development in imaging and molecular marker detection (early diagnosis), in surgical technique and adjuvant therapy (tumor specific targeting) have been achieved over the recent years. With respect to brain tumors, localization of the tumor may contra-indicate mass surgical removal and blood-brain barriers can also impede targeting, hence considerably prejudicing patient outcome.

To face these therapeutic hindrances, numerous studies have been conducted on tumorigenesis that revealed the role of overexpression, gene amplification or mutations of particular growth factor receptors - including ErbB proteins - in tumor proliferation and developing therapy resistance. After the discovery of their mitogenic potential, members of the ErbB family of type I receptor tyrosine kinases have undergone deep, comprehensive investigation. They were found to form homo- or heterodimers with each other that, stimulated by the enhancing effect of ligand binding, results in transphosphorylation on their tyrosine residues. This latter activation process leads to the recruitment of intracellular signaling molecules and translates into diverse cell fates. Heterodimerization - compared to

homodimerization - was shown to extend their transphosphorylating dynamism, yielding to more potent mitogenic signals.

To date, recent findings have also provided evidence for the functional crosstalk between certain cell adhesion molecules and receptor tyrosine kinases suggesting that they may contribute to therapy resistance. Given the phenomenon that foreign (e.g. brain) metastases of primarily invasive tumors are peculiarly isolated at their new localization - apparently losing their invasive ability to infiltrate - the role of molecular interactions of unique, organ and tumor specific cell adhesion and extracellular matrix molecules is suggested, which may restate the theory of "cell adhesion mediated therapy resistance".

2. MOLECULAR PATHOLOGY OF TUMORIGENESIS

2.1. The ErbB family of receptor tyrosine kinases

Research in the 1950's and 60's by Stanley Cohen on nerve growth stimulation with snake venom and then the unexpected "side effects" (precocious eyelid opening and incisor eruption in newborn mice) of the injected salivary gland extract led to an interesting finding - the discovery of a growth factor, later named EGF [6, 7]. His consecutive studies then disclosed its receptor (EGFR) [8, 9], which was proved to bear ligand-dependent tyrosine kinase activity - a revolutionary observation of molecular biology in the 1980s [10, 11]. After characterization of the erb-B oncogene of avian *er*ythro*b*lastosis virus, efforts revealed similarity between this viral erb-B oncogene and the human EGFR (therefore also termed ErbB1) [12, 13]. As other findings already supported the role of ErbB1 in tumorous transformation in animal studies [14], these latter results predicted a potential contribution of ErbB1 to human tumor development - setting up a new era of human cancer research.

Alterations of several tumor suppressors and oncogenes have been identified as being critical to the initial steps of transformation and progression to malignancy. Disregulated signaling processes starting from assemblies of cell surface molecules - including growth factor receptors - have been shown to play an important role in the pathogenesis and therapy resistance of tumors of different origin.

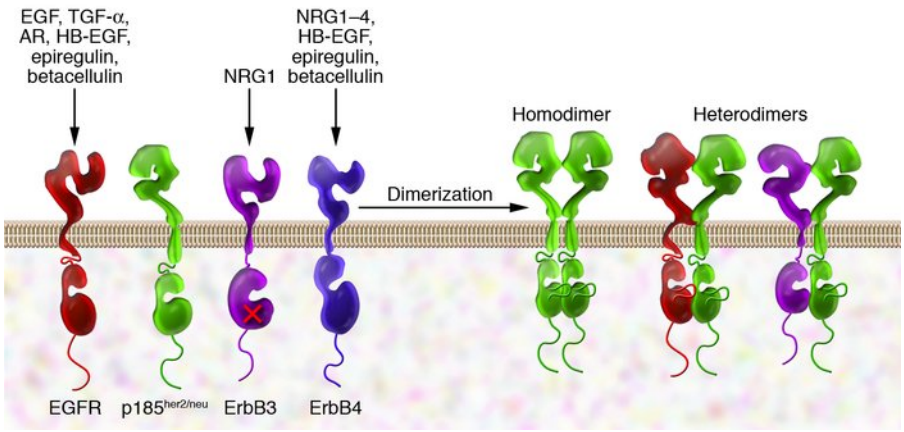

Figure 1. The ErbB family of type I receptor tyrosine kinases.
- from Hongtao Zhang et al., Journal of Clinical Investigation, 2007;117(8):2051-2058.

In this respect, members of the ErbB superfamily (ErbB1, ErbB2, ErbB3, ErbB4) of transmembrane receptor tyrosine kinases have been studied extensively [15-18]. ErbB2 was identified after the detection of an oncogene (*neu*) in rat *neu*roblastoma showing similarity to the viral erb-B oncogene. Since the purified protein product of the *neu* oncogene ($p185^{her2/neu}$)

did also appear to have high but not complete homology to the ErbB1 protein, it was termed ErbB2 [19, 20]. ErbB3 and ErbB4 were isolated and characterized by a targeted genomic screen in 1989 and 1993 (Fig. 1) [21, 22].

Members of the ErbB family are large glycoproteins that consist of an extracellular ligand-binding, a single chain transmembrane and an intracellular tyrosine kinase domain [23, 24]. The extracellular domain comprises four subdomains (I-IV), of which domain I and III serve for ligand binding, while the cysteine-rich domain II and IV are responsible for the dimerization. Upon ligand binding to domain I and III, a conformational change occurs that unseal the dimerization arm buried so far by domain II and IV in the autoinhibited, inactivated form of the receptor. The juxtamembrane and transmembrane chains contribute to the modification and activation of the receptor [25].

It has been revealed that certain tumor cells may express multiple ErbB family members, which can homo- and heteroassociate during signal transduction (see Fig. 1). Thorough investigations disclosed that dimerization and ligand binding leads to receptor transactivation and induction of versatile downstream signaling pathways via enhanced kinase domain activity [26]. Ligands of the ErbB family - including intramembrane proteins and their proteolytic products in plasma - regulate cell functions in auto-, para- or endocrine pathways:

- EGF - like ligands (EGF, TGFα, AR) binding to ErbB1
- neuregulins (NRG1-4 or HRGα/β) binding to ErbB3 and ErbB4
- HB-EGF, β-cellulin, epiregulin binding to ErbB1, ErbB3 and ErbB4

However, ErbB2 and ErbB3 stretch the point over this simplification as the former has no known ligand, whereas the latter has no kinase activity. Indeed, the dimerization arm of ErbB2 is in a constitutively exposed state rendering ErbB2 to act as a co-receptor for dimerization partners [16, 27], and present itself as an important integrator of transmembrane signaling by the ErbB family [28, 29]. It is probably for this reason that ErbB2 is clustered on the surface of breast tumor cells. The diameter of ErbB2-rich membrane domains is ~0.5 μm [30], and they are colocalized with ErbB3 proteins and lipid rafts that are liquid-ordered membrane microdomains, insoluble in non-ionic detergents at 4°C, rich in cholesterol, sphingomyelin and glycolipids [31]. Cell surface receptors are concentrated in lipid rafts, which can be considered as platforms either promoting or inhibiting signaling [32]. Nevertheless, besides the activation theory of allosteric oligomerization [33] - especially at these signaling platforms -, other observations suggested, however, the presence of preformed ErbB1 dimers in the membrane prior to getting activated by EGF [34].

2.2. The integrin family of cell adhesion molecules

Besides the association pattern of the ErbB molecules, tumor development, the proliferation and survival of cells also depend on the interactions between cells and their environment, including the ECM [35, 36]. Among the specific cell adhesion membrane protein species, integrins are the most dynamic and versatile group of adhesion molecules, from which downstream signals enable cancer cells to detach from neighboring ones, re-orient their polarity, and promote survival even in a foreign environment [37]. They also play a pivotal role in migration, attachment, cell cycle progression, programmed cell death and regulation of signal transduction pathways [38, 39].

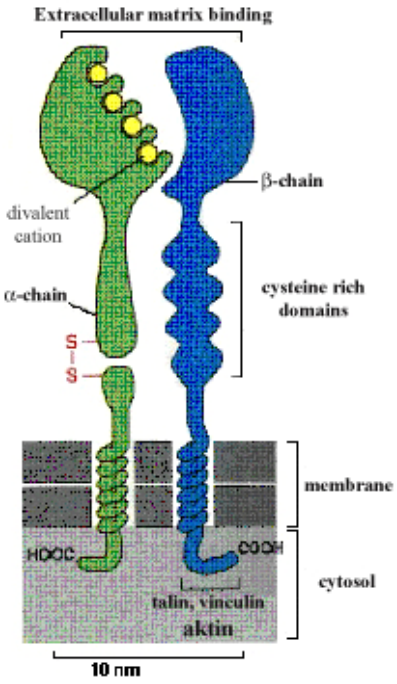

Figure 2. Schematic model of an integrin heterodimer.
- From the art of MBoC[3] © Garland Publishing, Inc., 1995 -

In the 1980's eager investigations were conducted on particular cell membrane receptors, which were termed position specific antigens in Drosophila [40], very late antigens of activation on human immune cells [41] or platelet glycoproteins [42]. After sequencing the cDNA and isolating the protein of chicken integrin β1 subunit in 1986, it was revealed that these membrane species belong to the same large cell adhesion molecule family, termed integrins, and carry a crucial role in signal transmission from the ECM to the cytoskeleton [43]. Integrins are evolutionarily ancient proteins, homologous sequences can be found even in bacteria and in prokaryotes [44]. They consist of two subunits (α and β), and bind to other cell adhesion molecules, ECM components or specific blood proteins (see Fig. 2). To date, 18 distinct α subunits and 8 β subunits have been characterized in humans, forming 24 distinct $\alpha\beta$ heterodimers (see Fig. 3) [45]. Activation and receptor conformation is regulated by special regions in subunit α (αI, MIDAS) and β (βI, ADMIDAS) upon ligand and ion (Ca^{2+} or Mn^{2+}) binding [46]. Repetitive conformational changes keep integrins in continuous motion that can be eloquently described as "bending like breathing" [47]. The subunit α determines ligand specificity, while β subunits are responsible for transmitting signals between the cell and its environment. A subset - eight members - of integrins recognizes RGD sequence in their ligands. Of the several α subunits, nine contain the

subdomain αI, which is unique in that it could be descended from the time tunicates diverged from invertebrates in the evolution, and holds a triple helical GFOGER recognition motif for binding collagens (α1, α2, α10, α11) and leukocyte specific proteins (αE, αM, αL, αD, αX) - which are thus not present in invertebrates [44, 48].

Other integrins (α4β1, α4β7, or heterodimers of β2) binds to LDV, IDAP or IDSP sequences of fibronectin or certain members of the immunoglobulin superfamily (ICAM-1, ICAM-2, VCAM-1, MadCAM), which may also define potential therapeutic targeting [49-51]. Most integrins recognize ECM proteins, such as fibronectin, vitronectin, tenascin, E-cadherin, laminins (LN-111, -211, -332, -411, -511), collagens (types I, II, IV and IX), members of the immunoglobulin superfamily (ICAM-1, -2, -3, -5, VCAM-1, MadCAM-1) or proteolytic products (endostatin, tumstatin, endorepellin) of ECM molecules [52]. Integrin β1 can associate with various α chains and consistently it was also found to be widely expressed throughout the human body (see Fig. 3).

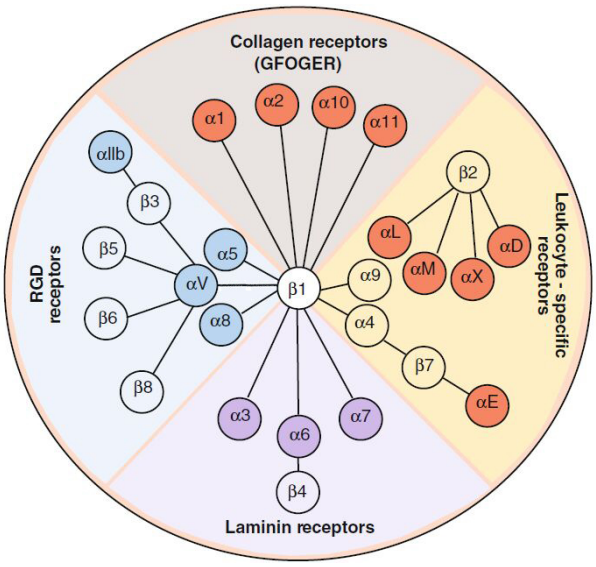

Figure 3. Diverse heteroassociation patterns of integrin *α* and *β* subunits.
Note that of the most promiscuous three chains - αV, β1 and β2 -, the integrin β1 can participate in such heterodimers that can form RGD receptors, collagen receptors, laminin receptors or even leukocyte-specific receptors, as well. - *from Barczyk et al., Cell Tissue Research 2010; 339:269-280.* -

Five splice variants ($\beta1_A$, $\beta1_B$, $\beta1_{C1}$, $\beta1_{C2}$ and $\beta1_D$) of the integrin β1 molecule have so far been described, differing in the cytoplasmic region [53, 54]. Interestingly, the widely expressed $\beta1_A$ was proved to be a stimulator, while $\beta1_C$ cytodomains are inhibitors of cell proliferation [55, 56]. The substantial role of integrin β1 was suggested in cell differentiation, migration, attachment, tumor progression and - as adhesion receptors - during metastasis, as well [57]. Disruption of basement membrane through downregulation of LN-1 and integrin $\beta1_C$ was also shown to contribute to tumor development [58, 59]. Indeed, epidermal stem cells

were also shown to express excess integrin β1 - a pontential candidate for screening as an epidermal stem cell marker. However, these data have to be carefully interpreted due to the dispersed expression profile and functionally diverse splice variants of integrin β1 [60].

When tissue cells spread out in the ECM, integrins (e.g. the α5β1 heterodimer) form multimeric clusters with structural and/or signaling roles in focal adhesion complexes [61]. The interaction of membrane proteins - including growth factor receptors and integrin molecules - at these focal adhesion sites then may mediate downstream signaling processes preventing rescue from apoptosis, and hence promoting cell survival [62].

2.3. Molecular markers and signal transduction pathways

EGF (acting through ErbB1), PDGF-A and B (acting through PDGFR-α and β), TGF-α (acting through ErbB1) and IGF-I (acting through IGF-IR) are often involved in stimulating tumor cell proliferation [63, 64]. The three key downstream signaling pathways that can show increased activity owing to aberrant receptor expression and/or interactions are the Ras/MAPK, PI-3K/Akt and PLC-γ/PKC signal routes (Fig. 4).

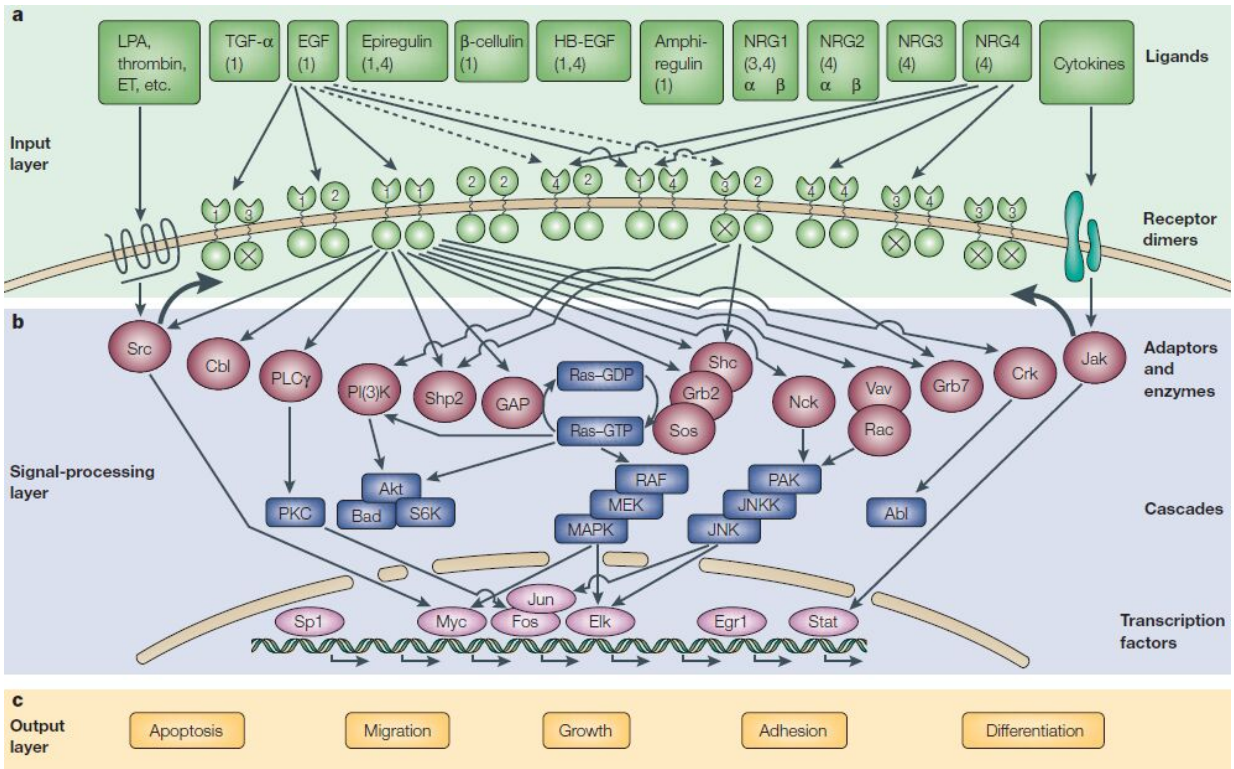

Figure 4. Signaling network of the ErbB tyrosine kinase receptor family.

- from Y. Yarden, Nature Reviews 2001; 2:127-137. -

The transphosphorylated ErbB tyrosine side chains are recognized by SH2 domains of Grb2 adaptor proteins that bridge Sos or Shc molecules through proline rich SH3 domains. This complex then functions as a GEF that recruits and activates Ras-GDP to form Ras-GTP. Thereafter, downstream signaling, via activation of Raf-1 and dual specificity (serine/threonine and tyrosine) MEK, leads to the phosphorylation of MAPK or ERK1/2 and various transcription factors like TCF, SRF, Elk-1, c-fos or c-myc that induce gene transcription by binding to SRE DNA sequences [65].

The other key signaling route of the ErbB receptors is regulated via the PI-3K protein, which is a heterodimer of a regulatory p85 subunit and a catalytic p110 subunit. The p85 is responsible for specific binding to ErbBs, while p110 produces IP_3 that functions as second messenger necessary for serine/threonine phosphorylation and thus for the activation of Akt (protein kinase B). Interestingly, direct docking sites for p85 are absent on ErbB1, however, it can activate the p85 subunit through docking the protein Gab-1.

The PI-3K signaling route is known to contribute to cell growth, invasion and anti-apoptotic processes [66], and has received much attention because it is negatively regulated by the PTEN protein. PTEN is an important regulator of the pathway as it dephosphorylates IP_3 and serves as a major tumor suppressor [67]. Deregulation of this protein was also shown the most common loss-of-function alteration in glioblastomas [68], and may be involved in trastuzumab responsiveness, as well [69]. Related downstream proteins also include GSK-3β and mTOR C1/2 complexes that regulate c-myc, cyclin degradation and translation, protein synthesis, redox status, autophagy, and apoptosis [70].

Downstream signaling events can also be mediated by docking SH2 domains of members of the PLC superfamily at phosphorylated tyrosine function groups of growth factor receptors as it was shown for ErbB1 [71]. In contrast, some isotypes of the PLC proteins (e.g. PLCβ) are activated by G-proteins (G_q, G_o). PLCγ cleaves PIP_2 to DAG and IP_3. Both cleaved products are necessary for the activation of PKC; intracellular calcium release via IP_3 regulated calcium channels translocates PKC to the cell membrane, where it gets activated by its cofactor, DAG. The affected cellular events via this signaling route diverge upon PLC and PKC isotype and substrate distribution profiles of different tissue types. Cell proliferation and survival can be influenced by signaling via PKCβII or PKCε, while PKCα, PKCβI or PKCδ are known to inhibit proliferation and drive apoptotic signals [72].

In addition, the cytoplasmic STAT proteins are also known to be mediating signaling from growth factor receptors. STAT monomers form homo- or heterodimers upon docking at each others' phosphorylated tyrosine residues via SH2 domains and then move into the nucleus to induce transcription of genes important in the regulation of cell cycle progression, apoptosis, tumor angiogenesis, tumor cell invasion and metastasis [73, 74]. Constitutive activations and perturbations of STAT3, STAT5 and STAT1 signaling were reported in numerous tumors [74, 75]. The Src kinase, named after the *src* gene of the chicken Rous-sarcoma virus, is also critically involved in tumorigenesis as it was published to interact with STAT proteins besides FAK and PI-3K [76], and thought to contribute to resistance to ErbB targeted therapies [77]. Moreover, the PI-3K/Akt pathway, known also to activate STAT proteins, was shown to modulate ErbB1-regulated activation of transcription factor NF-kappa-β involved in transformation pathways, as well (Fig. 4) [78].

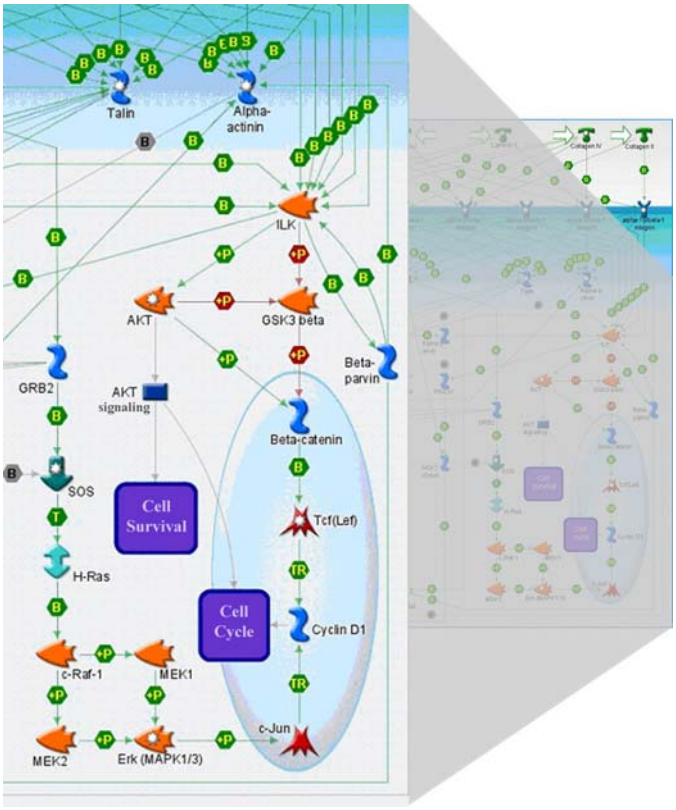

Figure 5. Signaling network of heterodimers formed by integrin β1 molecules. The most prominent Akt / ILK / GSK-3b interactions and signaling are higlighted.

- from Thomson Reuters, GeneGo, Pathway Map Details -

As discussed before, emerging evidence supports the assumption that growth factor signaling is frequently modulated by the interaction with certain cell adhesion molecules, which bear particular responsibility in tumor migration, attachment and progression. The focal adhesion complexes at the focal adhesion sites of migrating cells are known to be associated with talin, vinculin and the actin cytoskeleton. Signals from activated receptors in these complexes cause the activation and phosphorylation of FAK attached to talin. Thereafter, downstream signaling activates the PI-3K/Akt-PKB pathway, which promotes cell survival through inactivation of Bad, caspase-9 proteins and the transcription factor FKHRL-I [79, 80]. Recent studies on astrocytomas revealed that this FAK activation correlated and co-localized with ErbB1 and integrin α5β1 expression at the single cell level, which also provides evidence for a considerable cross-talk between ErbB1 and integrin molecules in human malignant

gliomas [81]. In addition, the ILK/GSK-3β mediated canonical β-catenin / Tcf-4 pathway involved in integrin signaling can also contribute to tumorigenesis by direct regulation of the Akt2 gene expression (Fig. 5) [82].

2.4. Associations of ErbBs and interactions with integrin β1

2.4.1. Homo- and heterodimerization of ErbB molecules

After ligand binding, ErbB1, ErbB3 and ErbB4 preferentially form a primary heterodimer with orphan ErbB2 proteins that translates into high tyrosine kinase and trans-phosphorylation activity [18]. Overexpressed ErbB2 is the preferred heterodimerization partner for other ErbB proteins [83] inhibiting ligand-induced receptor down-regulation [84] and playing a mediator role in lateral signal transmission and transmembrane signaling by its intrinsic tyrosine kinase activity [85]. The activated ErbB2 can form secondary dimers with other ErbBs starting divergent intracellular signaling pathways. Ligand binding affinity and intracellular activation patterns of the three primary dimers and those of the secondary dimers are different, which greatly diversifies the signaling capacity of the ErbB family [86].

Presence of ErbB1/ErbB3 and ErbB1/ErbB4 heterodimers has been rarely described, but they appeared only on cells where no ErbB2 was available. Dimers containing ErbB2 are more stable; they have higher ligand binding affinity and bear more potent tyrosine kinase activity. It is important to note that ErbB2 containing dimers are able to avoid degradation after internalization and they readily recirculate to the cell membrane. As opposed to this, ErbB1 containing dimers are down-regulated very fast after EGF activation. Therefore, ErbB1 down-regulation after activation by EGF may be an important negative feedback in the control of epithelial cell proliferation.

On cells with ErbB2 overexpression, spontaneous homodimerization of ErbB2 molecules can be observed because of the high receptor density [87]. The ErbB2 - ErbB3 heterodimer is the most mitogenic ErbB dimer, because ErbB2 enhances the ligand affinity and spectrum of ErbB3 towards EGF-like ligands. Phosphorylated ErbB2 serves as activation site for Shc coupling to the MAPK pathway, whereas ErbB3, if activated, is able to recruit PI-3K, and thus to signal via the Akt pathway [27]. This capacity of signaling through the MAPK pathway leading to proliferation and through the PI-3K/Akt pathway leading to survival, combined with the prolonged signaling caused by evaded internalization explains why the presence of the ErbB2/ErbB3 heterodimer is a bad prognostic factor [88].

2.4.2. Molecular interactions between ErbB and integrin β1 molecules

Transmembrane signaling mediated by the cooperation of integrins and growth factor receptors was underlined by several studies [89-91], and ligand binding induced formation of ErbB homo- and heterodimers was proved to activate a diverse network of second messenger systems [16].

In addition to the association patterns of ErbB molecules, tumor development, the proliferation and survival of cells also depend on the interactions between cells and their environment, including integrin molecules of the ECM [38, 39]. Similar to ErbB2, integrins were shown to be also raft-associated [92] and ErbB2 was shown to be associated with integrins α6β4 and α6β1 in human carcinoma cell lines [93]. Integrins containing a β1 subunit are receptors for collagen, laminin and fibronectin and function as adhesion receptors during metastasis (as described before) [57].

ErbB1 is also localized at these sites and can give rise to activation of the FAK and the PI-3K / Akt-PKB pathway, which promotes cell survival through inactivation of Bad, and caspase-9 as well as the transcription factor FKHRL-I [79, 80]. Interaction between ErbB1 and integrin β1 also enhances tumor cell detachment, migration, and metastatic ability [37] by displacing tensin-3 from the cytoplasmic tail of integrin β1 and consequently resulting in the disassembly of the actin cytoskeleton machinery [94]. Cooperative signaling between ErbB proteins and integrins [95, 96] is a common feature of invasive cancer cells and association of integrin β1 and ErbB proteins could provide a framework in which tumor cell metastasis could be better understood [97].

Recent findings also underlined the functional crosstalk between certain cell adhesion molecules and receptor tyrosine kinases, suggesting that they may contribute to developing chemo- and radioresistance [98]. The coactivation of multiple receptor tyrosine kinases and cell adhesion molecules then may drive redundant inputs into the cytoplasm, maintain downstream signaling and affect the response of tumor cells to targeted therapies [99].

2.5. Analysis of multi-faceted molecular interactions of membrane proteins

One of the best methods for mapping molecular interactions is measuring FRET, which enables resolving molecular associations in the 1-10 nm range, far exceeding the diffraction limit of the conventional microscope. The FRET phenomenon was first described by

Theodore Förster in the late 1940s [100]. In the process, energy is transferred from the first excited electronic state (S_1) of a donor (D) to a neighboring acceptor molecule (A) in a nonradiative, dipole-dipole interaction under favorable conditions. The rate of FRET (k_T) is proportional to the negative 6^{th} power of the separation distance between the donor and acceptor molecules and eventually results in the quenching of the donor and the increase of the acceptor fluorescence (sensitized emission) (Fig. 6-7) [101]. Applications for measuring FRET between cell membrane species were established for flow cytometry and confocal microscopy [102, 103]. The FCET technique provides statistically accurate information on the distribution of FRET efficiency on thousands of cells [90, 104], whereas microscopic FRET measurements can reveal the heterogeneity of the expressions and interactions of membrane proteins within even a single cell [105, 106].

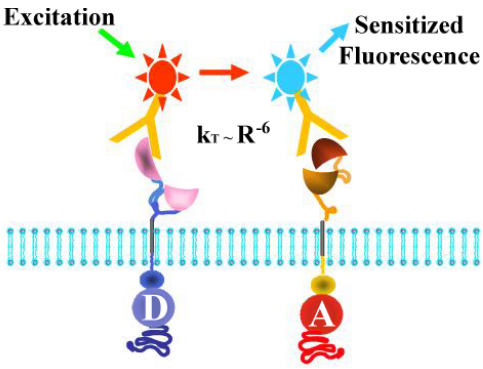

Figure 6. The FRET phenomenon. Energy is transferred from an excited donor (D) to a nearby acceptor (A) molecule. The FRET rate is proportional to the negative 6^{th} power of their separation distance.

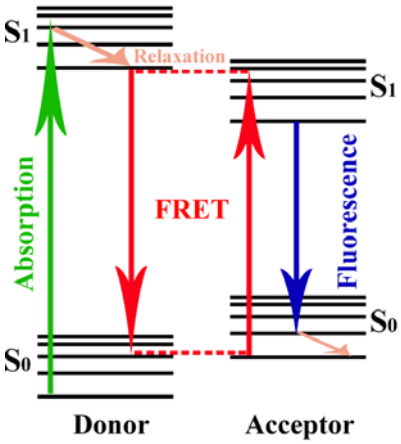

Figure 7. Mechanism of FRET. Energy is transferred in a nonradiative, dipole-dipole interaction

In conventional FRET measurements, molecular associations are investigated between two molecules regardless the interactions with other nearby molecules. Thereby, the implementation of a new method, characterizing the relationship of distinct molecular interactions could greatly extend our knowledge of multi-component complexes and signaling mechanisms. Steadily improving FRET techniques have now evolved to the potential of characterizing molecular interactions in tissue sections [107, 108]. Indeed, precisely quantitating molecular interactions on individual samples *in situ* could be conjoined with clinical data to better define prognosis or optimal therapy [109, 110].

Regarding these results, the need for further functional assays is raised for better understanding the molecular interactions between certain mitogenic cell surface species and surrogate markers of stem cell survival. Translation of future results into clinics may allow us to fine-tune the right mixture of drugs that target specific molecules of tumors and lead to respective marker development for individualized treatment and patient selection [111].

3. ERBB MOLECULES IN TUMOR DEVELOPMENT – THE MEDICAL ASPECT

In addition to their exceptional disposition "to fine-tune" the hierarchical structure of signaling processes that regulate tissue and organ development and differentiation during ontogenesis, growth factor receptors are also well known to contribute to tumorigenesis.

Members of the ErbB family of type I receptor tyrosine kinases are influential representatives of the growth factor receptors responsible for tumorous transformations since deregulation, overexpression, amplification or mutations of these cell membrane proteins are common and quite frequent events that occur in the first steps of tumor development. After discovering their mitogenic potentials, the ErbB proteins have undergone comprehensive investigations that shed light on their pivotal role in the tumorigenesis.

3.1. Alterations of ErbB2 in breast cancer

Amplification of ErbB2 was first reported in human breast and ovarian cancer [112], but its overexpression can also often be responsible for other malignancies, such as colon, pancreas, ovarian, bladder, head-and-neck, non small cell lung cancers, Wilm's tumors and neuroblastoma [113].

In breast cancers, ErbB2 is overexpressed in 60% of the inflammatory and in 25% of the non-inflammatory ductal invasive breast cancers [114] and due to its high dimerization potential, heteroassociation with other members of the ErbB family or with extraneous diverse cell membrane proteins can induce versatile signaling events that eventually drive uncontrollable tumor growth from *in situ* to invasive carcinoma [115]. Hence, targeting ErbB2 in adjuvant or neoadjuvant regimens may potentially bring about improvement in the otherwise poor clinical outcome of patients suffering from advanced breast cancer.

3.1.1. Epidemiology and diagnosis of breast cancers - a general outline

Breast cancer had a 98.1 / 100.000 crude incidence rate (62.8 / 100.000 ASR) and 30.5 / 100.000 crude mortality rate (ASR 16.7) in the European region as of 2008, at which time these parameters were 99.2 (ASR 56.8) and 40.1 (ASR 18.6), respectively, in Hungary [1]. In numbers, death of 139.829 women in Europe and of 2.108 women in Hungary could be attributed to breast cancer in 2008. Despite decreasing mortality - due to advance in early diagnosis and more optimized therapy over the recent years in developed countries - breast cancer still remains the leading cause of tumorous death in women.

Diagnosis is based upon clinical symptoms (local, paraneoplastic and systemic), imaging (mammography, ultrasound or MR in challenging or disseminated cases) and pathological analysis of surgical samples (core needle biopsy). Therapeutic intervention schemes are based on histological diagnosis according to the ever-latest WHO classification [116] and TNM - staging that now includes ER, PgR and ErbB2 status (IHC, and FISH/CISH for gene amplification assessment) of the tumor, as well. Mutations of the "caretakers" BRCA1/2 genes are also sought for in patients at high risk (i.e. specific ethnic groups) as these genes are known to be incriminated in hereditary high-grade ductal mamillary carcinomas - in ~5 % of all cases - that usually do not bear ER or ErbB2 positivity as compared to sporadic cases. In addition, mutations in susceptibility genes (TP53, PTEN, STK11/LKB1, CDH1, CHEK2, ATM, MLH1, MSH2) have also been implicated in the development of hereditary breast tumors [117]. In the cases of sporadic breast cancers, overexpression of the ErbB2 protein was revealed in 20 - 30 % of the patients, and targeting this molecule is now in clinical routine [118].

3.1.2. Treatment options for breast cancer

Therapy of breast cancer is multidisclipnary: surgery, radiotherapy and (neo)adjuvant chemotherapy. Post-surgical radiotherapy is strongly recommended to avoid early recurrence. Patients with different degree of endocrine responsiveness (ER, PgR status) are treated with endocrine therapy with or without combining chemotherapeutic regimens. Neoadjuvant chemotherapy is planned upon predictive factors in order to down-size locally extended primary tumor to reach a mammary stage eligible for breast conservation surgery. For adjuvant chemotherapy, anthracycline and taxane based regimens are usually administered that now include trastuzumab, as well [119].

Upon revealing the pathogenic role of ErbB2 overexpression or gene amplification in breast cancer development, targeting this molecule at the cell surface was pointed out as a treatment option. To date, trastuzumab (the recombinant, humanized version of an anti-ErbB2 mouse monoclonal antibody, 4D5) is included not only in the management of metastatic disease but also in adjuvant regimens [120]. As ErbB2 overexpression was found to predict poor prognosis even in primarily small and node negative tumors, it was opted to be included in neoadjuvant systemic regimens, as well [121, 122]. Relapse rate was shown to be significantly decreased, however resistance to trastuzumab has been observed in ~50 % of ErbB2 overexpressing cases, many of them developing during treatment. To counter this hindrance, intensive research is going on worldwide, and yet more recent trials have proposed

the integration of lapatinib (inhibiting both ErbB1/2 kinase activity) along with bevacizumab (against VEGF) and everolimus (an mTOR kinase inhibitor, derivative of tacrolimus) into neoadjuvant chemotherapeutic regimens [123]. Other tyrosine kinase inhibitors such as neratinib/foretinib with irreversible panErbB inhibition [124] and pazopanib/sunitinib with multitargeted potential against VEGFR, PDGFR, c-Kit, RET, FLT-3 and CSF-1R have also reached clinical phase [125]. Downstream blocking agents targeting the Akt protein or both PI-3K and mTORs (perifostine, NVP-BEZ235) were reported to overcome trastuzumab and even associated lapatinib resistance [126]. In addition, several second-generation HSP90 inhibitors (e.g. alvespimycin) [127], thioether-linked conjugates of cytotoxic tumor activated prodrugs (e.g. the anti-microtubule mertansine, DM1) are under trials for primary metastatic breast cancers. Moreover, promising studies are conducted with the use of variant ErbB2 targeting antibodies such as pertuzumab that effectively blocks ErbB2 from forming heterodimers [128], the monoclonal, bi-specific, tri-functional antibody ertuxomab that drives CD3 positive T-cells and macrophages to ErbB2 overexpressing cancer cells [129], and defucosylated trastuzumab antibodies that were proven to enhance ADCC [130].

3.1.3. Therapy resistance to trastuzumab in the management of breast cancers

As mentioned above, ErbB2-mediated transmembrane signaling is a key target of novel anticancer agents such as trastuzumab that binds to the juxtamembrane region of the domain IV of ErbB2 responsible for dimerization [131]. Trastuzumab is thought to lead to down-modulation and internalization of ErbB2 that results in reduced downstream signaling via inactivation of the MAPK and PI-3K pathways [28, 132, 133]. Others suggested that trastuzumab induced internalization may be achieved preferentially by mono-ubiquitination of ErbB2 through recruiting c-Cbl - an E3 ubiquitin-protein ligase - to site, which leads to accelerated endocytotic removal of ErbB2 from the cell surface [134]. However, in contrast to these observations, additional data revealed that down-regulation is not the main mechanism of trastuzumab action *in vivo*, and that instead the antibody recycles back to the membrane with ErbB2 after endocytosis [135].

It did also soon become clear that domain IV comprises a clevage site for matrix-metalloproteases and shedding thereby results in a 110 kDa extracellular domain of the 185 kDa full-length ErbB2, which is then released and circulates in the serum *in vivo* [136]. The membrane-associated, amino-terminally truncated, residual 95 kDa fragment then gains increased dimerization activity that can be inhibited by trastuzumab binding [137]. Moreover, membrane translocation and activation of PTEN - via sustained dephosphorylation due to

reduced Src activity by dissociation from ErbB2 upon trastuzumab binding - was proved to also contribute to the inhibitory effect of trastuzumab via inhibiting Akt and downstream mTOR kinases [138]. Upon administration, trastuzumab was observed to induce cell cycle arrest at the G1 / S boundary, accompanied by an increase in $p27^{kip1}$ level and a decrease in cyclin D1 and cyclin-dependent kinase 2 activity [139], whereas others published that trastuzumab inhibited angiogenesis by modulating the equilibrium between pro- and anti-angiogenic factors and angiopoietin-2 expression, which thereby finally resulted in decreased tumor vascularization and supply [140, 141]. Various additional mechanisms have been also suggested to explain trastuzumab resistance including autocrine production of EGF-related ligands [142], activation of the IGF-I receptor pathway [143, 144], and masking of the target epitope of trastuzumab by MUC4/sialomucins or CD44/hyaluronic acid complexes [145].

Several documented inter-molecular and downstream signaling events - detailed above - substantiated the anti-proliferative effect of trastuzumab *in vitro*, whereas consequent research proved that the majority of the inhibitory effect of trastuzumab *in vivo* is attributable to ADCC [146].

Along this line, a cell line - termed JIMT-1 - provided a useful model system that was established from an ErbB2-overexpressing, trastuzumab-resistant breast cancer patient [147]. Besides sterically hindering ErbB2-trastuzumab interaction, MUC4 was shown to hamper the exertion of NK immune-cells responsible for ADCC [148, 149], and increase the transforming activity of the ErbB2-ErbB3 heterodimer by direct interaction between ErbB2 and the EGF-like domain of the ASGP-2 subunit of the MUC4 heterodimer (ASGP-1/2) glycoprotein [150, 151]. Using xenografts from the JIMT-1 cell line in mice, it was proved that circulating and disseminated - i.e. metastatic - tumor cells (CTCs, DTCs) re-gain response to trastuzumab by ADCC, even though tumor cells at the primary site retain resistance, which gives the idea that administration of trastuzumab in advanced - virtually resistant - breast cancer is still relevant in terms of preventing metastasis [152].

Based on other findings, the inactivation of PTEN [138], down-regulation of the $p27^{kip1}$ protein [153, 154], gain-of-function mutations of the PIK3CA gene [155, 156], disturbed ADCC by the polymorphism of the FCGR3A gene [157], the decreased expression of the BAD BH3-only pro-apoptotic protein or interactions with Brk/PTK6 have also received great attention as possible predictors of trastuzumab resistance [158, 159]. To date, combination of anti-ErbB2 vaccine and trastuzumab in ErbB2 overexpressing breast cancer patients has also been proposed to overcome resistance and sustain specific immunity [160].

Although clinical application of this specific anti-tumor targeting therapeutic approach has drastically improved therapy outcome for patients with ErbB2 positive breast tumors, success is far from complete, as resistance to trastuzumab is quite frequent; initial efficacy is 30-50%, and many of the initial responders have a relapse after 6-9 months [161]. The background of this common resistance to trastuzumab thus seems to be multitudinous and may vary case by case, which can significantly limit the potential of this new treatment modality [162, 163].

3.2. Alterations of ErbB1 in astrocytoma

Ever since Stanley Cohen first described the EGF and its receptor EGFR (later termed ErbB1), intense and thorough investigations were initiated on its suspected mitogenic potential in human tumorigenesis. Substantial evidence demonstrated that alterations in the ErbB1 signaling route, and overexpression or gain-of-function mutations of the ErbB1 protein (e.g. ErbB1vIII or delta2-7 EGFR - the most frequent class III mutants, which harbor constitutive kinase activation by a deletion in its extracellular domain) can be frequently accounted for gliomagenesis [164].

Based on these and additional findings on multitudinous interactions of ErbB1 with other cell surface species, newly proposed anti-tumor therapies tended to include anti-ErbB1 agents, however yet inextricable difficulties in facing the observed common therapy- and radioresistance raised the need to address combined therapeutic modalities for the treatment of astrocytic tumors.

3.2.1. Epidemiology and diagnosis of astrocytomas - a general outline

Tumors of the central nervous system are the second most frequent causes of cancer mortality under age 35 with a slight peak in children between 6 and 9 years old [4, 165]. Brain tumors had a 6.9 / 100.000 crude incidence rate (5.2 / 100.000 ASR) and 5.3 / 100.000 crude mortality rate (ASR 3.7) in the European region as of 2008, at the same time these parameters were 6.1 (ASR 4.3) and 6.4 (ASR 4.0), respectively, in Hungary [1]. In numbers, death of 47.451 people in Europe and of 640 people (both sexes) in Hungary could be accounted for tumors of the central nervous system in 2008.

Only in the United States, ~44 thousand new cases of primary malignant and benign brain tumors are diagnosed per year, of which ~45% are gliomas [165]. Of these tumors, high grade astrocytomas show particularly bad prognosis, and although there is no firm consensus

yet, most studies of time trends in developed countries disclosed a dramatically increased incidence (up to 300%) and mortality of brain tumors over the past decades [5]. Despite significant advances in neuroimaging, surgical technique and adjuvant therapy over the past 50 years, malignant glioma remains a highly invasive and virtually incurable disease, of which treatment is frequently hampered by the decreased chemo- and radiosensitivity of the tumor cells [166].

Diagnosis is based upon clinical symptoms (due to the expanding intracranial mass), imaging (mainly MR) and histopathological analysis of surgical samples (resection or stereotactic biopsy). The staging is based on the histopathological grade - according to the latest revised WHO classification [167] - and imaging results. As astrocytomas do rarely disseminate over the brain, staging of other organs is not necessary for treatment planning.

Multiform glioblastoma is recognized to show significant cellular heterogeneity – as its name implies; it is composed of cells of many different morphologies and varying expression of biomarkers. Recently, human malignant gliomas have been shown to be organized hierarchically based on a small subpopulation of tumor cells having stem cell properties [168-170]. A cancer stem cell or tumor initiating cell is defined as a cell within a tumor that possesses the capacity to self-renew and to regenerate the heterogenous lineages of cancer cells that comprise the tumor [171]. They have been reported to be enriched in the fraction of CD133+ cells - also known as Prominin-1 (PROM1) or AC133 coding for a 120 kDa pentaspan transmembrane glycoprotein on chromosome 4p16.2 [172, 173]. Radiobiological assays have provided evidence that cancer stem cell content and the intrinsic radiosensitivity of cancer stem cells or tumor stroma varies between tumors, thereby affecting their radiocurability [174, 175].

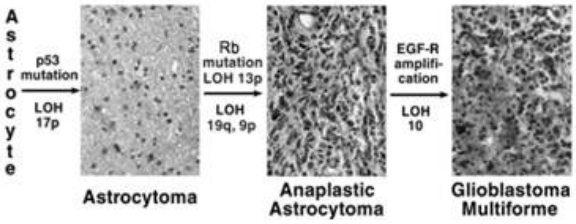

Figure 8. Development of secondary glioblastoma by accumulation of mutations.
- The WHO classification of tumors affecting the central nervous system, Stephen B. Tatter, 1993 -

Molecular genetic data gathered since the early 1990s suggest that histologically defined subtypes of malignant gliomas are even more diverse at the biological level. Primary glioblastomas arising *de novo* without clinical or histological evidence of a less malignant precursor lesion share two common mechanisms of gliomagenesis: overactive growth factor (mitogen) signaling and disruption of cell cycle control (perturbations of $p16^{INK4a}$ and $p14^{ARF}$ tumor suppressors). In contrast, secondary glioblastomas develop more slowly by malignant progression from lower-grade gliomas, and the accumulation of genetic alterations (p53 mutation, PDGF-A / PDGFR-α

overexpression, retinoblastoma (RB) gene alteration, PTEN mutation, loss of heterozygosity 10q and loss of DCC expression) over time is characteristic of these tumors (Fig. 8) [176]. Furthermore, proof has been published that molecular genetic analysis of fresh frozen samples on loss of heterozygosity on chromosome 1p / 19q, epigenetic silencing of the MGMT gene promoter or IDH mutations can help identify patients at risk with potential unresponsiveness to chemotherapy [177, 178].

Amplification and mutations of the ErbB1 molecule have also long been recognized as the most common gain-of-function perturbations in malignant gliomas. Indeed, increased expression of the ErbB1 protein on the cell surface has been shown to correlate with decreased radiosensitivity in high grade astrocytoma cells [179].

3.2.2. Treatment options for astrocytoma

The actual therapeutic strategy of glial tumors consists of surgical resection as complete as achievable, and treatment of the remaining tumor with adjuvant radio- and/or chemotherapy. If resection is contra-indicated due to the localization of the tumor, stereotactic serial biopsy has to be undertaken for histopathological diagnosis. For grade IV astrocytomas, concomitant chemo-radiotherapy is now the standard of care [180, 181].

Adjuvant systemic chemotherapy means almost exclusively the administration of temozolomide (atypical alkylating agent) approved also for newly diagnosed cases by the FDA in 2005 March, combined usually with radiotherapy. Other therapeutic trials were conducted on the use of PCV regimens (procarbazine, CCNU, vincristine) [182, 183], implantation of nitrosourea (BCNU) impregnated biodegradable polymer (Gliadel wafer) into the resection cavity [184], or of novel tyrosine kinase inhibitors against overexpressed or mutant ErbB1 (erlotinib) [185], PDGFR (imatinib) [186] and VEGF (bevacizumab) alone or in combination with irinotecan [187].

Inhibition of integrin αVβ3 signaling with the RGD mimetic peptide cilengitide has also reached the clinical phase, however, the positive outcomes were more likely attributable to direct effects on endothelial cells and tumor vascularization [188-190]. Furthermore, ongoing preclinical studies now address PI-3K-related pathway inhibitors (NVP-BEZ235, LY294002, enzastaurin) that suggest a potential to sensitize chemotherapy-induced apoptosis via disrupting the PI-3K / Akt / mTOR / GSK-3β signaling routes [70]. However, overall survival of patients with astrocytoma is still devastatingly low, though huge international research efforts are apparent. Recurrence generally occurs within a year after diagnosis

despite broadening therapeutic modalities that try to target and abolish, *inter alia*, the yet actually uncontrollable infiltrative property of this kind of tumor.

As emerging evidence has proven interactions between ErbB family proteins and other cell surface adhesion species, some new treatment strategies are increasingly focusing on cell adhesion mediated therapy resistance, since the challenge of treating malignant gliomas arises from their infiltrative extension rather than from mass expansion.

3.2.3. Therapy resistance to irradiation in the management of astrocytomas

Several resistance mechanisms to irradiation have been proposed so far, but the underlying molecular interactions still remain elusive. Principally, ionizing radiation kills cancer cells through causing DNA damage by producing strand breaks. Neutrons and α-particles affect DNA directly, whereas X-rays and γ-rays first interact with intracellular water-molecules producing free hydroxyl radicals, which then damage the DNA [176]. Maintained DNA damage triggers apoptosis (programmed cell death) or senescence, therefore the ability to repair DNA breaks is of crucial importance concerning cellular survival.

In addition to accumulating evidence that greater radioresistance correlated with more efficient repair of DNA damage, ErbB proteins appeared to participate in the response of tumor cells to ionizing radiation [179, 191, 192], and increased expression of ErbB1 correlated with decreased radiosensitivity in high grade astrocytoma cells [193]. The balance between cytoprotective and cytotoxic responses to ErbB1 activation during single and repeated radiation exposures was shown to depend on the relative expression levels and activities of different cell surface receptors via mediating overall cellular responses of proliferation and apoptosis [194, 195]. Several studies demonstrated that PI-3K / Akt signaling – the most prominent glial activation pathway – has a crucial role in enhanced DNA repair and the development of radioresistance through Src-dependent ErbB1 activation [196, 197]. Indeed, further investigation strengthened the assumption on molecular interactions between ErbB1 and integrin β1 molecules in tumor cell migration and metastasizing ability via upregulation of cten, a tensin family member, and consequent disintegration of the actin cytoskeleton [94].

The high frequency of these signaling pathway alterations has recently led to the identification and increasing administration of small-molecule inhibitors in radiation oncology [198], and most recent studies have also revealed that stem cell-related "self-renewal" signature and high ErbB1 expression were associated with resistance to concomitant chemo-radiotherapy [199].

Taking together the emerging knowledge on radioresistance of brain tumors, increasing evidence has been provided on the interactions of certain growth factor receptors and cell adhesion molecules, especially ErbB1 and integrin β1, also in cancer stem cells that constitute only the minority of the whole tumor. The integrin β1 mediated PI-3K / Akt-PKB signaling was also shown to be critically involved in glioma cell adhesion and prolonged cell survival [200]. Moreover, most recent findings highlighted integrin β1 inhibitors as potentially promising radiosensitizers for glioblastoma *in vitro* [201, 202].

Accordingly, interactions of ErbB1 and integrin β1 could play an important role in the development of increased radioresistance and may present a novel therapeutic target. The importance of these interactions has so far been raised on the basis of *in vitro* and *xenograft* models. However, expression profiles and molecular associations of ErbB and integrin molecules may differ on individual human glioblastoma tumors *in situ*, which may prejudice treatment and patient outcome. As developing FRET techniques now potentially enable the characterization of molecular interactions in tissue sections [107, 108], the quantitation of specific molecular interactions and downstream signaling on individual clinical tumor samples *in situ* may allow for discerning prognostically diverse patient subgroups and finding optimal combinations of therapies [109, 110].

4. OBJECTIVES

Based on recent emerging findings on the importance of integrins in ErbB2-mediated transmembrane signaling, we first set out to demonstrate the interaction of ErbB2 and integrin β1 proteins and to compare the functional significance of this interaction in trastuzumab sensitive and resistant cell lines. We aimed

- to determine the molecular interactions of ErbB2 and integrin β1 on ErbB2 positive tumor cell lines and
- to compare the expression patterns and the degree of homo- and heteroassociation of ErbB2 and integrin β1 molecules on trastuzumab sensitive and resistant cell lines.

As molecular interactions can be influenced by other neighboring proteins - especially at signaling membrane platforms (lipid rafts) harboring multimolecular complexes - we proposed to establish a new method, two-sided FRET, to characterize multimolecular interactions

- to measure the relationship between the association states of two molecule-pairs of three arbitrarily chosen molecular species and
- to untangle the correlation of ErbB2 homoassociation and ErbB2 - integrin β1 heteroassociation on trastuzumab sensitive and resistant cell lines.

Given the critical contribution of integrins to growth factor downstream signaling in glioma cell survival and adhesion, we set out to characterize the interaction of these proteins in clinical samples and cellular models of glioma. We wished

- to determine the extent and molecular background of chr7 or erbB1 gene gain-related radiation resistance of U251-derived astrocytoma subclones,
- to assess the contribution of ErbB1 overexpression and ErbB1 interaction with integrins to radioresistance on erbB1 gene transfected astrocytoma cell lines and
- to quantitate *in situ* the molecular interactions of ErbB1 and integrin β1 molecules on fresh frozen intraoperative astrocytoma sections and correlate findings with clinical data as well as with results from the *in vitro* model system.

5. MATERIALS AND METHODS

5.1. Antibodies

Monoclonal antibodies 528 (Mab 528) against ErbB1, TS2 against integrin β1, L368 against β2-microglobulin, W6/32 against HLA-A,B,C and Hermes3 against CD44 were purified from supernatants produced by the hybridoma cell lines 528 (IgG2a, #HB-8509), TS2/16.2.1 (IgG1, #HB-243), L368 ($IgG1_{\kappa}$, #HB-149), W6/32 (IgG_{2a}, #HB-95) and Hermes3 (IgG2a, #HB-9480) (ATCC, Manassas, VA, USA), respectively, using Sepharose 4B Fast Flow Protein G beads in the case of IgG2a antibodies or protein A beads in the case of IgG1 antibodies (Sigma-Aldrich, St. Louis, MO, USA). Against the ErbB2 molecule, 2C4, 7C2 (a gift from Genentech Inc., South San Francisco, CA), trastuzumab (Hoffman-La Roche AG, Germany) and their Fab' fragments were used. ErbB3 and ErbB4 were targeted with the H3.90.6 (against ErbB3) and 72.8 or 77.16 (against ErbB4) (NeoMarkers, Lab Vision Corporation, Fremont, CA). The monoclonal antibodies anti-CD29/integrin β1, anti-CD104/integrin β4, anti-ITGB5/integrin β5 (Sigma, St. Louis, MO and Research Diagnostics Inc., Flanders, NJ), anti-CD61/integrin β3 (Dako-Cytomation, Carpinteria, CA), anti-CD49a/integrin α1, anti-CD49b/integrin α2, anti-CD49d/integrin α4, anti-CD49f/integrin α6, anti-CD51/integrin αV (Research Diagnostics Inc., Flanders, NJ) were used for labeling members of the integrin family. Cy3- and Cy5-conjugated goat anti-mouse antibodies (GaMIg) and Fab' fragments (Jackson ImmunoResearch, West Grove, PA) were used for indirect secondary labeling of unconjugated primary antibodies. The monoclonal antibody MEM75 against transferrin receptor was a gift from Vaclav Horejsi (Institute of Molecular Genetics, Academy of Sciences, Prague, Czech Republic).

Labeling of antibodies with Cy3 and Cy5 mono-reactive sulfoindocyanine N-hydroxysuccinimidyl esters (Amersham Biosciences Europe, Freiburg, Germany), Alexa Fluor® 546, Alexa Fluor® 555, Alexa Fluor® 647 monosuccinimidyl-esters and X-fluorescein-isothiocyanate (XFITC) (Molecular Probes, Invitrogen Corp., CA) was carried out according to the manufacturers' specifications. The dye to protein labeling ratio determined by spectrophotometry was in the range of 2:1 - 3:1 and 1:1 in the case of whole IgGs and Fab's, respectively.

5.2. Labeling of cells with antibodies

For flow cytometric measurements, cells were trypsinized and resuspended at 1 x 10^6 cells in 50 µl PBS supplemented with 0.1 % bovine serum albumin (BSA). Labeling was done with saturating concentrations (10–20 µg/ml) of AlexaFluor 546 and/or AlexaFluor 647-conjugated antibodies on ice (4°C) for 30 minutes, then cells were washed three times in PBS and fixed in 500 µl of 1% formaldehyde solution in PBS.

For microscopic measurements, medium was discharged and adherent cells were washed three times in PBS. After labeling with saturating concentrations of X-FITC, Cy3, Alexa555 or Cy5-conjugated antibodies (alone or in mixture) on ice for 30 minutes cells were washed three times in PBS and fixed in 500 µl of 4% formaldehyde-PBS for 20 minutes. Coverslips were mounted in glycerol or in Mowiol 4-88 reagent (#475904, Calbiochem, Merck KGaA, Darmstadt, Germany) onto precleaned silanized microscopic slides, whereas samples on chambered coverglasses were measured under 500 µl of 1% formaldehyde solution in PBS.

Lipid rafts were labeled with 8 µg/ml Alexa488- or Cy5-labeled subunit B of cholera toxin (Alexa488-CTX: Sigma, St. Louis, MO; Cy5-CTX: Molecular Probes, Eugene, OR) for 30 minutes on ice. For cross-linking of lipid rafts, incubation with CTX-B was carried out at 37°C for 30 minutes. Cross-linking of integrins β1 was done using secondary antibodies at 37ºC for 30 minutes after labeling with primary anti-integrin β1 antibodies. After cross-linking, samples were placed on ice for 15 minutes before continuing the labeling protocol.

5.3. Cell cultures

The breast cancer cell lines SK-BR-3 (#HTB-30, American Type Culture Collection (ATCC) Manassas, VA, USA) and JIMT-1 (from Jorma Isola, University of Tampere, Tampere, Finland), and the gastric adenocarcinoma cell lines MKN-7 (Immuno-Biological Laboratories Cell Bank, Gunma, Japan) and NCI-N87 (#CRL-5822, ATCC) were grown to subconfluence according to their specifications.

The parental U251 NCI cell line (National Cancer Institute, Bethesda, MD - hereafter U251) was grown to subconfluence in MEM EBSS + 10% FCS + Non Essential Amino Acids at 37°C, in 5% CO2 [203]. Previously, subclones of the U251 parental line were established by transferring extra chr7 pieces (carrying the erbB1 gene) into them through fusion with microcells made from mouse A9 hybrids of human chr7 [204]. We used a set of U251 subclones – c5, c9, and c55 – with increasing amounts of chr7 along with parallel increasing radioresistance [205]. As a control line, the U251 Hyg+ subclone was used that did not carry

extra chr7, but also expressed the hph gene product confering resistance to hygromycin B that was used at 0.4 mg/ml to maintain selection pressure. After reaching subconfluence, cells were harvested by trypsinization for flow cytometric experiments or subcultured on 12 mm diameter coverslips or on Lab-Tek II chambered coverglass for microscopic experiments (Nalge Nunc International, Rochester, NY, USA).

5.4. Fresh frozen sections

Intraoperative tumor samples were stored at -80 ºC in the Brain Tumor and Tissue Bank of the Department of Neurosurgery, Medical Health Science Center, University of Debrecen with permission of the Regional Ethical Committee and the National Research Ethical Committee. Each patient signed an informed consent form prior to surgery. Histological classification of the tumors was done as part of the routine clinical pathology process at the Department of Pathology, Medical Health Science Center, University of Debrecen. In our study, we used samples immediately adjacent to the region that were used for the histopathological diagnosis. They were collected during the surgical intervention and were snap-frozen in isopentane (Sigma-Aldrich, St. Louis, MO) cooled in liquid N_2. After embedding in Tissue-Tek O.C.T. (Sakura Finetek, Torrance, CA), 15 μm thick sections were cut by a cryostat-microtome system (Shandon Cryotome, AS-0620E, Thermo Fisher Scientific Inc., Waltham, MA) at -20 ºC. Sections were placed onto precleaned silanized slides and then dried, fixed in 4% formaldehyde solution in PBS for 30 minutes and blocked in 1% BSA solution in PBS for 30 minutes. Labeling was performed with 20 μg/ml Cy3-528 (anti-ErbB1) and 20 μg/ml Cy5-TS2 (anti-integrin β1) antibody overnight in a wet chamber at 4 ºC, then cells were washed three times and mounted in glycerol.

5.5. Cellular Model Systems

5.5.1. Chromosome 7 transferred U251 NCI subclones

Earlier it has been shown that gain of chr7 material in glioblastoma is associated with radiation resistance [205], which coincides with independent findings that ErbB1 overexpression is associated with decreased radiosensitivity [179] and with the fact that the erbB1 gene (coding for ErbB1) is located on chr7p.

To reveal the extent and molecular mechanisms of chr7 gain-related radiation resistance attributable to disturbed signaling by ErbB1, we used U251 NCI subclones transferred with extra chr7 pieces through fusions of these cells with microcells made from mouse A9 hybrids of human chr7 [204]. The U251 NCI cell line was established from a grade IV astrocytoma (glioblastoma multiforme) and the parental cell line was shown to be considerably sensitive to X-ray radiation. Subclones that acquired pieces of 7p together with proximal 7q were radiation resistant, whereas those that acquired smaller pieces of distal 7q remained more sensitive.

We used a set of U251 fusions – c5, c9, c55 – to explore the mechanisms behind radiation resistance through the evaluation of cell surface expression levels of, interactions between, and downstream signaling by ErbB1 and integrin β1 molecules. The clones c5, c9, c55 were derived from the parental U251 NCI cell line by transferring increasing amount of extra chr7, respectively. The U251 Hyg+ clone was used as a control line, carrying no chr7 pieces but also expressing the hph gene product (phosphotransferase) that confers resistance to hygromycin B (aminoglycoside antibiotics) used to maintain selection pressure on the chromosome-transferred clones. Thus, all compared lines could be grown under equivalent conditions, in MEM EBSS + 10% FCS + Non Essential Amino Acids supplemented with 400 μg/ml Hygromycin B at 37°C, in 5% CO_2. The radiosensitivity of this set (U251 parental, c5, c9 and c55) was characterized previously in agar colony forming assay (LD_{50} values of 4, 4.7, 5, and 5.7 Gy, respectively) at our collaborating institute (Barrow Neurological Institute / St. Joseph's Hospital and Medical Center, Phoenix, AZ, USA).

5.5.2. Stable erbB1 gene transfected U251 NCI subclones

To confine the results to the clear effect of ErbB1 overexpression to radiation resistance, in order to differentiate from the regulatory effect of other genes coded on chr7p, U251 transfectant sublines that express various amounts of extra ErbB1 were generated. The erbB1 gene in the plasmid pCDNA3, carrying geneticin resistance (a kind gift from Yosef Yarden, Weizmann Inst. of Science), was introduced by electroporation using the nucleofector device of Amaxa (Cologne, Germany) with solution V and protocol T-20 [206]. The functionality of this expression vector was demonstrated in preceding experiments with transfecting eGFP-ErbB1 fusion protein (GFP reporter fused C-terminally to the ErbB1) into CHO (Chinese Hamster Ovarian) cells ordinarily not expressing ErbB1. Proper membrane expression and EGF-induced autophosphorylation of this tagged receptor, as well as calcium transients could be detected in these confirmatory experiments.

U251 cells transfected with erbB1 were selected with 0.4 mg/ml geneticin, and sorted in a FACSVantage SE with DiVa option (Becton Dickinson, Franklin Lakes, NJ) into subclones of low, medium and high ErbB1 expressors. Further cultivation under selection pressure resulted in the splitting of the medium expressor population, yielding subpopulations similar to the low and high expressors. Furthermore, in spite of selection pressure, a subset of the high ErbB1 expressors gradually drifted to low expression, and thus flow cytometric sorting had to be repeated several times. Eventually, a low ErbB1 (~150 thousand copies per cell, U251 E1L) and a high ErbB1 (~1 million copies per cell, U251 E1H) transfectant subclone was created and stocked, which could be reliably used as a stable expression system under selection pressure for 3-4 passages.

5.6. Determination of radiosensitivity

We estimated the radiosensitivity of the transfectant U251 subclones both in conventional proliferation assay using EZ4U (colorimetric indicator of mitochondrial activity) (Biomedica, Budapest, Hungary), and in colony forming analysis after exposure to 0, 2, 4, 6 and 8 Grays of ^{60}Co γ-irradiation. Aliquots of parental U251 and U251 E1L were also treated with 20 nM wortmannin (Sigma-Aldrich, St. Louis, MO) starting 1 hour before 2 Gy irradiation. Six replicates of 200 single cells of each subline were cultured and incubated until attachment in a flat bottom 96-well plate, and irradiated through indicator-free DMEM medium. To minimize radiation scattering, plates were submerged into water bath and irradiating doses were corrected for the absorbance of the thickness of the liquid layer. Cells were stained with methylene-blue (0.2% w/v in 70% ethanol) seven days after irradiation and colonies were counted in a Nikon Eclipse TS100 (Nikon Instruments, Inc., Melville, NY) microscope. Alternatively, colony clusters were contoured and counted in an imaging cytometer (CompuCyte Corp, Cambridge, MA, USA) using 633 nm transmission imaging. Surviving fractions were calculated and normalized according to the following equation

$$SF(D) = \frac{\text{Colonies Counted}}{\text{Number of Cells Plated} \cdot PE_{D_0}} \qquad \text{(Eq.1.)}$$

where PE_{D_0} denotes the plating efficieny of non-irradiated cells as follows:

$$PE_{D_0} = \left[\frac{\text{Colonies Counted}}{\text{Number of Cells Plated}} \right]_{Dose=0} \qquad \text{(Eq.2.)}$$

Survival curves were fit and plotted using the Linear Quadratic Model with Sigmaplot v10.0 (Systat Software, Inc., Chicago, IL) according to Eq. 3.

$$S(D) = e^{-(\alpha \cdot D + \beta \cdot D^2)} \quad \text{(Eq.3.)}$$

where D indicates the irradiation dose, α (Gy^{-1}) means the initial slope of the survival curve characterizing the direct action of single ionizing events causing DNA double strand breaks, and β (Gy^{-2}) represents the quadratic component of cell killing describing the sublethal DNA damage (i.e. single strand breaks) that can be restored.

5.7. Flow cytometric determination of cell surface receptor expressions

Evaluation of receptor expression was carried out on a FACSVantage SE with DiVa option (Becton Dickinson, Franklin Lakes, NJ) using the FL-6 channel (excitation at 633 nm, detection through a 650 nm long pass filter) in linear mode after labeling with respective Alexa-647 conjugated antibodies. The background corrected mean of histograms from 20,000 events was converted to antigen numbers using QIFIKIT (DakoCytomation, Glostrup, Denmark) according to the manufacturer's instructions. Unconjugated primary antibodies were detected with AlexaFluor 647 conjugated goat-anti-mouse (H+L) secondary antibodies (Molecular Probes, Invitrogen Corp., CA).

5.8. Assessing the molecular interactions of ErbB and integrin molecules

5.8.1. Fluorescence resonance energy transfer (FRET)

Measuring FRET is one of the best methods for evaluating molecular interactions, which is sensitive for estimating intra- or intermolecular distances and enable to resolve molecular associations and conformational changes in the 1-10 nm range. Let us consider a system with two different fluorophores in which the molecule with higher energy absorption is defined as the donor (D) and the one with lower energy absorption is defined as the acceptor (A). If the donor is in the excited state, it will lose energy by internal conversion until it reaches the ground vibrational level of the first excited state. If the donor emission energies overlap with the acceptor absorption energies, through weak coupling, the following resonance can occur:

$$D^* + A \Leftrightarrow D + A^* \quad \text{(Eq.4.)}$$

where D and A denote the donor and the acceptor molecules in ground state, and D^* and A^* denote the first excited states of the fluorophores (see section 2.5.) [104].

According to the theory of Förster, the rate (k_T) and efficiency (E) of energy transfer can be estimated as:

$$k_T = const * J * n^{-4} * R^{-6} * \kappa^2 \quad \text{(Eq.5.)}$$

$$E = \frac{k_T}{k_T + k_F + k_D} \quad \text{(Eq.6.)}$$

where k_F is the rate constant of fluorescence emission of the donor and k_D is the sum of the rate constants of all other excitation processes of the donor. R is the separation distance between the donor and acceptor molecules, and κ^2 is an orientation factor, which is a function of the relative orientation of the donor's emission dipole and the acceptor's absorption dipole. Other parameters are n, the refractive index of the medium, and J, the spectral overlap integral, which is proportional to the overlap in the emission spectrum of the donor and the absorption spectrum of the acceptor [104].

5.8.2. Flow cytometric fluorescence resonance energy transfer measurements (FCET)

To determine the homo-, and heteroassociation states of the labeled receptors, FCET measurements were performed either on the FACSVantage SE instrument with DiVa option equipped with 488, 532 and 633 nm lasers or on a FACSArray bioanalyzer (Becton Dickinson) equipped with 532 and 635 nm lasers.

In experiments on the FACSVantage SE instrument, the FRET efficiencies were calculated with cell-by-cell correction for autofluorescence [90]. The distribution of cells in forward and side scattering channels was used for discarding debris and dead cells. The cellular autofluorescence was measured in the FL1 channel (excited by the 488 nm laser) through a 530/30 nm band pass filter. Donor intensities were recorded in the FL4 channel through a 585/42 nm bandpass filter, while acceptor and sensitized acceptor intensities were detected in FL6 and FL5 channels, respectively, through 650 nm long pass filters. The donor (Alexa546) and acceptor (Alexa647) molecules were excited by the 532 and 633 nm laser lines, respectively.

In measurements on the FACSArray bioanalyzer the donor intensities (excited by the 532 nm laser) were recorded in the Yellow channel through a 585/42 nm bandpass filter, while the acceptor and sensitized acceptor intensities were excited by the 633 nm and the 532 nm lasers, respectively, and were detected in the Red and Far-Red channels through a 661/16 nm

bandpass and a 685 nm long pass filter, respectively. List mode data were stored in FCS 3.0 file format. Calculation of cell-by-cell FRET efficiency was carried out using the software REFLEX with correction for autofluorescence [207]. FRET efficiencies are presented as mean values - indicating the standard error of the mean - of approximately normally distributed, unimodal FRET histograms of 20,000 cells.

Illustrative representation of characteristic FRET histograms of ErbB1 homoassociations and ErbB1 – integrin β1 heteroassociations are shown in Figure 9.

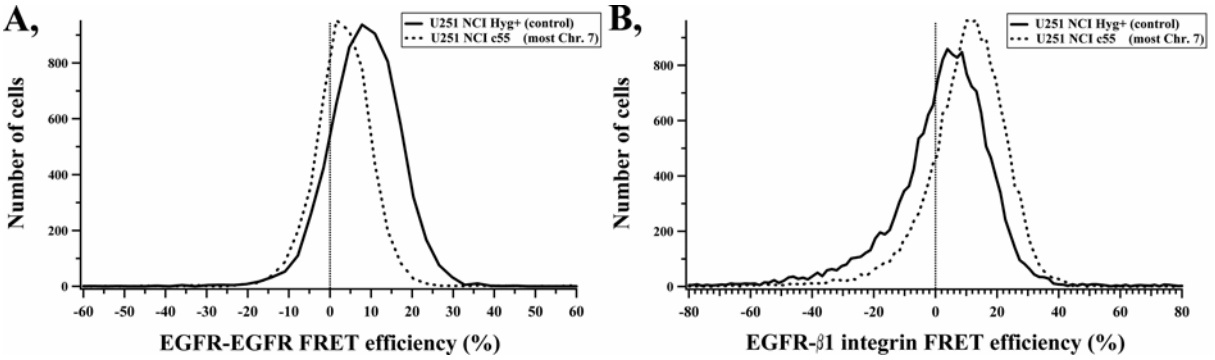

Figure 9. FCET measurements were performed on U251 NCI clones. Characteristic FRET histograms of ErbB1 (EGFR) homoassociation (A) and ErbB1 – integrin β1 heteroassociation (B) are shown in the most radiosensitive U251 NCI Hyg+ control line and in the most radioresistant U251 NCI c55 line, which latter bears the most extra chr7 material.

5.8.3. Confocal microscopy

For microscopic imaging of cells, we used a Zeiss LSM 510 confocal laser-scanning microscope (CLSM, Carl Zeiss AG, Jena, Germany) equipped with a Plan-Apochromat 63×/1.40 NA oil immersion objective and an UV/488/543/633 beam splitter. X-FITC, Cy3 and Cy5 fluorophores were excited at 488, 543 and 633 nm (argon ion and He-Ne lasers) and detected through 505-535 nm and 560–605 nm bandpass, and 650 nm longpass filters, respectively. Cells were imaged in horizontal, 1 - 3 μm thick, 4-times averaged optical sections (512 x 512 pixels at 12 bit) using 2.51 μs pixel dwell time and 3× zoom (100 nm per pixel, 2 times oversampling) in frame mode. Before abFRET measurements, we determined the optimal time for bleaching the Cy5 fluorescence to less than 20 percent of the initial value. Expression levels of proteins on fresh frozen astrocytoma tissue sections were imaged in tile mode that enabled the observation of broad tissue areas, while maintained the high resolution and confocality, as well. Images were acquired in multi-track mode to avoid crosstalk between channels. The alignment of detection channels was regularly checked with samples of FocalCheck fluorescent microspheres (Molecular Probes, Invitrogen Corp., CA).

5.8.4. Calculation of molecular colocalization

Image cross-correlation values (*C*), describing the colocalization between two different molecules labeled with fluorescent dye conjugated antibodies was calculated according to Pearson's formula:

$$C = \frac{\sum_i (S1_i - S1_{aver})(S2_i - S2_{aver})}{\sqrt{\sum_i (S1_i - S1_{aver})^2 \sum_i (S2_i - S2_{aver})^2}} \qquad \text{(Eq.7.)}$$

where $S1_i$ and $S2_i$ are the intensities of the ith pixel in the first and second images, respectively, $S1_{aver}$ and $S2_{aver}$ are the average fluorescence intensities of the first and second images, respectively. Low intensity pixels were excluded from the analysis. The value of the cross-correlation coefficient (*C*) can range from +1 to -1. Values close to 1, 0 and -1 indicate high (1) and low (0) degree of colocalization, and anticorrelation (-1), respectively. *C* values were computed using the Zeiss LSM v3.2 software or a home-made software written in LabView (National Instruments, Austin, TX) [208].

5.8.5. Acceptor photobleaching method (abFRET)

While flow cytometric FRET is reliable and has good cellular statistic power, it is not applicable to assessing *in situ* interactions of molecules on adherent cells (such as glioblastoma lines are), which probably has increased importance in the case of looking at cell adhesion molecules such as integrin β1. Furthermore, in the case of tissue samples obtained during brain tumor surgery, FCET is also of little use. Thus, a microscopic method needs to be applied to measure FRET in adherent cells and tissues.

A quick and simple method is based on irreversibly destroying the acceptor fluorophore by photobleaching it and thereby de-quenching the donor molecule [209]. FRET efficiency (*E*) in each pixel can be measured using this protocol [210] and is calculated as follows:

$$E = 1 - \frac{F^B_{D_{(i,j)}} - S_4^{avr} * F^B_{A(i,j)}}{\gamma^{avr} * F^A_{D_{(i,j)}}} \qquad \text{(Eq.8.)}$$

where $F^B_{D_{(i,j)}}$ and $F^A_{D_{(i,j)}}$ are the background subtracted donor fluorescence values before (B) and after (A) photobleaching the acceptor, respectively, and $F^B_{A(i,j)}$ denotes the background subtracted acceptor fluorescence value of pixel (i,j) before photobleaching the acceptor.

γ^{avr} is a factor correcting for the photobleaching of the donor during the whole protocol, calculated as the median of

$$\gamma_{(i,j)} = \frac{F_{D_{(i,j)}}^{ref_D,B}}{F_{D_{(i,j)}}^{ref_D,A}} \quad \text{(Eq.9.)}$$

where $F_{D_{(i,j)}}^{ref_D,B}$ and $F_{D_{(i,j)}}^{ref_D,A}$ are the background subtracted donor intensities in pixels (i, j) before (B) and after (A), respectively, running an identical acceptor photobleaching protocol on a reference sample labeled with donor only (ref_D) [210]. S_4^{avr} is also a correction factor compensating for the crosstalk of the acceptor label into the donor channel. It is the median of

$$S_{4_{(i,j)}} = \frac{F_{D_{(i,j)}}^{ref_A}}{F_{A_{(i,j)}}^{ref_A}} \quad \text{(Eq.10.)}$$

where $F_{D_{(i,j)}}^{ref_A}$ and $F_{A_{(i,j)}}^{ref_A}$ are the background subtracted donor (D) and acceptor (A) intensities in pixels (i, j) of a reference sample labeled with acceptor only (ref_A). Correction for incomplete acceptor bleaching was not necessary, because samples with less than 80% depletion of the acceptor were not evaluated. Control experiments revealed that calculated FRET values showed negligible dependence on the extent of acceptor bleaching, if at least 80% of the acceptor was bleached (see Fig. 10).

The measurement protocol was implemented on an LSM 510 confocal laser scanning microscope (CLSM, Carl Zeiss AG, Jena, Germany) equipped with a Plan-Apochromat 63×/1.40NA oil immersion objective and an UV/488/543/633 beam splitter. Adherent U251 NCI clone cells were washed three times in PBS, labeled with saturating concentrations of Alexa555 (donor) – and/or Cy5 (acceptor)-conjugated antibodies on ice for 30 min, then washed three times in PBS and fixed in 500 µl of 4% formaldehyde solution in PBS for 20 min. Coverslips were mounted in glycerol onto precleaned microscopic slides. Alexa555 and Cy5 fluorophores were excited at 543 and 633 nm and detected through 560–605 nm bandpass and 650 nm longpass filters, respectively. Horizontal, 1 - 3 µm thick, 4-times averaged optical sections (512 x 512 pixels at 12 bit) were taken of either the top or bottom flat layer of the cell membrane using 2.51 µs pixel dwell time and 3× zoom (100 nm per pixel, 2 times oversampling) in frame mode. Before abFRET measurements, the optimal bleaching time for reducing Cy5 fluorescence to less than 20% of the prebleach value was determined.

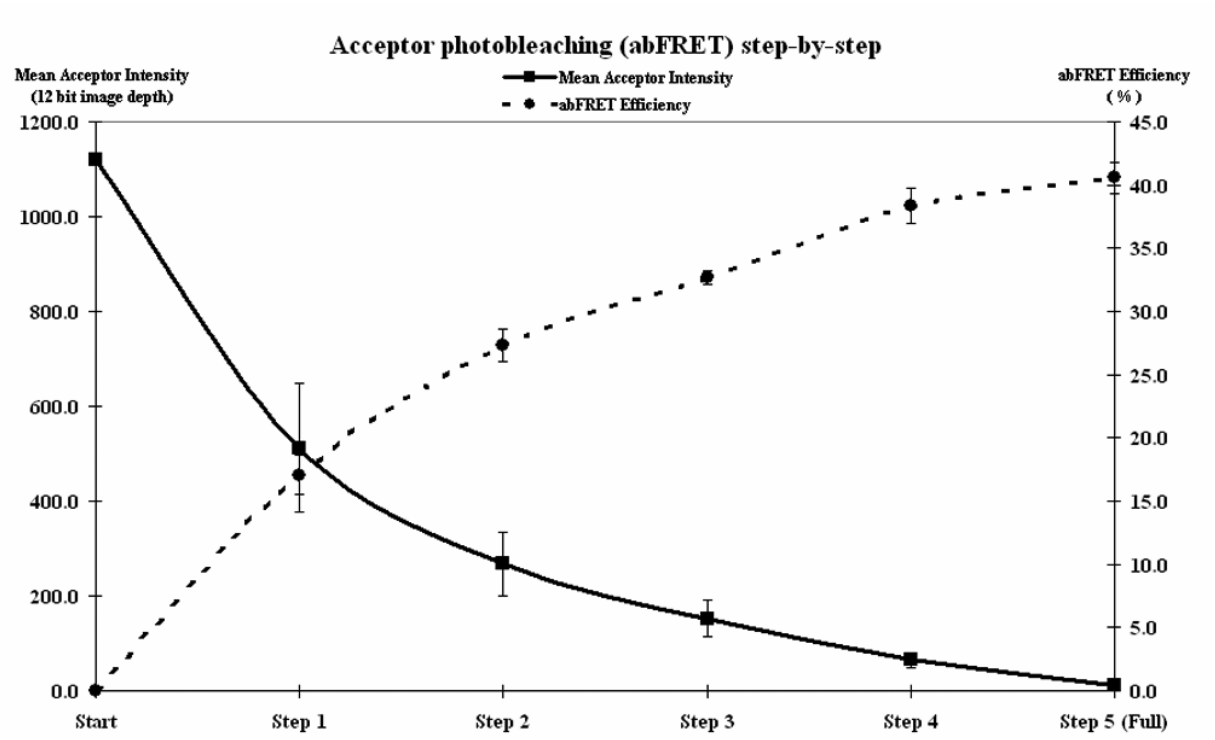

Figure 10. Dependence of abFRET efficiency on the bleaching time and hence the retained acceptor intensity in confocal microscopic abFRET measurements.

Images were acquired in multi-track mode to avoid crosstalk between channels. The alignment of detection channels was regularly checked with samples of FocalCheck fluorescent microspheres (Molecular Probes, Invitrogen Corp., CA, USA). A custom C algorithm was written and used in SCIL Image (TNO, Institute of Applied Physics, Delft, The Netherlands [211]) and an also custom written ImageJ plugin AccPbFRET [212] was used to evaluate image sequences and calculate average FRET efficiency after background subtraction, correction for shift and Gauss filtering for pixels above threshold in each frame, usually containing 2–5 cells. Output results were stored in standard image cytometry data (ICS 1.0) format [213]. Representative illustration of images obtained in abFRET measurements can be seen on Fig. 11.

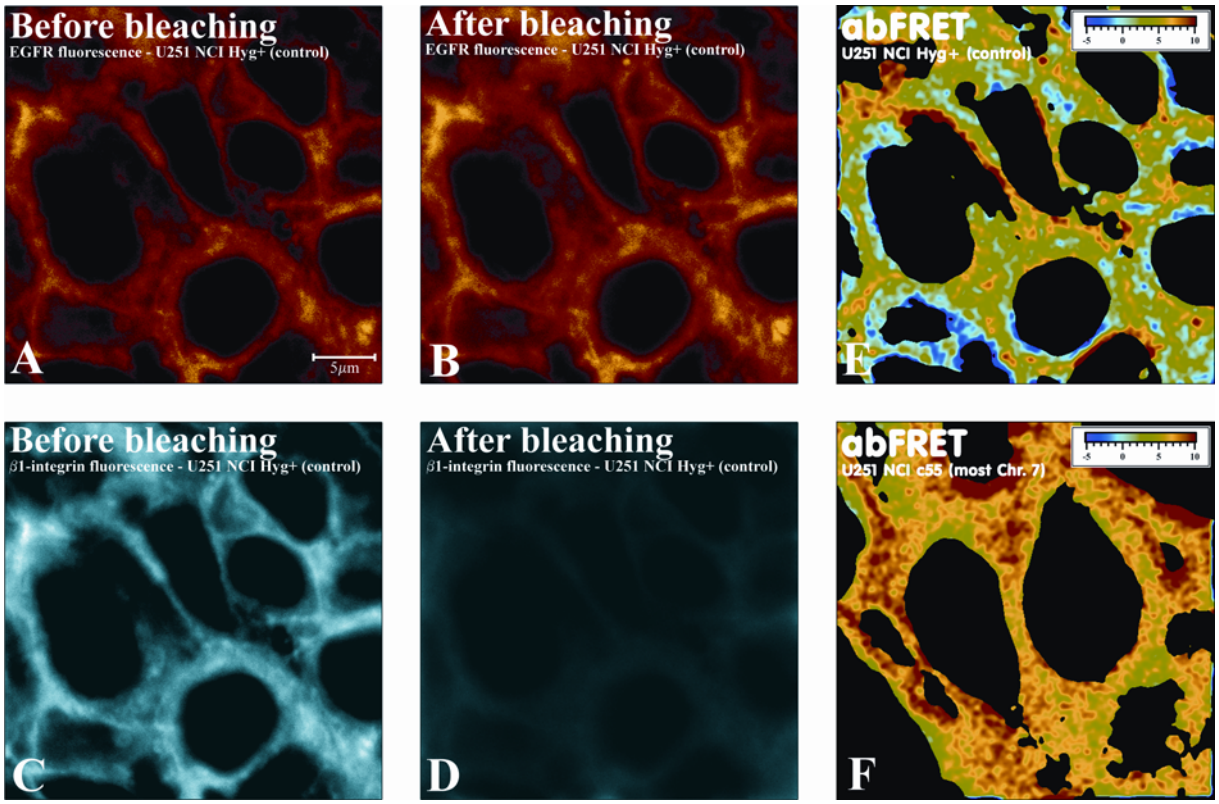

Figure 11. Representative images of abFRET measurements.

Microscopic abFRET measurements were performed on U251 NCI clones. Images of ErbB1 (EGFR) fluorescence, serving as a donor and integrin β1 fluorescence, serving as an acceptor in the protocol, are displayed before photobleaching (A and C) and after photobleaching (B and D), respectively. The false color abFRET images of ErbB1 – integrin β1 heteroassociation are shown on U251 NCI Hyg+ (E) and on U251 NCI c55 (F) clones.

5.8.6. Donor photobleaching method (dbFRET)

The dbFRET method was introduced by Jovin and Arndt-Jovin in 1989 [214]. The procedure is based on quenching the donor fluorescence (XFITC) in the presence and the absence of an acceptor fluorophor (Cy3) and calculating the dbFRET efficiency from the change of the donor photobleaching kinetics. In these experiments the specimens were bleached by acquiring 40-50 images as time series using the 488 nm Ar-ion laser at high (20-40%) power. Images were median or low-pass filtered (3x3 kernel, LSM v 3.2 software), and fit pixel-by-pixel after thresholding by the dbFRET software [215], yielding images of time constants describing the photobleaching kinetics of the donor (Fig. 12). Assuming that the donor photobleaching occurs from the excited singlet state, it can be derived, that:

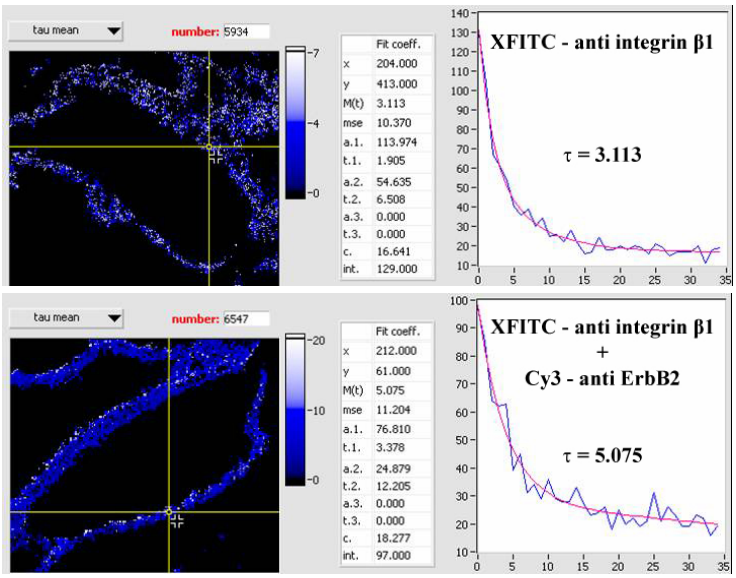

$$E = 1 - \frac{\overline{\tau}_{ble}}{\tau^{A}_{ble}} \qquad \text{(Eq.11.)}$$

Figure 12. Representative images of a dbFRET experiment between ErbB2 and integrin β1 molecules. Distribution of the time constant in the absence (τ_{ble}, upper) and the presence (τ_{ble}^{A}, lower) of the acceptor (Cy3-anti ErbB2 antibody), and the photobleaching kinetics of the donor (XFITC-anti integrin β1) in the marked pixels (yellow cross on the image) are displayed. Energy transfer efficiency is calculated according to Eq.11.

where *E* denotes the FRET efficiency, τ_{ble} and τ_{ble}^{A} are the photobleaching time constants in the absence and the presence of the acceptor, respectively. The τ_{ble}^{A} images were converted to *E* images according to (Eq.11.) using the corresponding mean τ_{ble} value as constant. The output *E* maps were visualized in false color images.

5.9. Stimulation of cells with EGF, heregulin and trastuzumab

Cells were treated with 50 ng/mL EGF (R&D Systems, Minneapolis, MN, USA), 50 ng/mL β1-heregulin (R&D Systems) or 50 μg/mL trastuzumab (Herceptin®) on coverslips or in suspension for 30 minutes in a CO_2 incubator in serum-free medium followed by washing three times in PBS and labeling with fluorescent dye conjugated antibodies according to the previous sections.

5.10. Western blot analysis

To assess the activation of the ErbB2 molecule in experiments on breast cancer lines or that of the PI-3K/Akt-PKB survival pathway in experiments on U251 astrocytoma subclones, we performed Western blot analysis on ErbB2, p-ErbB2 and Akt, p-Akt proteins, respectively. As activation of signaling pathways can vastly depend on their initial equilibrium, both serum-starved and serum-fed cells were tested. Cells were serum starved overnight in SFM and then treated with EGF or trastuzumab, or undergone cross-linking experiments as described previously. PBS-washed cell pellets were solubilized in 5x SDS-sample buffer, sonicated, centrifuged at 16,000x g for 5 min, and supernatants were subjected to standard SDS-PAGE (7% gel) followed by ECL-visualized, peroxidase-based immunoblotting. Akt, pAkt (Upstate/Millipore, Billerica, MA) and cErbB2 (Ab3-OP15, Calbiochem-Merck Biosciences, Schwalbach, Germany), pErbB2 (PY99-sc7020, Santa Cruz Biotechnology, Santa Cruz, CA) was detected with specific antibodies and as loading control, β-actin (AC40, Sigma-Aldrich) was used. For each lane, signal intensities of the specific bands were quantified by densitometry, corrected for background, and normalized to β-actin.

5.11. Statistical analysis

Data analysis was achieved with SigmaStat version 3.5.0.54 (Systat Software, Inc.). Parameters of Grade II and IV astrocytic tumor groups were compared with Student's t-test or upon lack of normality with Mann-Whitney rank sum tests after checking normality according to Kolmogorov-Smirnov with Lilliefors' correction. Normally distributed variables of more than two classes were compared using ANOVA, followed by Tukey's post hoc test. Predicting power of ErbB1 and integrin β1 expression, and ErbB1 – integrin β1 heteroassociation on survival and recurrence time was assessed by stepwise forward multiple regression, and on the grade of tumor by stepwise multiple binary logistic regression. Overall and relapse-free survival were analyzed by the Kaplan-Meier method comparing Grade II against grade IV tumors, as well as pairs of groups created by splitting the whole cohort into below and above average values of ErbB1 or integrin β1 expression or ErbB1 – integrin β1 heteroassociation. Patients enrolled later than the start of the observation time and still alive at the end of the study were censored from further analysis at their survival time point. Those undergone incomplete tumor resection were also censored in the analysis of relapse-free survival. Statistical comparison and the estimation of p were done with the log-rank test followed by pairwise multiple comparison *post-hoc* Holm-Sidak methods.

6. RESULTS

6.1. Interactions of ErbBs and integrin β1 on breast and gastric cancer cell lines

6.1.1. Lower ErbB2 expression is accompanied by higher integrin β1 levels

Since membrane protein associations depend on their relative densities, we first characterized the expression levels of ErbB1-4 proteins, as well as integrins β1-, β3- and α6 in trastuzumab resistant and sensitive cell lines by flow cytometry (Table I). Trastuzumab resistant cell lines showed lower ErbB2 and higher integrin β1 expression levels. The trastuzumab resistant JIMT-1 line displayed an extremely high integrin β1 level, whereas its trastuzumab sensitive counterpart, the SK-BR-3 cell line, had the lowest expression level. Expression levels of other ErbB and integrin molecules revealed no characteristic differences among the sensitive and resistant cell lines.

Table I. Number of ErbB and integrin molecules on the cell lines studied.[1]

	SK-BR-3[2]	JIMT-1[3]	N87[2]	MKN-7[3]
ErbB-1	130,000	92,000	50,000	100,000
ErbB-2	800,000	112,000	1,200,000	500,000
ErbB-3	30,000	30,000	17,000	30,000
ErbB-4	70,000	20,000	40,000	60,000
integrin β1	81,000	2,460,000	122,000	566,000
integrin α6	15,000	50,000	30,000	20,000
integrin β3	70,000	n.d.	15,000	40,000

[1]Number of ErbB molecules and integrins were determined from flow cytometric measurements taking the ErbB2 expression level of SK-BR-3 cells as a standard.

[2]Trastuzumab sensitive cell line

[3]Trastuzumab resistant cell line

n.d.=not determined

6.1.2. Colocalization of ErbB2, integrin β1 and lipid rafts upon treatments

Given the important role played by the association between ErbB2 and integrin β1 in malignant cells [96] and the altered local environment of ErbB2 in the trastuzumab resistant JIMT-1 cell line [149], a different interaction in the ErbB2-integrin axis between trastuzumab sensitive and resistant cells seemed reasonable to assume. To quantitatively compare the cell lines, cross-correlation coefficients between ErbB2 and integrin β1 were calculated from confocal images of adherent cells (Fig. 13).

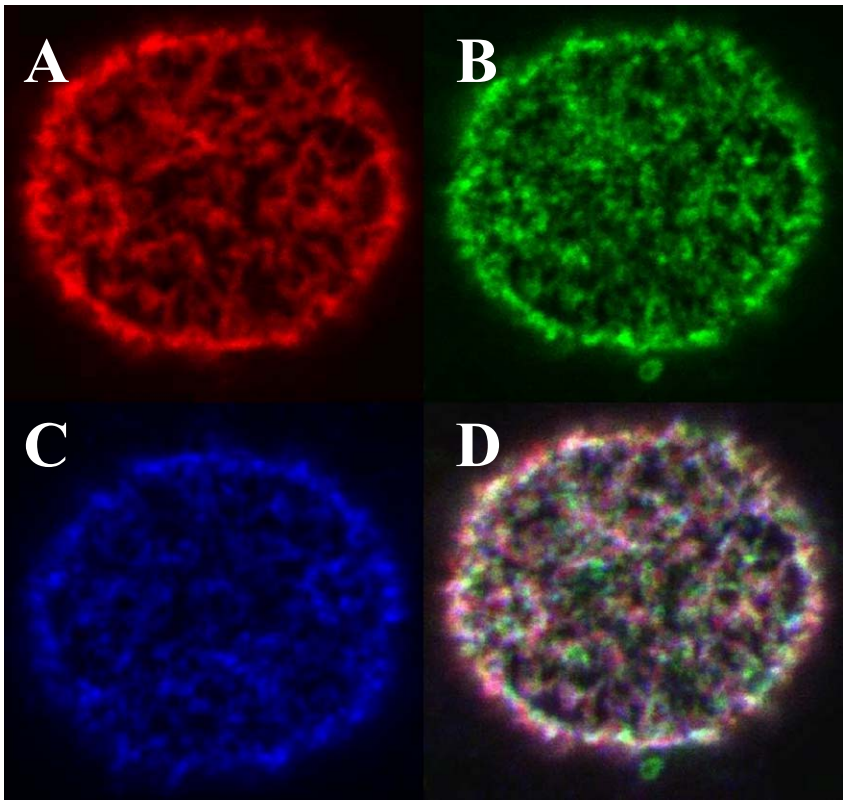

Fig. 13. Triple colocalization. Confocal images of an N87 cell showing the distribution of ErbB2 (Cy3-2C4) (A), lipid rafts (Alexa488-CTX-B) (B) and integrin β1 (anti-CD29 + secondary Cy5 GaMIg Fab') (C). The overlay image (D) shows high overlap of these membrane areas confirmed by cross-correlation values of 0.66, 0.78 and 0.74 for ErbB2 - lipid rafts, ErbB2 - integrin β1 and integrin β1 - lipid raft pairs, respectively.

- with permission; used already in the Ph.D. thesis of my co-author Maria-Magdalena Mocanu, Univ. of Bucharest, 2005 -

Significant colocalization was found between ErbB2 and integrin β1 on all the examined tumor cell lines (Table II), which was independent of trastuzumab resistance. Additionally, both ErbB2 and integrin β1 were found in lipid rafts. Interestingly, the gastric cell lines (MKN-7 and N87) showed significantly higher integrin β1 - lipid raft and ErbB2 - lipid raft colocalization than the breast cancer cell lines (SK-BR-3 and JIMT-1). The previously documented, spatially non-overlapping transferrin-ErbB2 receptor pair [216] was chosen as a negative control, yielding a *C* value of 0.13±0.02. Positive control samples, labeled with two non-competing monoclonal antibodies against ErbB2 (Cy5-2C4, Cy3-trastuzumab), yielded a *C* value of 0.75 ± 0.06.

Table II. Cross-correlation values measured between integrin β1 and ErbB2 on double labeled tumor cells.[1]

Treatment	SK-BR-3	JIMT-1	N87	MKN-7
quiescent	0.70 ± 0.05	0.61 ± 0.08	0.76 ± 0.02	0.76 ± 0.02
trastuzumab	0.61 ± 0.02	0.55 ± 0.07	0.77 ± 0.03	0.69 ± 0.04
EGF	0.62 ± 0.04	0.60 ± 0.08	0.76 ± 0.02	0.69 ± 0.03
heregulin	0.56 ± 0.05	0.51 ± 0.06	0.79 ± 0.02	0.67 ± 0.01

[1]Cells were labeled with anti-CD29 against integrin β1 followed by secondary labeling with Cy3 GaMIg Fab' and Cy5-2C4 against ErbB2. Cross-correlation values are calculated according to Pearson's formula. The mean (±SEM) values are presented in the table. Negative control samples were labeled against transferrin receptor (Cy5-MEM75) and ErbB2 (Cy3-trastuzumab), and yielded a cross-correlation value of 0.13 ± 0.02. Positive control was labeled against ErbB2 on two different epitopes (Cy5-2C4, Cy3-trastuzumab), and yielded a cross-correlation value of 0.75 ± 0.06. - *with permission; used already in the Ph.D. thesis of my co-author Maria-Magdalena Mocanu, Univ. of Bucharest, 2005* -

In order to mimic trastuzumab therapy and ligand-induced signaling, further colocalization measurements were carried out on cells treated with trastuzumab, EGF and heregulin. None of the treatments changed the ErbB2 / integrin β1 colocalization significantly (Table II). On the other hand, trastuzumab-treated breast cancer cells showed a significant decrease in the integrin β1 - lipid raft and ErbB2 - lipid raft colocalization, whereas no change was observed on gastric cancer cells (Fig. 14).

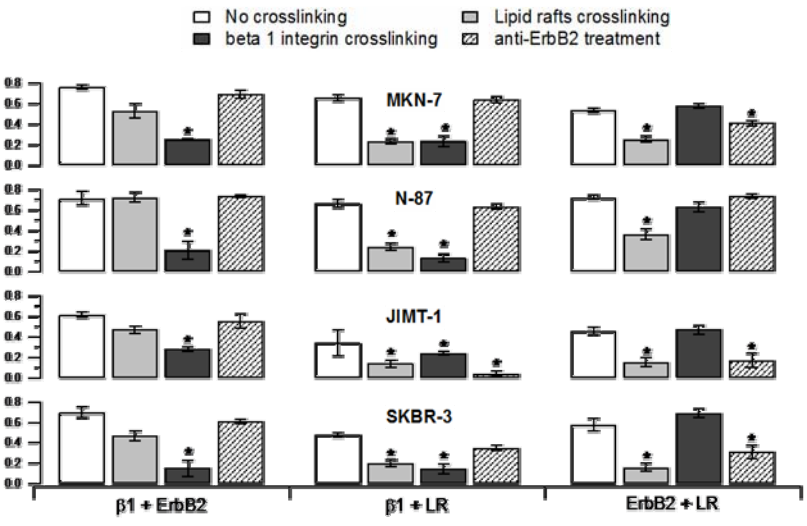

Figure 14. MKN-7, N87, SK-BR-3 and JIMT-1 cells were labeled for integrin β1, ErbB2 and lipid rafts. Treatments were done as described before. Error bars show the SEM. Asterisks indicate significant difference from untreated cells using Student's *t*-test ($p<0.05$). (LR= Lipid Raft) *- with permission; used already in the Ph.D. thesis of my co-author Maria-Magdalena Mocanu, Univ. of Bucharest, 2005 -*

6.1.3. Crosslinking of integrin β1 or lipid rafts disrupts their colocalizations

We carried out crosslinking experiments in order to estimate the strength of interaction and the preferred association partners of the proteins. CTX-B-induced crosslinking of lipid rafts significantly decreased colocalization of lipid rafts with both ErbB2 and integrin β1 on all cell lines studied (Figs. 14 and 15). The separation of ErbB2 and integrin β1 from the aggregated lipid rafts suggested that these proteins are not tightly raft-associated, i.e. they did not co-migrate with rafts. This is supported by the finding that the ErbB2/integrin β1 colocalization was either unchanged or only slightly decreased on all cell lines, i.e. their mutual interaction is stronger than their respective raft association.

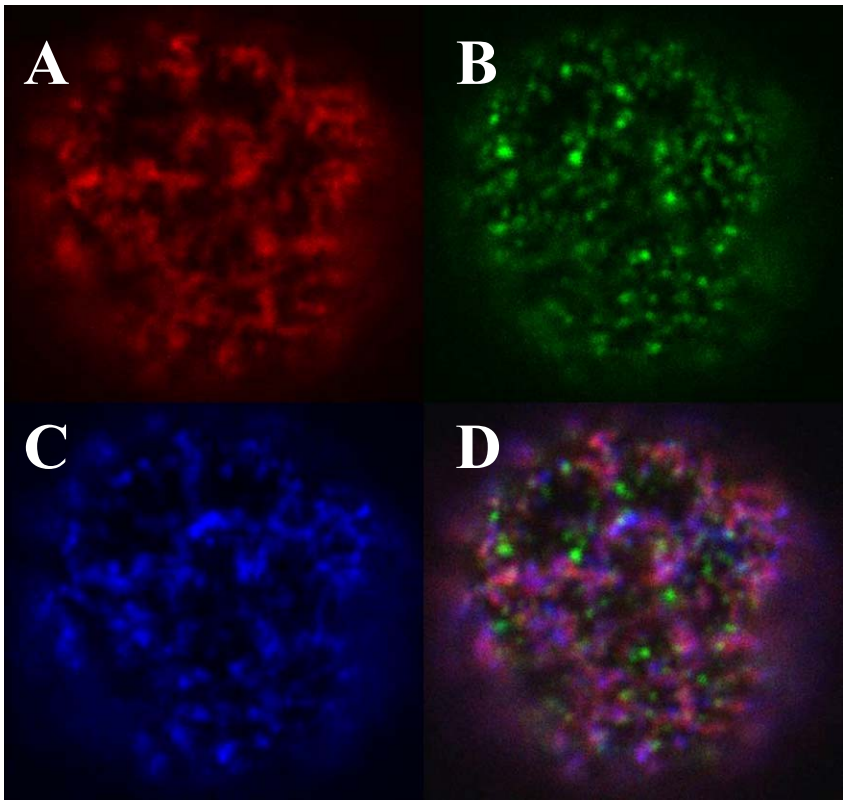

Figure 15. Cross-linking of lipid rafts. Distributions of ErbB2 (A) and integrin β1 (C) are settled, while they get mutually dismissed from lipid rafts (D) confirmed by cross-correlation values of 0.82, 0.19 and 0.27 for ErbB2/integrin β1, ErbB2/lipid rafts, and integrin β1/lipid raft pairs, respectively.
- with permission; used already in the Ph.D. thesis of my co-author Maria-Magdalena Mocanu, Univ. of Bucharest, 2005 -

Secondary antibody-mediated cross-linking of integrin β1 caused a decrease in all colocalization values involving integrin β1 (integrin β1/ErbB2, integrin β1/lipid rafts) in all cell lines (Fig. 14) implying that cross-linking liberated integrin β1 from its complex with ErbB2 and lipid rafts. This is consistent with the finding that the ErbB2/lipid raft association was largely unaffected by integrin cross-linking indicating that the raft-association of ErbB2 was not perturbed.

As both ErbB proteins and integrin β1 are known to interact with the actin cytoskeleton - having a potential to influence their compartmentalization [92, 217] -, additional triple colocalization measurements were performed on cytochalasin D-treated cells (10 μg/ml, 2.5 hours in serum-free medium at room temperature) followed by crosslinking as above. There were no significant differences in any of the colocalization values measured on cytochalasin D treated cells compared to untreated ones indicating that binding to the actin cytoskeleton does not affect the interactions of ErbB2, integrin β1 and lipid rafts with each other (data not shown).

6.1.4. ErbB2 - integrin β1 interaction is independent of integrin β1 expression level

Colocalization measurements proved that ErbB2 and integrin β1 are located in the same membrane domains, but FRET measurements were needed to estimate their molecular interactions. The heteroassociation of ErbB2 and integrin β1 was always measured using the more abundant of the two proteins as the acceptor. Significant interaction between ErbB2 and integrin β1 was detected on JIMT-1 and N87, whereas FRET for this heteroassociation was lower on SK-BR-3 and MKN-7 cells (Table III).

Table III. Flow cytometric measurement of FRET efficiencies (±SEM, %) between integrin β1 and ErbB2 on the cell lines studied.[1]

Association /cell line	SK-BR-3	JIMT-1	N87	MKN-7
ErbB2 homoassociation	16.1 (±1.2)	2.9 (±0.8)	11.5 (±0.1)	3.9 (±1.2)
ErbB2 intramolecular	56.2 (±2.4)	58.2 (±1.5)	65.4 (±0.3)	56.7 (±1.4)
ErbB2 - integrin β1[2]	n.d.[2]	9.7 (±1.8)	n.d.[2]	5.8 (±2.2)
integrin β1 - ErbB2[2]	3.3 (±2.0)	n.d.[2]	7.1 (±1.3)	n.d.[2]
integrin β1 homoassociation	9.8 (±1.9)	6.4 (±1.0)	5.2 (±1.9)	6.4 (±2.8)

[1]Average energy transfer values determined from histograms of 10,000 cells. Cells were treated in suspension as described in materials and methods.

[2]On the trastuzumab sensitive SK-BR-3 and N87 cell lines FRET efficiency was measured only with integrin β1 as donor (Alexa546-TS2) and ErbB2 as acceptor (Alexa647-2C4), since measuring in the opposite direction would have given unreliable results owing to the low expression level of integrin β1 on these cell lines. Similarly, owing to the lower expression level of ErbB2 in JIMT-1 and MKN-7, only data obtained with ErbB2 as donor (Alexa546-2C4) and integrin β1 as acceptor (Alexa647-TS2) are shown. (n.d. = not determined)

High level of homoassociation of ErbB2 was detected on the trastuzumab sensitive SK-BR-3 and N87 cells using the 2C4 antibody, while the resistant JIMT-1 and MKN-7 cells showed FRET below 5%. The degree of homoassociation of ErbB2 correlated with its expression level, since the cell lines expressing a high number of ErbB2 molecules (SK-BR-3, N87) displayed the strongest ErbB2 homoassociation. Weak homoassociation of integrin β1 was detected on all cell lines except for SK-BR-3, which showed almost 10% FRET for integrin β1 homoassociation.

None of the cell lines showed significant changes in FRET after treatment with trastuzumab or heregulin, however, EGF treatment resulted in increased FRET efficiency values for all ErbB1 associations (ErbB1-ErbB1, ErbB1-ErbB2 and ErbB1-integrin β1) (Table IV). These results promoted that there is not only colocalization, but also molecular association between ErbB2 and integrin β1 based on the FRET measurements.

Table IV. Effects of EGF, trastuzumab or heregulin treatments on diverse molecular interactions in trastuzumab sensitive (SK-BR-3) and resistant (JIMT-1) breast cancer cell lines.[1]

Cell lines / **Associations**	**SK-BR-3**				**JIMT-1**			
Trastuzumab resistance	-	-	-	-	+	+	+	+
Treatment	no	EGF	trastuzumab	HRG	no	EGF	trastuzumab	HRG
ErbB1-ErbB1	27.9 ± 1.4	42.0 ± 3.9	24.8 ± 2.9	28.1 ± 9.3	3.4 ± 0.5	14.3 ± 1.3	5.3 ± 1.2	4.1 ± 1.4
ErbB1-ErbB2	14.7 ± 1.4	27.9 ± 6.7	11.6 ± 1.7	12.7 ± 3.1	1.9 ± 0.5	7.9 ± 0.0	2.0 ± 0.5	3.0 ± 0.8
ErbB1-integrin β1	22.7 ± 2.1	36.3 ± 2.8	18.1 ± 1.8	1.8 ± 4.9	19.7 ± 2.1	32.6 ± 4.5	21.2 ± 1.9	18.3 ± 9.7
ErbB1-MHCI	22.6 ± 3.8	41.7 ± 2.7	19.5 ± 1.3	30.5 ± 5.9	12.5 ± 1.0	17.4 ± 3.8	14.7 ± 0.7	10.6 ± 0.3
ErbB2-MHCI	15.1 ± 2.9	28.4 ± 6.6	15.8 ± 6.8	11.3 ± 2.0	6.4 ± 0.6	7.9 ± 2.0	8.0 ± 0.8	5.9 ± 0.5
integrin β1-MHCI	22.8 ± 2.4	27.0 ± 2.4	20.7 ± 1.7	4.2 ± 7.7	12.1 ± 0.8	9.4 ± 1.0	12.6 ± 0.7	12.8 ± 2.3
ErbB2 intramolecular	53.7 ± 3.1	59.9 ± 7.6	n.d.	51.5 ± 0.4	47.6 ± 2.0	49.9 ± 0.0	n.d.	n.d.
MHCI intramolecular	27.7 ± 4.1	35.5 ± 2.2	28.0 ± 3.2	34.3 ± 4.5	18.4 ± 1.9	n.d.	n.d.	n.d.

[1]Average energy transfer values determined from histograms of 10,000 cells. Cells were treated in suspension as described in the Materials and methods. In the cases of treatments with trastuzumab, measurements of the intramolecular FRET on ErbB2 molecule was omitted because of the influencing effect of the antibody used for the treatment. (HRG=heregulin, n.d. = not determined)

6.1.5. ErbB2-integrin β1 interaction do not alter trastuzumab-mediated phosphorylation

Since integrins have been shown to modulate ErbB-mediated signal transduction [96], it seemed possible that the high expression level of integrin β1 on the trastuzumab resistant cell lines affects trastuzumab-mediated ErbB2 tyrosine phosphorylation to a greater extent. We stimulated serum-starved SK-BR-3 and JIMT-1 cells with trastuzumab with or without prior crosslinking integrin β1 molecules. ErbB2 tyrosine phosphorylation was lower on non-stimulated JIMT-1 than SK-BR-3 cells in accordance with previous results [149]. Trastuzumab induced the tyrosine phosphorylation of ErbB2 both in the trastuzumab sensitive and resistant cell lines (Fig. 16). Cross-linking of integrin β1 did not alter the level of trastuzumab-induced ErbB2 tyrosine phosphorylation even in the trastuzumab resistant JIMT-1 cell line that expressed a high amount of integrin β1. These findings suggested that in spite of the high cell surface density of integrin β1 on JIMT-1 the first signaling steps initiated by trastuzumab are not affected.

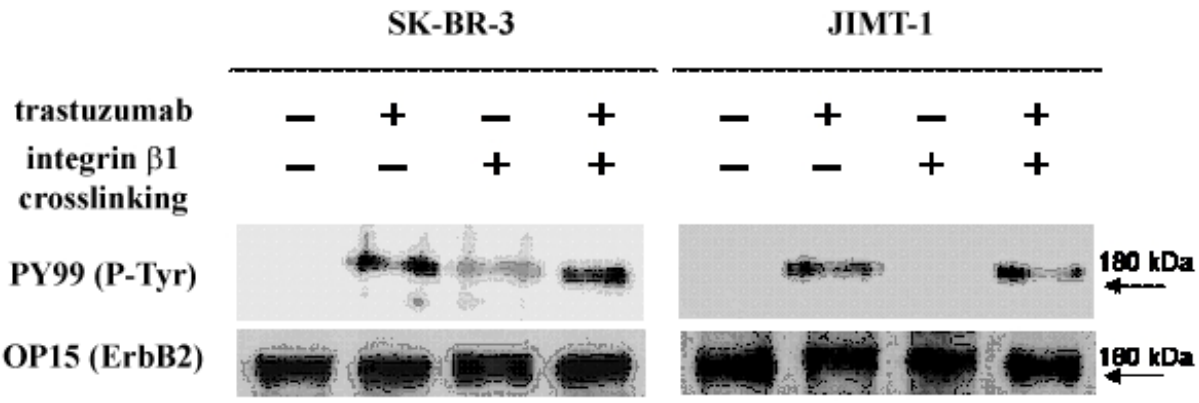

Figure 16. High expression of integrin β1 did not change trastuzumab-induced ErbB2 tyrosine phosphorylation. Integrin β1 was crosslinked in SK-BR-3 and JIMT-1 cells with anti-CD29 and secondary goat anti-mouse antibodies followed by stimulation of cells with 10 μg/mL trastuzumab for 20 minutes, where indicated. Cells were then lysed and ErbB2 was immunoprecipitated with OP15. Proteins were resolved by SDS-PAGE and membranes were labeled with PY99 or OP15.

6.2. Associations of ErbBs are dynamically modulated by integrin β1 molecules - application of the newly established two-sided FRET method

6.2.1. Excess integrin β1 inversely correlates with ErbB2 level on trastuzumab resistant cells

A general assumption in oncology is that the expression level and interaction partners of proteins determine the malignant phenotype of cancer cells. Given the previous results implying that association states of ErbB2 may dynamically modulated by neighboring membrane species - e.g. integrin β1 - we aimed at investigating concurrent association states of three molecules on the cell surface to gain more information on attributable intermolecular changes in the background of trastuzumab resistance. First, we recharacterized the expression levels of ErbB1, ErbB2, integrin β1 extended for that of CD44 and MHC-I on trastuzumab resistant (JIMT-1, MKN-7) and sensitive (SK-BR-3, N87) cell lines by flow cytometry. Trastuzumab resistant cell lines showed lower ErbB2, but higher integrin β1 and CD44 expression levels than the sensitive ones. The relative numbers of ErbB1 and MHC-I did not reveal characteristic differences between the resistant and sensitive cell lines (Fig. 17).

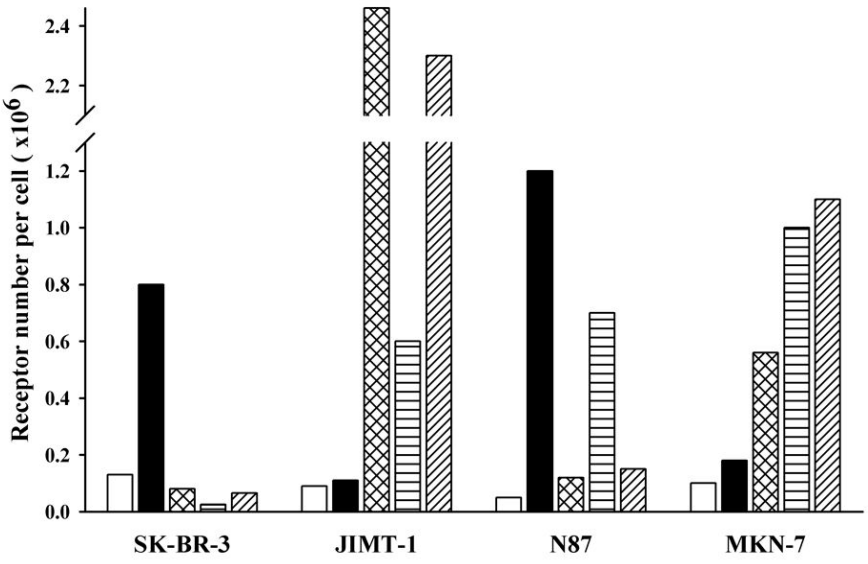

Figure 17. Expression profile of trastuzumab resistant (JIMT-1, MKN-7) and sensitive (SK-BR-3, N87) cell lines. Number of ErbB1 (□), ErbB2 (■), integrin β1 (⊠), MHC-I (▤) and CD44 (▨) molecules were determined by flow cytometry. Note, that the trastuzumab resistant cell lines showed lower ErbB2, but higher integrin β1 and CD44 expression levels than the sensitive ones.

6.2.2. ErbB2 interactions are shifted towards heteroassociations with integrin β1

As we observed differences in the expression levels of ErbB2, integrin β1 and CD44 in the cell lines, we then assessed the molecular associations of these proteins using FCET (Table V). The homoassociation of ErbB2 correlated with its expression level giving rise to high ErbB2 homoassociation in trastuzumab sensitive cell lines, in which the expression level of ErbB2 was high [93]. The heteroassociations were usually measured using the more abundant cell surface protein as acceptor. Significant interaction between ErbB2 and integrin β1 was detected on the resistant JIMT-1 cell line, while MKN-7 and N87 cells displayed moderate and SK-BR-3 cells low (<5%) FRET in this respect. Heteroassociation of CD44 with integrin β1 or ErbB2 was high on the resistant JIMT-1 cell line, but weak on the similarly resistant MKN-7 cells (Table V).

Table V. FCET measurements on the trastuzumab sensitive and resistant cell lines.[1]

Association / Cell line	**SK-BR-3**	**JIMT-1**	**N87**	**MKN-7**
ErbB2 homoassociation	16.1 (±1.2)	2.9 (±0.8)	11.5 (±0.1)	3.9 (±1.2)
ErbB2 intramolecular	56.2 (±2.4)	58.2 (±1.5)	65.4 (±0.3)	56.7 (±1.4)
ErbB2 – integrin β1[2]	n.d.	13.1 (±1.1)	n.d.	9.1 (±1.2)
integrin β1 – ErbB2[2]	3.3 (±2.0)	n.d.	7.1 (±1.3)	n.d.
integrin β1 homoassociation	9.8 (±1.9)	6.4 (±1.0)	5.2 (±1.9)	6.4 (±2.8)
ErbB2 – CD44	n.d.	19.9 (±1.5)	n.d.	4.2 (±0.7)
integrin β1 – CD44	n.d.	10.5 (±1.0)	n.d.	3.7 (±0.5)
MHC-I – integrin β1	n.d.	14.9 (±1.3)	n.d.	5.2 (±0.5)

[1]Mean energy transfer efficiency determined in flow cytometry. Mean ± SEM of 20,000 cells. [2]Heteroassociations were always measured using the more abundant cell surface protein as acceptor. (n.d. = not determined owed to low expression levels)

6.2.3. Model system for two-sided FRET (tsFRET)

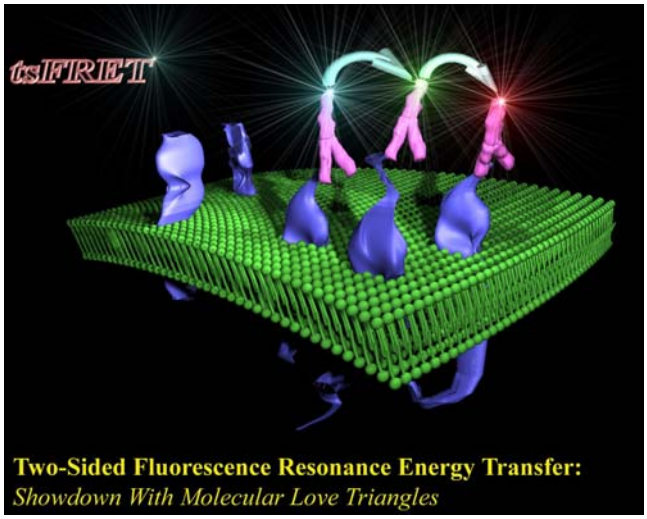

As proof-of-concept for the tsFRET approach, we devised a triple labeled model system applicable in CLSM. In this, the first fluorophore (XFITC) is a donor dye of the first FRET pair (D1), and its acceptor (A1) is the second fluorophore (Cy3 or Alexa555). This dye also acts as a donor (D2) for the third fluorophore (Cy5), which is the acceptor in this second FRET pair (A2). Consequently, the second fluorophore is both an acceptor and a donor (A1≡D2), although in two different measurement protocols.

In the above system, the energy transfer efficiency can be measured sequentially using the abFRET method (between A1≡D2 and A2) followed by the dbFRET method (between D1 and A1≡D2). Using appropriately chosen fluorophores, the abFRET and dbFRET methods can be combined consecutively, since the excitation wavelengths (543 and 633 nm corresponding to the absorption of A1≡D2 and A2, respectively) used in abFRET do not excite the first fluorophore (XFITC) (see Fig. 18).

To demonstrate the feasibility of this approach, we used the ErbB2 molecule labeled with three non-competing monoclonal antibodies as a model system. On the basis of the nearly full-length ErbB2 model [218], it was known that the 7C2, 2C4 and 4D5 antibodies do not compete with each other. We labeled N87 cells with XFITC-7C2 (D1), Cy3 or Alexa555-conjugated 2C4 (A1≡D2) and Cy5-4D5 (A2) (Fig. 18A).

Both dbFRET and abFRET efficiency values demonstrated the proximity of the labeled antibodies as expected. Then we generated the contour plot from the corresponding pixel-by-pixel dbFRET (axis ‘x’) and abFRET (axis ‘y’) efficiencies. The pixel-by-pixel 2D matrix of the contour plot was calculated on 5 - 10 % FRET ranges by a macro written for the software Sigmaplot. The resulted 2D matrix was then plotted by using the contour plot function of the software Igor Pro.

We derived the dependence of the two FRET efficiencies on each other by calculating a trendline. The dbFRET axis was divided into several bins depending on the number of data points, and the mean abFRET value corresponding to pixels in the bin was calculated and plotted against the binned dbFRET values. The contour plot and the trendline (slope = 0.003 by linear regression) showed no correlation between the FRET values, since these energy transfer efficiency values showed a Gaussian distribution. This finding was in accordance with expectations, since in this case both dbFRET and abFRET values represented intramolecular distances, which are constant (see Fig 19.).

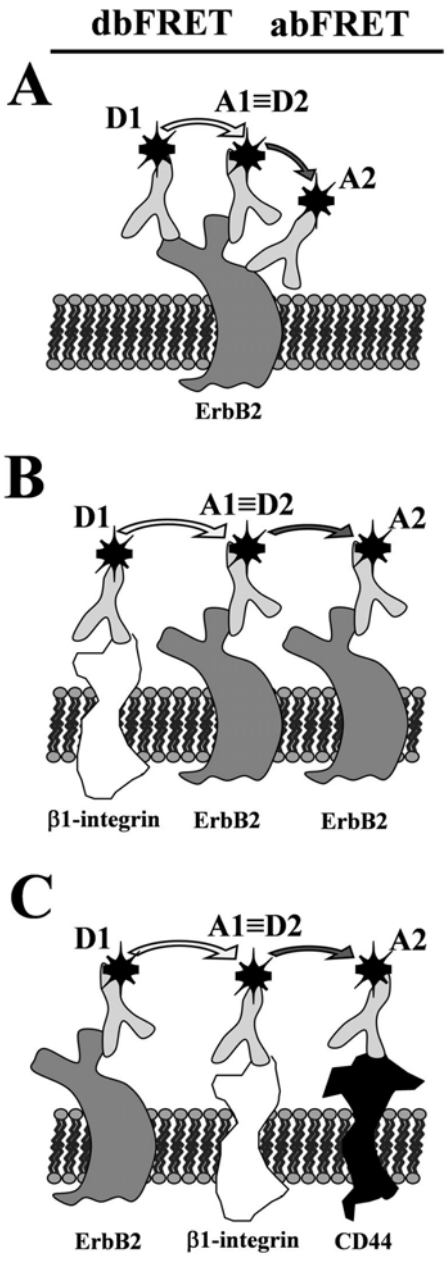

Figure 18. Schematic models of two-sided FRET measurements on CLSM.

D1 denotes XFITC, the donor in dbFRET, A1≡D2 refers Cy3 or Alexa555 acting as an acceptor in dbFRET (A1) and a donor in abFRET (D2), while A2 indicates Cy5, the acceptor in abFRET. The energy transfer efficiency can be measured sequentially using the abFRET method (between A1≡D2 and A2) followed by the dbFRET method (between D1 and A1≡D2).

(**A**) The model system. ErbB2 was labeled with XFITC-7C2 (D1), Cy3-2C4 or Alexa555-2C4 (A1≡D2) and Cy5-4D5 (A2).

(**B**) Influence of integrin β1 - ErbB2 heteroassociation on the ErbB2 homoassociation. Cells were labeled with XFITC-TS2 (D1), Cy3-2C4 or Alexa555-2C4 (A1≡D2) and Cy5-2C4 (A2).

(**C**) Relationship of ErbB2 – integrin β1 and integrin β1 – CD44 heteroassociation. Cells were labeled with XFITC-2C4 (D1), Cy3-TS2 or Alexa555-TS2 (A1≡D2) and Cy5-Hermes3 (A2).

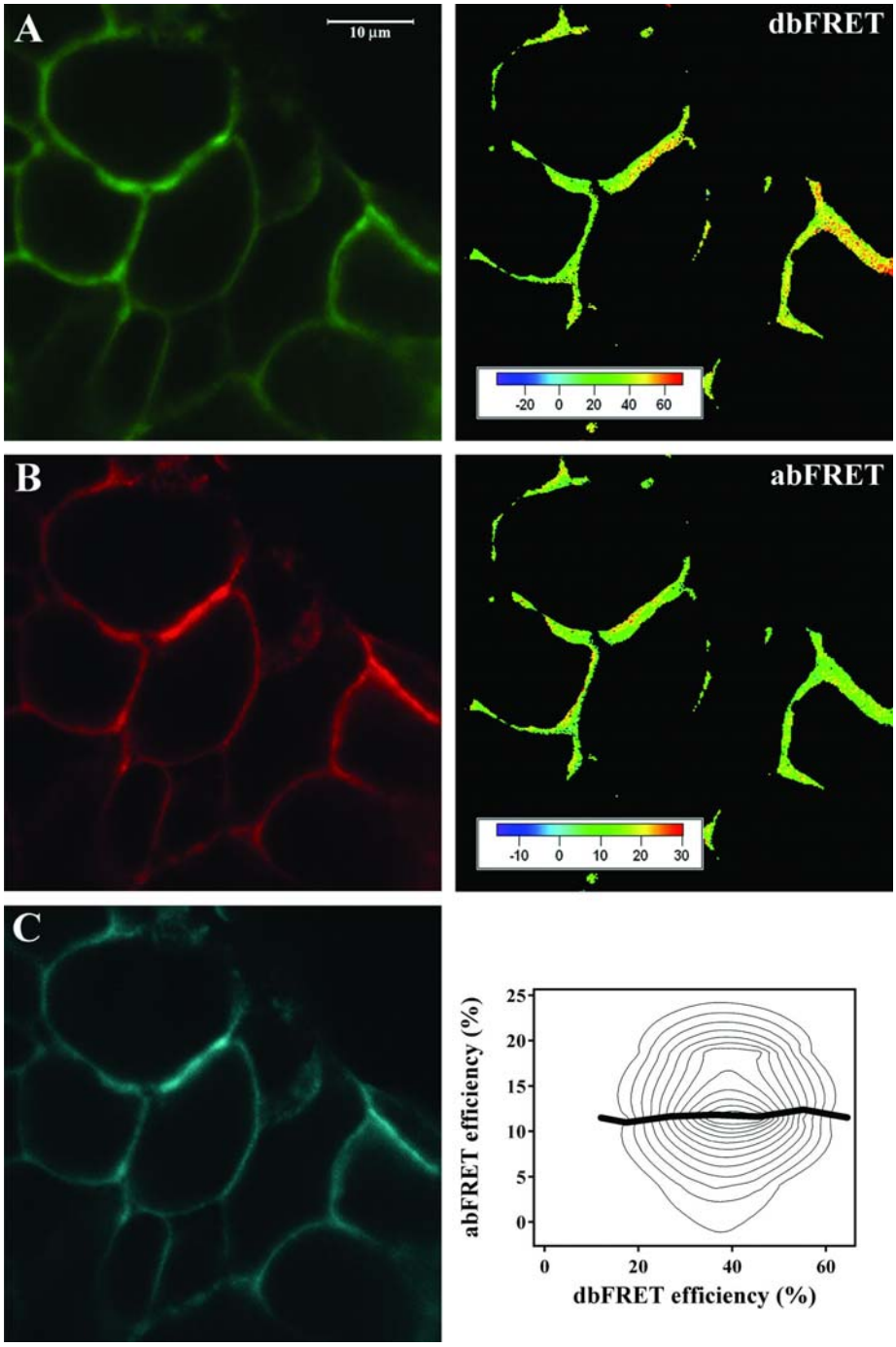

Figure 19. Two-sided FRET on N87 cells triple-labeled with anti-ErbB2 antibodies.

The raw, green color coded XFITC-7C2 (D1) image (**A**), red color coded Cy3-2C4 (A1≡D2) image (**B**), blue color coded Cy5-4D5 (A2) image (**C**), the false color dbFRET efficiency image (*right top*), the false color abFRET efficiency image (*right middle*) and the contour plot derived from pixel values of the corresponding dbFRET and abFRET images (*right bottom*) are displayed.

6.2.4. Application of tsFRET: ErbB2 homoassociations are disintegrated by integrin β1

As we successfully implemented the tsFRET method for evaluating the correlation of two different molecular interactions, we wished to characterize the relationship of ErbB2 - integrin β1 heteroassociation (measured by dbFRET) and ErbB2 homoassociation (measured by abFRET) on trastuzumab sensitive cell lines (SK-BR-3, N87). The schematic model of the experiment can be seen in Fig. 18B. The JIMT-1 and MKN-7 trastuzumab resistant cell lines were not investigated in this respect, because the ErbB2 homoassociation was low on both cell lines as determined by FCET (Table V) and abFRET, as well [219]. On the contour plot for N87 cells, two different peaks could be identified at 13 % (abFRET) – 20 % (dbFRET) and at 7 % (abFRET) – 30 % (dbFRET) and the trendline runned with a slope of -0.042 (Fig. 20A). This finding suggested an anti-correlation between integrin β1 – ErbB2 heteroassociation (dbFRET) and ErbB2 homoassociation (abFRET), as the higher the dbFRET efficiency, the lower the abFRET efficiency was pixel-by-pixel, and vice versa. Similar tendency could be detected on SK-BR-3 cells based on the trendline showing also a decrease with a slope -0.080, however the contour plot displayed only a single peak at about 12 % (abFRET) – 26 % (dbFRET) (Fig. 20B).

The trastuzumab resistant cell lines (JIMT-1, MKN-7) were investigated in respect of the influential effect of CD44 (integrin β1 – CD44, abFRET) on ErbB2 - integrin β1 interaction (dbFRET) behind the resistant phenotype, because the CD44 expression level was saliently high on the resistant cell lines contrary to the sensitive ones, and previous data have already proposed its possible role in trastuzumab resistance. The schematic model of these experiments is displayed in Fig. 18C. On the contour plot of MKN-7 cells two discrete peaks were distinguishable at 10 % (abFRET) – 22 % (dbFRET) and at 20 % (abFRET) – 32 % (dbFRET) and the trendline showed an increase with a slope 0.077 (Fig. 20C). This implied a modest positive correlation, as higher dbFRET values adjoined with higher abFRET values. On the contrary, there was only one peak at 12 % (abFRET) – 21 % (dbFRET) on the contour plot for JIMT-1 cells, and the trendline runned with a slope -0.002 (Fig. 20D). Thus, neither a positive nor negative correlation could be presumed between ErbB2 – integrin β1 and integrin β1 – CD44 heteroassociations on JIMT-1 cells.

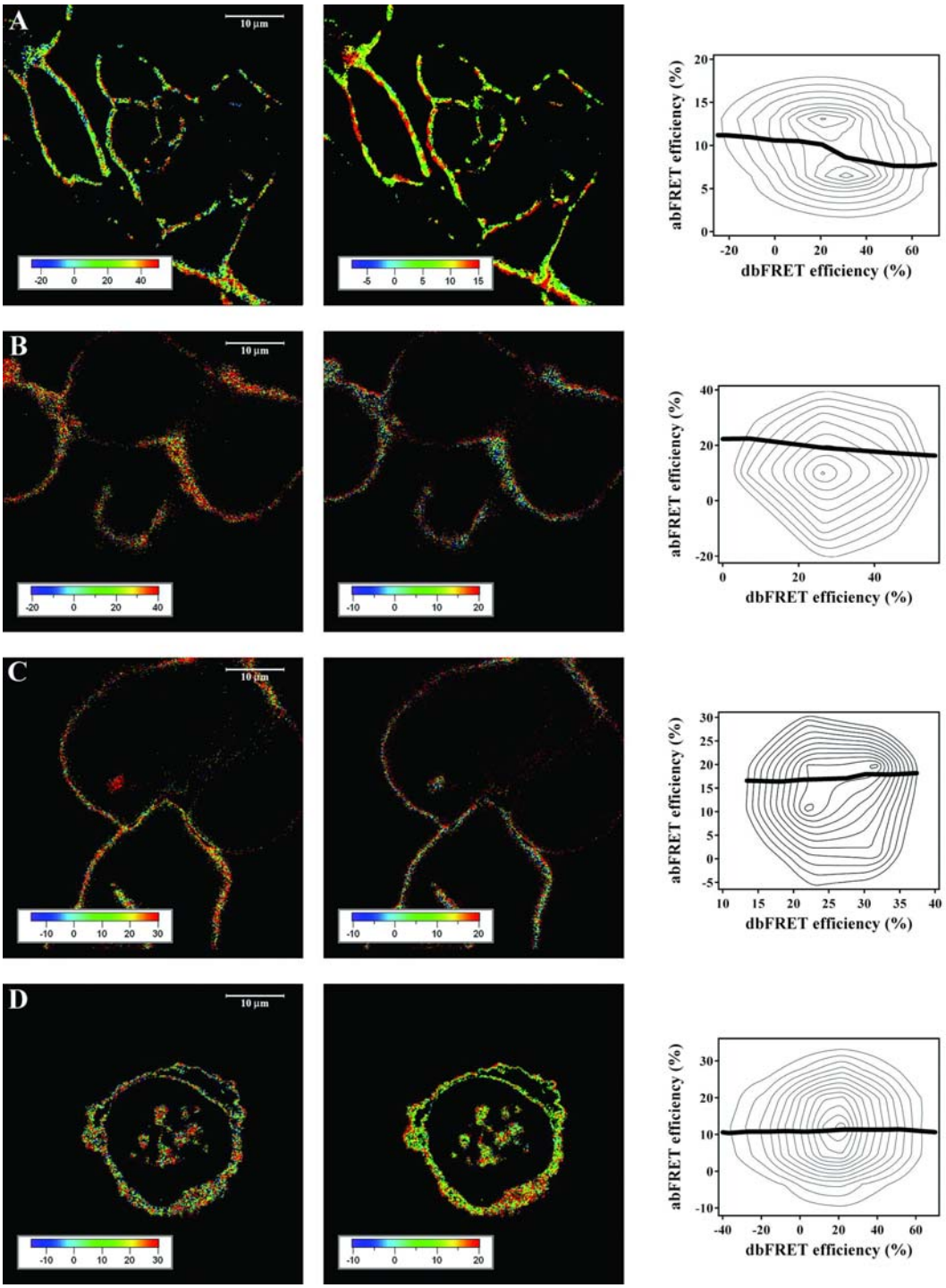

Figure 20. tsFRET measurements of two molecule-pairs of three arbitrarily chosen molecules.
N87 (**A**) and SK-BR-3 (**B**) cells were labeled for integrin β1 with XFITC-TS2 (D1), and for ErbB2 with Cy3- or Alexa555-2C4 (A1≡D2) and Cy5-2C4 (A2) antibodies. MKN-7 (**C**) and JIMT-1 (**D**) cells were labeled for ErbB2 with XFITC-2C4 (D1), integrin β1 with Cy3- or Alexa555-TS2 (A1≡D2) and for CD44 with Cy5-Hermes3 (A2) antibodies. Consecutive abFRET and dbFRET measurements were performed and the false color maps of dbFRET (*left column*) and abFRET (*middle column*) efficiencies as well as the contour plots of the corresponding pixel-by-pixel dbFRET and abFRET efficiency values (*right column*) are shown.

In addition, we planned to trace the possible effect of the ErbB1 – ErbB2 heteroassociation on the ErbB2 homoassociation in SK-BR-3 cells, as our former FCET results (Table IV) implied a plausible impact of ErbB1 - ErbB2 heteroassociation on ErbB2 mediated signaling in the studied breast cancer cell lines. However, according to the mean dbFRET and abFRET efficiency values together with their contour plot distribution and trendline slope (summarized in Table VI) no clear correlation could be detected between these molecular interactions.

Table VI. *Two-sided FRET measurements among three distinct molecular species on trastuzumab sensitive (SK-BR-3 and N87) and resistant (JIMT-1 and MKN-7) cells.*[1]

Cell line	D1	A1≡D2	A2	dbFRET	abFRET	slope
JIMT-1	ErbB1	integrin β1	MHC-I	*16.6 (±4.3)*	*7.2 (±0.4)*	*n.d.*
	ErbB2	integrin β1	CD44	*12.0 (±0.8)*	*9.2 (±1.5)*	*-0.002*
MKN-7	ErbB2	integrin β1	CD44	*15.2 (±2.4)*	*21.2 (±3.4)*	*0.077*
	integrin β1	ErbB2	CD44	*18.2 (±2.3)*	*6.0 (±4.0)*	*n.d.*
SK-BR-3	ErbB1	ErbB2	ErbB2	*21.0 (±1.7)*	*11.2 (±1.5)*	*-0.017*
	integrin β1	ErbB2	ErbB2	*26.3 (±1.3)*	*16.0 (±2.8)*	*-0.080*
	ErbB2[2]	ErbB2[2]	ErbB2[2]	*37.0 (±3.4)*	*23.0 (±1.1)*	*0.003*
N87	integrin β1	ErbB2	ErbB2	*19.0 (±2.4)*	*9.3 (±1.8)*	*-0.042*

[1]Mean dbFRET and abFRET efficiency values (% ± SEM) and the slopes of the trendlines along contour plots determined from corresponding dbFRET and abFRET images. [2]ErbB2 molecules were triple-labeled with 7C2 (D1), 2C4 (A1≡D2) and 4D5 (A2) antibodies tagged by the corresponding XFITC, Cy3 or Alexa555 and Cy5 fluorescent dye for consecutive abFRET and dbFRET measurements. All other ErbB2 indicated in the table denotes labeling with 2C4 antibody. (n.d. = not determined)

6.2.5. Cell function related distribution of membrane receptors

We also wished to investigate whether the membrane distribution of molecules along the 'z' axis (from the bottom to the top of the cell) affect the results achieved by microscopic FRET methods. This was exceptionally of interest, because FCET values of integrin β1 – ErbB2 heteroassociation on SK-BR-3, N87 and MKN-7 cells and those of integrin β1 – CD44 interaction on MKN-7 cells were significantly lower (Table V) than the corresponding microscopic FRET values (Table VI). Therefore, we wanted to discriminate and comprehend

the possible altering effect of trypsinization used before FCET measurements and the indeterminate overestimating effect of microscopic FRET methods.

We measured, thus, the rate of ErbB2 - integrin β1 heteroassociation by dbFRET on trypsinized, cyto-centrifuged SK-BR-3 and MKN-7 cells, which were found to be significantly lower (1.1% ± 0.3 %, 3.8 ± 0.5 %) than the corresponding dbFRET values measured on adherent, non-trypsinized cells (see Table VI). Moreover, integrin β1 was found in a remarkably higher density at the adhering (bottom) surface of cells than towards the top, whereas ErbB2 displayed a more homogeneous distribution all over the cell membrane both in adherent and trypsinized cells. Consequently, we performed both dbFRET and abFRET measurements for the ErbB2 - integrin β1 heteroassociation on MKN-7 and N87 cells in various optical slices to gain insight into the dependence of dbFRET and abFRET on the distance from the plane of adherence toward the top of the cell. We observed that along with decreasing expression level of integrin β1 both abFRET (Fig. 21) and dbFRET (data not shown) efficiency values subsided towards the top of the cell. This finding implied that the association of integrin β1 and ErbB2 is significantly higher at the adhering surface of the cells.

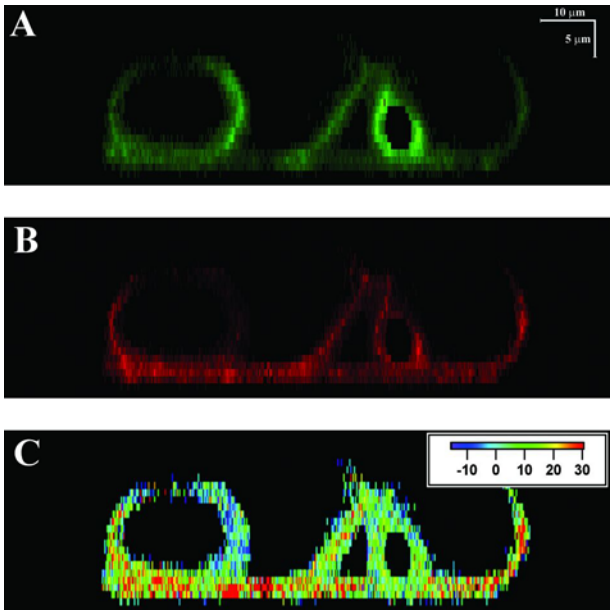

Figure 21. Z-section images of ErbB2 – integrin β1 heteroassociation on adherent MKN-7 cells.
MKN-7 cells were labeled with Alexa555-2C4 and Cy5-TS2 in chambered coverglass. Z-section image was taken as a series of line scans recorded with 1 μm depth interval. The Alexa555-2C4 as donor (**A**), the Cy5-TS2 as acceptor (**B**) and the false color energy transfer efficiency image (**C**) are displayed. It can be seen that the association state of ErbB2 and integrin β1 is decreasing from the plane of adherence (bottom of the images) toward the top of the cell.

6.3. Molecular interactions of ErbB1 and integrin β1 molecules reliably predict clinical outcome and correlate with radioresistance of astrocytic tumors

6.3.1. Higher ErbB1 and integrin β1 levels correlate with pronounced radioresistance

As preliminary data have already supported the contribution of integrin molecules in the chemo- or radioresistant phenotype [220], we screened the expression level of integrins αV, α1, α2, α4, α6, β1, β3, β4 and β5 on U251 chr7 transferred subclones Hyg+, c5, c9 and c55 (Fig. 22). Previously, the radioresistance of these subclones was determined by agar colony forming assay as LD_{50} of 4.0, 4.7, 5.0, and 5.7 Gy, respectively [204]. The results revealed that in parallel with increasing extra chr7 material and radioresistance, Hyg+, c5, c9, and c55 clones expressed not only increasing numbers of ErbB1 (65, 77, 83, and 270 thousand per cell), but also increscent numbers of integrin β1 (360, 400, 420, and 540 thousand per cell), respectively (Fig. 23A).

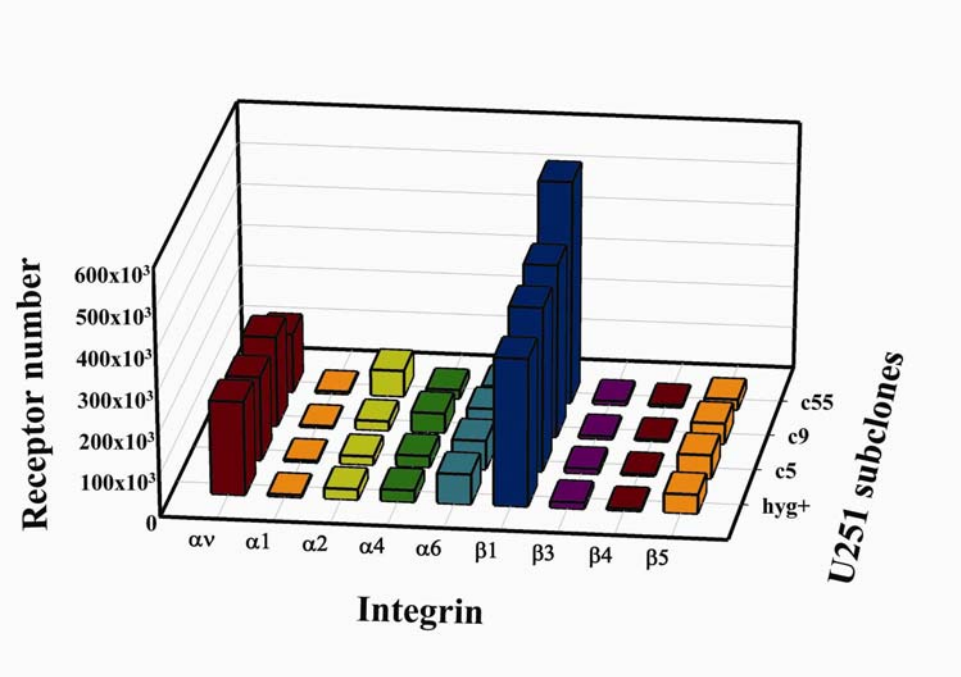

Figure 22. Integrin expression profile of U251 parental cell line and subclones c5, c9 and c55.
Number of the screened integrin molecules on the cell surface of U251 parental line and subclones transferred with extra chr7 material were quantitated by flow cytometry using QIFIKIT. Note the prominent receptor numbers of integrin β1 and the still markedly elevated expression of integrin αV molecules.

6.3.2. Overexpression of ErbB1 alone is also accompanied by higher integrin β1 levels

To differentiate from the regulatory effect of other genes coded on chr7p, we determined the expression levels of ErbB1 and integrin β1 in erbB1 gene transfected U251 subclones. The high and low ErbB1 expressing U251 E1H and E1L subclones, respectively, were followed up through 28 passages, and we found that the U251 E1H subclone incrementally split into two subpopulations: a low and a high ErbB1 expresser, designated as U251 E1H/L and U251 E1H/H, respectively. All subclones (E1L, E1H/L and E1H/H) expressed an increased number of ErbB1 and integrin β1, compared to the parental U251 cell line (Fig. 23B), which was stably sustained, while the ratio of the E1H/H subpopulation within the U251 E1H subclone decreased to 5% gradually over the passages. Notably, the U251 E1H/H subpopulation did not show statistically significant further increase in integrin β1 expression over the E1L, despite the extreme increase in ErbB1.

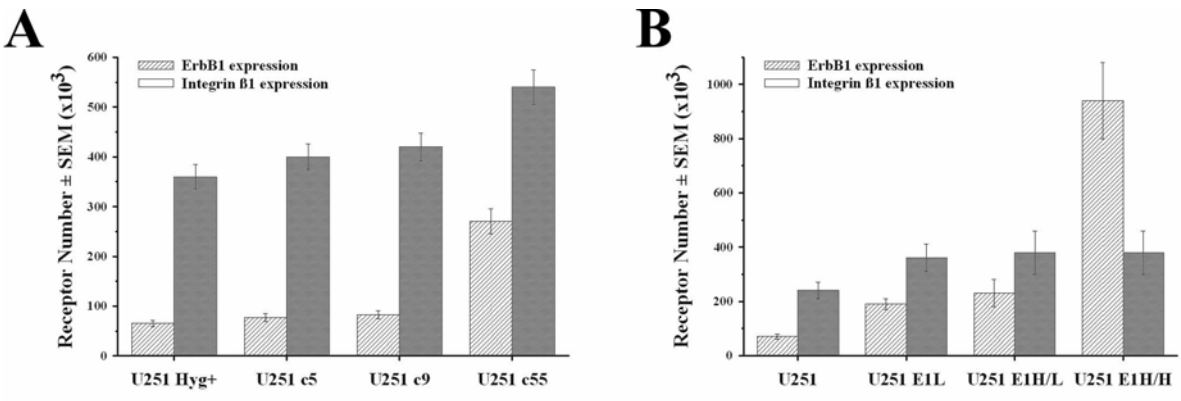

Figure 23. Expression profile of U251 sublines armed with extra chr7 (c5, c9, c55) or transfected with erbB1 gene (E1L, E1H/L, E1H/H).

U251 subclones were labeled for ErbB1 with AlexaFluor 546-528 and for integrin β1 with AlexaFluor 647-TS2 antibodies, as described in the Material and methods.

A-B, Number of ErbB1 (▨) and integrin β1 (■) molecules on the cell surface of U251 subclones transferred with extra chr7 material (**A)** or transfected with erbB1 gene (**B**) were quantitated by flow cytometry using QIFIKIT calibration.

6.3.3. Integrin β1 contributes to survival, whereas ErbB1 promotes colony forming ability

We analyzed the radiosensitivity of the parental U251 and the transfectants U251 E1L and E1H after applying 2, 4, 6 and 8 Gy irradiation. The survival rate of the transfectants increased alongside with their expanding ErbB1 and integrin β1 expression levels, but the

further extreme increase in the ErbB1 expression of the U251 E1H subclone did not assign significantly higher survival rate over the E1L (Fig. 24A). In the linear-quadratic model, both the parameters α and β differed significantly between the transfectants E1H, E1L and the parental U251, but not between the two transfectants (Table in Fig. 24A), implicating the dependence of these factors on the integrin β1 expression level. However, presence of additional surplus ErbB1 promoted the colony forming capability of U251 E1H compared to the parental U251 and even to the U251 E1L (Fig. 24B).

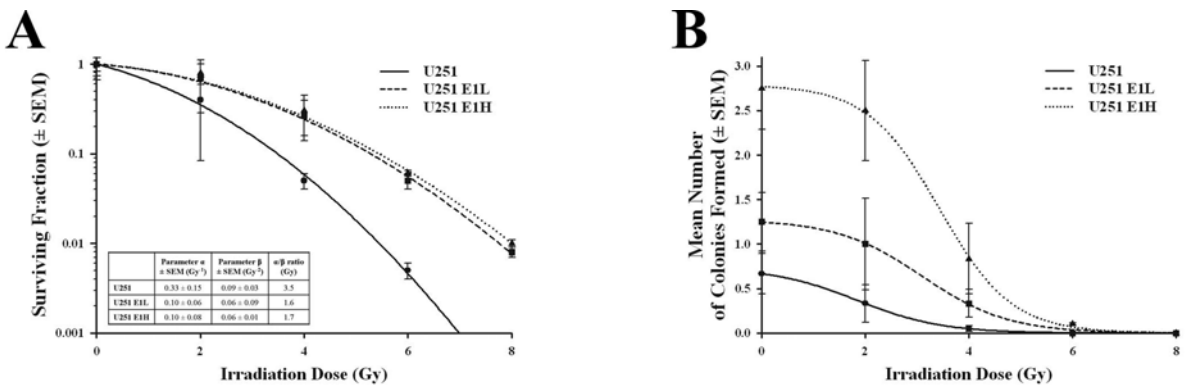

	Parameter α ± SEM (Gy⁻¹)	Parameter β ± SEM (Gy⁻²)	α/β ratio (Gy)
U251	0.33 ± 0.15	0.09 ± 0.03	3.5
U251 E1L	0.10 ± 0.06	0.06 ± 0.09	1.6
U251 E1H	0.10 ± 0.08	0.06 ± 0.01	1.7

Figure 24. Survival rate and colony forming capability after ionizing radiation.
A, Surviving fraction of U251 parental (●—●), U251 E1L (■- - -■) and U251 E1H (▲. . .▲) subclones after exposure to 2, 4, 6 and 8 Gy irradiating dose. On every irradiated U251 cell line, the parameter α - describing the direct ionizing effect -, the parameter β - reflecting the sublethal effect of the irradiation - and the α/β ratio - giving the irradiating dose, at which the linear and quadratic components of cell killing are equal - were calculated according to the linear quadratic model. **B,** Colony forming ability of U251 parental (●—●), U251 E1L (■- - -■) and U251 E1H (▲. . .▲) sublines after exposure to 2, 4, 6 and 8 Gy irradiating dose.

6.3.4. Increased integrin β1 is critical for radioresistance avertible by inhibition of PI-3K

Next, we wished to assess the suspected perturbation of the most prominent glial survival pathway, the PI-3K/Akt signaling route behind the increasing radioresistance. We performed western blot analysis of Akt and pAkt proteins, which disclosed a significant, 85% increase in pAkt levels of both U251 E1L and E1H transfectant subclones as quantitated by densitometry (Fig. 25A). After EGF treatment, the pAkt/Akt ratio also increased in both U251 E1L and E1H transfectant subclones (1.6 ± 0.2 and 1.8 ± 0.2, respectively) comparing with that of the parental U251 (1.1 ± 0.1). However, the additional increase of pAkt/Akt ratio in E1H opposed to E1L transfectants was low juxtaposing the extreme increase in ErbB1 expression of E1H (Fig. 25B). Combining wortmannin to inhibit PI-3K reverted the initially increased radioresistance of U251 E1L transfectants after 2 Gy irradiation (Fig. 25C).

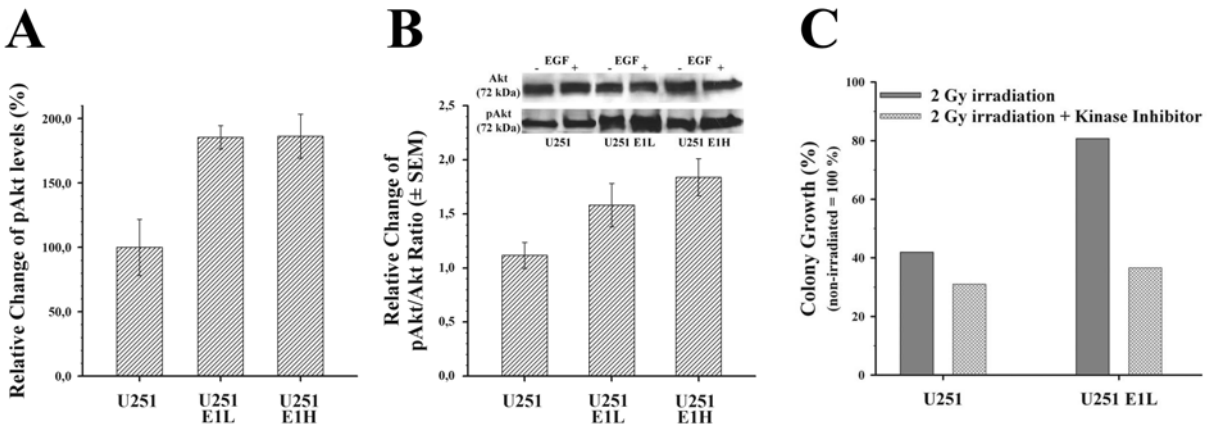

Figure 25. PI-3K inhibition, and change of the pAkt/Akt equilibrium after EGF treatment.

A, The relative change of pAkt levels in U251 and its transfectant sublines determined by densitometry of Western blots (mean±SD of 3 experiments). **B,** The pAkt/Akt ratio upon EGF treatment and corresponding Western blot image of starved U251 transfectant sublines. Note that survival rate and increase of pAkt in U251 E1H and U251 E1L transfectants does not show significant difference, while their colony forming ability is remarkably higher in U251 E1H, and is also accompanied by a higher responsivity of Akt phosphorylation to EGF stimulus. **C,** Relative percentage of well coverage in comparison to the respective, non-irradiated U251 and U251 E1L subclones after exposure to 2 Gy irradiation alone (■) or combined with the inhibition of PI-3K with wortmannin (▨).

6.3.5. ErbB1 interactions are shifted towards heteroassociations with integrin β1

FCET measurements: shift of balance towards ErbB1-integrin β1 heteroassociations

We carried out FCET measurements on ErbB1 homoassociation and ErbB1 - integrin β1 heteroassociation to explore the potential role of these molecular interactions behind the Akt-mediated radiation resistance. As positive reference control, MHC-I – β2-microglobulin intramolecular FRET efficiency was determined (28±2%). The results revealed anticorrelation between decreasing ErbB1 homoassociation (11±1%, 6±1%, 4±1%, 1±0.5%) and increasing ErbB1–integrin β1 heteroassociation rates (6±1%, 7±1%, 8±1%, 9±2%) on Hyg+, c5, c9, c55 U251 clones, as well as on parental U251, E1L, E1H/L and E1H/H transfectants (13±1%, 10±0.1%, 10±0.2%, 7±0.5% and 5±1%, 7±0.5%, 7±0.5%, 10±1%, respectively) (Fig 26. A and B). FRET was also measured in the opposed direction (integrin β1–ErbB1) by reversing the donor-acceptor labeling, and a similar tendency was observed (2%, 3%, 4%, 18%).

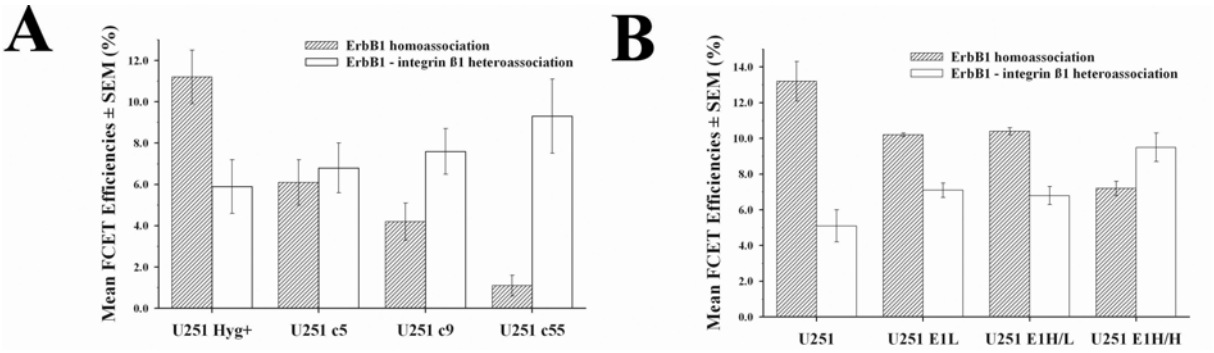

Figure 26. ErbB1 homoassociation and ErbB1 – integrin β1 heteroassociation states on U251 subclones.
On U251 subclones, double labeled for ErbB1 with AlexaFluor 546-528 and for integrin β1 with AlexaFluor 647-TS2 antibodies, FCET experiments were performed as described before. **A-B,** Autofluorescence corrected FCET efficiency values of ErbB1 homoassociation (▨) and ErbB1 – integrin β1 heteroassociation (□) were calculated from flow cytometric data with a custom written software Reflex on U251 subclones transferred with chr7 material (**A**) or transfected with erbB1 gene (**B**). MHC-I – β_2-microglobulin intramolecular FCET efficiency was determined as positive reference control (28 ± 2 %).

tsFRET experiments: integrin β1 recruits ErbB1 from ErbB1 homoclusters

Based on our FCET results, we further wished to analyze the inter-dependence of ErbB1 homoassociation and ErbB1 - integrin β1 heteroassociation on U251 transfectants E1H and E1L at the submicron scale of microscopic resolution. Therefore, we performed tsFRET measurements regarding these molecular interactions, as tsFRET was preliminary proved to be a feasible process to assess the correlation of two distinct molecular interactions. The experimental setup is demonstrated schematically in Fig. 27.

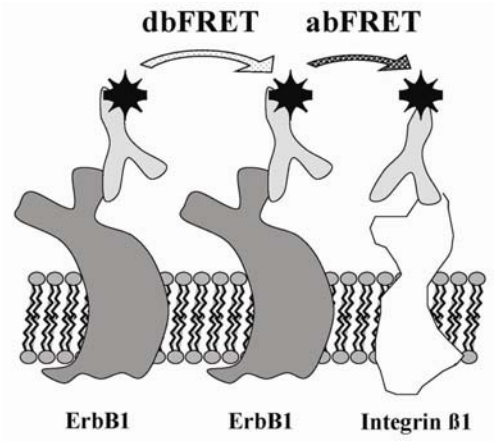

Figure 27. Schematic model of tsFRET experiments. U251 transfectant cells were triple labeled for ErbB1 with XFITC-528 (*left*) and Cy3-528 (*middle*) and for integrin β1 with Cy5-TS2 (*right*) antibodies. Consecutive abFRET (between Cy3-528 and Cy5-TS2) and dbFRET (between XFITC-528 and Cy3-528) measurements were performed.

The ErbB1 homoassociation correlated negatively with ErbB1 – integrin β1 heteroassociation on both E1H/L and E1H/H transfectants, indicating, at the submicroscopic level, a competition by excess integrin β1 for ErbB1. Furthermore, overall tendencies of stronger hetero- and lesser homoassociation in E1H/H over E1H/L, indicated by contour plot peaks and change of the

steepness of trendlines (-0.3373 to 0.090 in E1H/L to E1H/H, respectively), are also of notice coherently with the flow cytometric data. These findings gave rise to an explication that neighboring integrin β1 molecules recruited ErbB1 receptors by disintegrating the ErbB1 homoclusters, observed more prominently on the more radioresistant and high ErbB1 expressing U251 E1H/H subclone (Fig. 28).

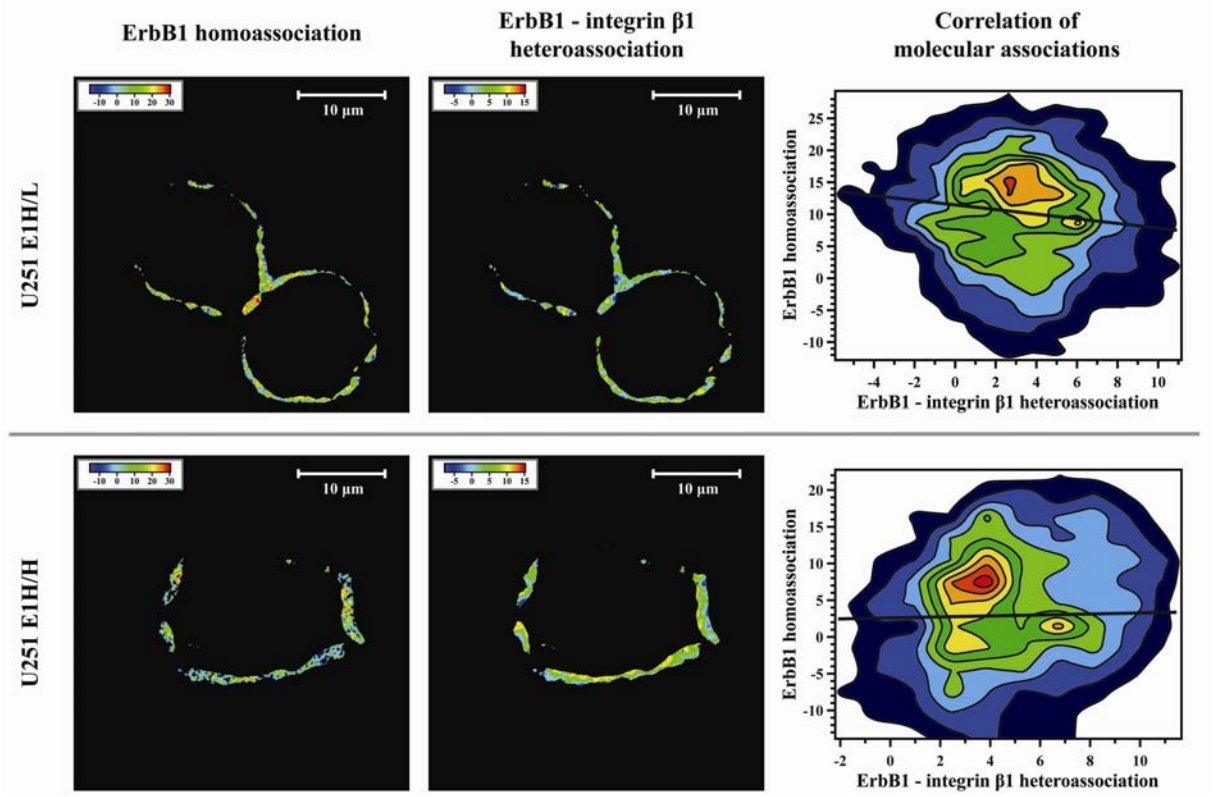

Figure 28. Correlation of ErbB1 homoassociation and ErbB1 - integrin β1 heteroassociation in tsFRET experiments on U251 subclones.

The false color maps of dbFRET (ErbB1 homoassociation, *left*) and abFRET (ErbB1 - integrin β1 heteroassociation, *middle*) efficiencies as well as the contour plots and trendlines (*right*) of the corresponding pixel-by-pixel dbFRET and abFRET efficiency values on U251 E1H/L (*upper series*) and E1H/H (*lower series*) subclones are shown. Note the increase of ErbB1 - integrin β1 heteroassociation and the decrease of ErbB1 homoassociation on U251 E1H/H subclone. Consider the discrete peaks on both contour plots and the shift of peaks toward stronger ErbB1 - integrin β1 heteroassociation and decreased ErbB1 homoassociation underlined by the change of trendline steepness on the more radioresistant U251 E1H/H subclone.

6.3.6. Grade IV astrocytoma exhibit higher ErbB1 and integrin β1 expression than grade II

We determined the ErbB1 and integrin β1 expression on intraoperative fresh frozen tissue sections of grade II and grade IV astrocytoma tumors, in order to corroborate our *in vitro* findings and eventually to explore their possible relevance in comparison with clinical data. Ten patients with grade II (age 18 to 59 years, mean 37.8 years, 5 males and 5 females) and 10 patients with grade IV (age 42 to 73 years, mean 61.4 years, 3 males and 7 females) astrocytoma were involved in the study. Relevant clinical data are summarized in Table VII. Background corrected mean fluorescence intensities of immunofluorescence labeled tissue sections were overall higher in grade IV than in grade II tumors both for ErbB1 and for integrin β1 (Fig. 29). Moreover, two cases in the grade IV group (T53, T82) showed saliently high integrin β1 expression level with less more, but still prominent increase in ErbB1 expression.

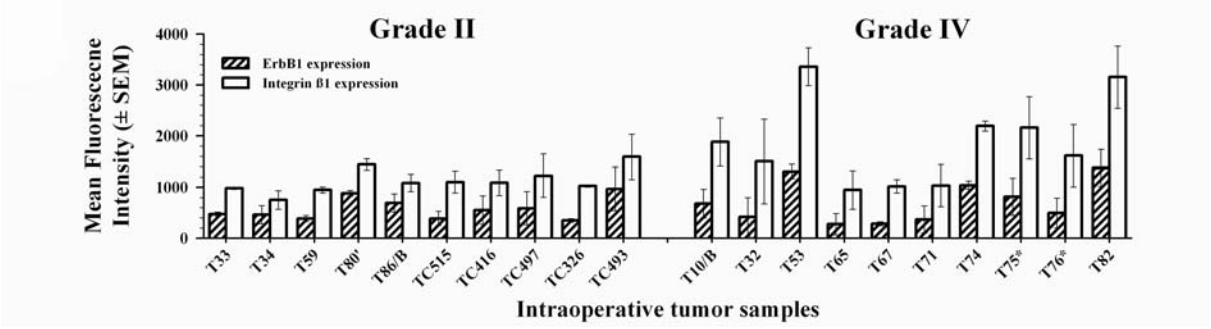

Figure 29. Expression profiles of ErbB1 and integrin β1 molecules on clinical, fresh frozen tissue sections of grade II and IV astrocytoma tumors *in situ*.

Confocal microscopic background corrected mean fluorescence intensity values of ErbB1 (▨) and integrin β1 (□) molecules on grade II (*on the left*) and grade IV (*on the right*) intraoperative astrocytoma tissue sections are shown.

Table VII. Clinical findings, therapy and survival profiles of patients studied.[1]

	N°	Code	Therapy	Relaps	Survival
Astrocytoma, Gr. II.	II./1.	T33	Op+Op	48 months	>82 months (alive)
	II./2.	T34	Op+Rx	50 months	77 months
	II./3.	T59	Op+Rx	residual tumor	42 months
	II./4.	T80'	Op+Rx+Op+Op	15 months	31 months
	II./5.	T86/B	Op+T	14 months	16 months
	II./6.	TC515	Op	-	>34 months (alive)
	II./7.	TC416	Op	33 months	>40 months (alive)
	II./8.	TC497	Op+Op+Rx	32 months	>36 months (alive)
	II./9.	TC326[2]	Op+Op	-	>41 months (alive)
	II./10.	TC493	Op+Rx	3 months	16 months
Astrocytoma, Gr. IV. Glioblastoma multiforme	IV./1.	T10/B	Op+Rx	biopsy	10 months
	IV./2.	T32	Op+Rx	4 months	7 months
	IV./3.	T53	Op+Rx+Op+T	2 months	4 months
	IV./4.	T65	Op+Rx+Op	4 months	8 months
	IV./5.	T67	Op+Rx	4 months	7 months
	IV./6.	T71	Op+Rx+Op+Rx+Op	12, 12, 6 months	40 months
	IV./7.	T74	Op+Rx	13 months	16 months
	IV./8.	T75*	Op+Rx	4 months	10 months
	IV./9.	T76*	Op+Rx+BCNU	4 months	8 months
	IV./10.	T82	Op+Rx	2 months	4 months

[1]List of the intraoperative astrocytoma tumor samples and the clinical findings, therapeutic interventions, outcomes and survival profiles of the corresponding patients with glial tumors are summarized. Abbreviations: Op=Operation, Rx=Radiotherapy, BCNU=BCNU chemotherapy, T=temozolomide chemotherapy.

[2]In the case of TC326 the start of the follow-up time in this study was actually a second operation; the tumor first had been diagnosed and resected as a grade I astrocytoma 7 years before.

6.3.7. ErbB1–integrin β1 association is increased in grade IV versus grade II astrocytoma

Next, we planned to analyze the ErbB1 - integrin β1 interaction in clinical samples. For this purpose, we successfully adapted the confocal microscopic abFRET method on fresh frozen tissue sections *in situ*. Thus, the ErbB1 - integrin β1 heteroassociation could be quantitated on the samples enrolled in the study. As positive control, MHC-I – β2-microglobulin intramolecular abFRET efficiency was determined and was 14 ± 0.3 %. Exemplary images of ErbB1 (donor) and integrin β1 (acceptor) fluorescence, and the false color map of pixel-by-pixel abFRET efficiency values on grade II and grade IV astrocytoma samples (TC515 and T82, respectively) are shown in Fig. 30. The representative abFRET images reflect apprehensively that grade IV astrocytoma (T82) showed higher ErbB1 - integrin β1 heteroassociation than grade II (TC515) did.

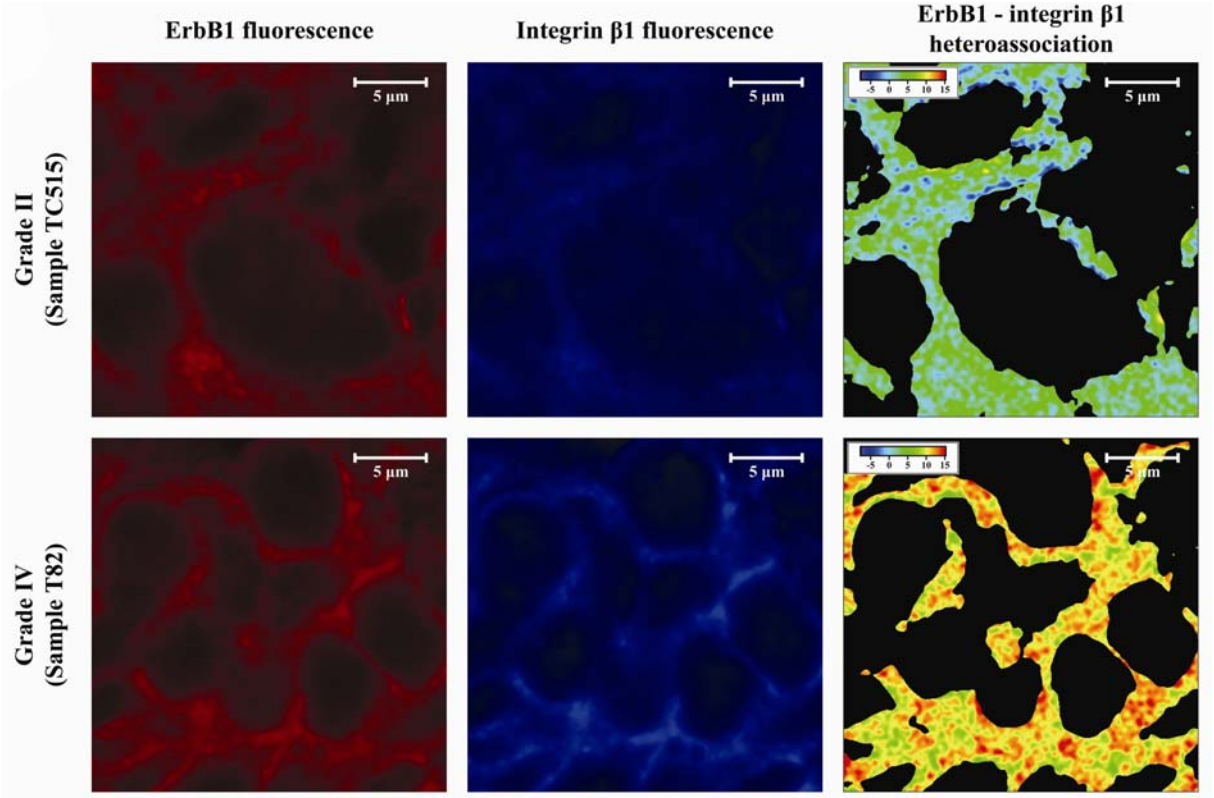

Figure 30. Microscopic abFRET experiments on ErbB1 - integrin β1 heteroassociation states in clinical, fresh frozen tissue sections of grade II and IV astrocytoma tumors *in situ*.

abFRET measurements were performed between ErbB1 and integrin β1 on double labeled astrocytoma sections (Cy3-528 for ErbB1 and Cy5-TS2 for integrin β1) in the cases of grade II (sample TC515, *upper series*) and grade IV (sample T82, *lower series*) intraoperative astrocytoma tissue sections according to the technical steps detailed in the Material and methods. Of the investigated grade II and grade IV astrocytomas, representative fluorescence images of ErbB1 (*left*) and integrin β1 (*middle*) expressions and the false color abFRET images (*right*) are shown. Intra-molecular abFRET efficiency between MHC-I and β_2-microglobulin was determined as positive reference control (14.1 ± 0.3 %).

Overall, abFRET on grade IV tumors showed stronger ErbB1 - integrin β1 heteroassociation than did on grade II tumors (Fig. 31A). The clear separation of the two disease groups was verified by binary logistic regression. Furthermore, stepwise binary logistic regression on ErbB1 expression, integrin-β1 expression and ErbB1 - integrin β1 abFRET efficiencies identified this heteroassociation as a single determinant of tumor grade (Fig. 31B).

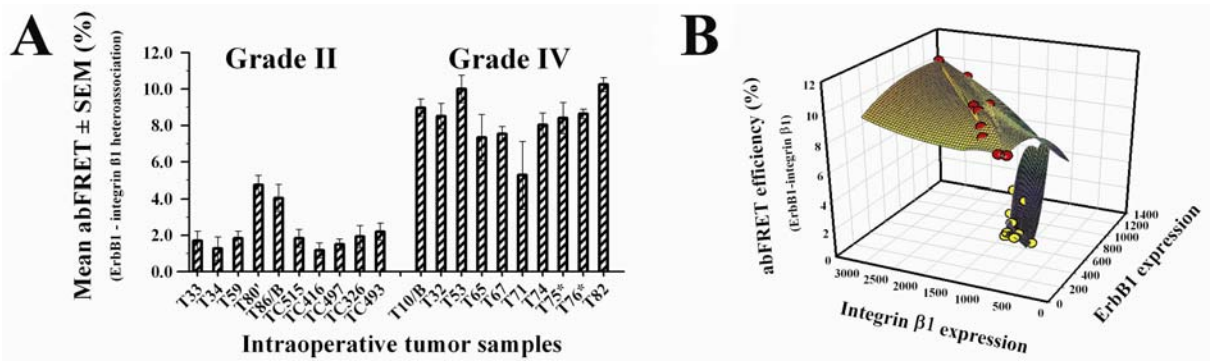

Figure 31. ErbB1 - integrin β1 heteroassociation states and 3D distribution of the results on clinical, fresh frozen tissue sections of grade II and IV astrocytoma tumors *in situ*.

A, Summarized results of abFRET experiments on the investigated clinical, fresh frozen tissue sections of grade II (*left*) and grade IV (*right*) astrocytomas *in situ* are shown. **B,** Elucidatory three dimensional correlation of ErbB1, integrin β1 expression levels and the corresponding ErbB1 - integrin β1 abFRET efficiencies on grade II (*yellow dots*) and grade IV (*red dots*) astrocytoma tissue sections. Note the clear separation of the cases by the abFRET efficiencies (*axis Z*).

6.3.8. Statistical analysis: ErbB1-integrin β1 association potentially predicts therapy outcome

Integrin β1 expression levels were significantly higher on grade IV tumors than on grade II tumors (p=0.038), and integrin β1 was proved to significantly contribute to the prediction of survival in multiple stepwise linear regression analysis, as well (p=0.05). However, despite the well documented contribution of ErbB1 overexpression to gliomagenesis and remarkable salience in ErbB1 expression levels in two cases of the grade IV group (T53, T82), the overall difference of ErbB1 expression levels between grade II and IV tumors was not significant in this study (p=0.379). Alongside with significantly higher ErbB1 - integrin β1 heteroassociation states on grade IV tumors (p<0.001), this interaction was proved to be a single determinant of tumor grade as described above (Fig. 31B, *OR*=8716). In addition to showing prognostical significance in survival analysis of pooled grade II and grade IV cases (p<0.001), multiple stepwise linear regression highlighted ErbB1 - integrin β1 abFRET efficiency values as the predictors of time-to-relapse both for pooled grade II and IV samples and for the grade IV cases alone (p=0.094 and 0.085, respectively).

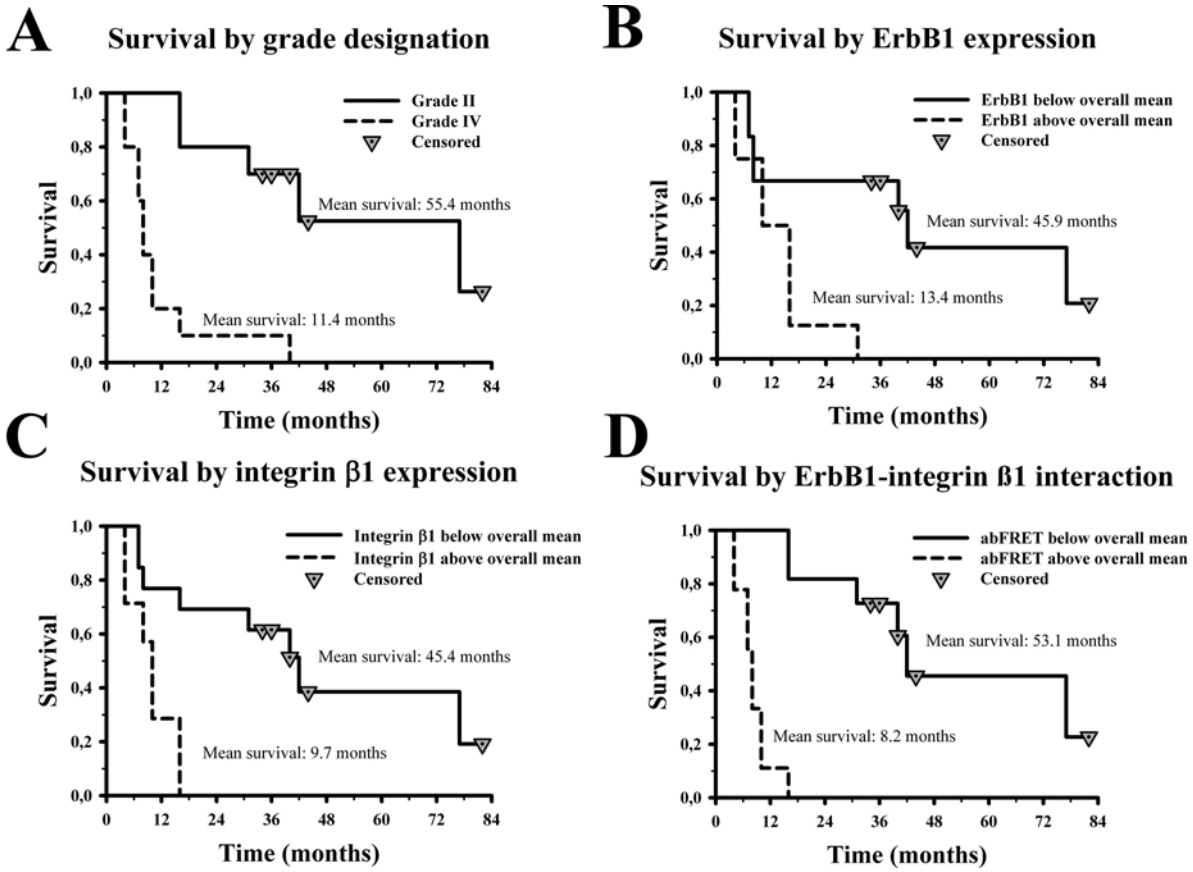

Figure 32. Prognostic significance of ErbB1, integrin β1 expression levels and that of the degree of their heteroassociation in patients with astrocytic tumors.

Overall survival by grade designation (grade II and IV tumors) was determined by the Kaplan-Meier method **(A)**. Survival of patients with tumors showing ErbB1 (**B**), integrin β1 (**C**) expression levels and abFRET efficiency states (**D**) below (▬) or above (▬ ▬) the overall mean, respectively, were also compared. Statistical comparison of the indicated patient-groups was estimated by the log-rank test followed by *post-hoc* Holm-Sidak procedures. Significance values are given as *p* values ($p<0.001$, $p=0.014$, $p=0.004$ and $p<0.001$ for grade, ErbB1, integrin β1 and the ErbB1 – integrin β1 heteroassociation, respectively).

Overall, survival of patients was coherent with known differences between grade II and grade IV astrocytoma (Fig. 32). Patients with grade II tumors all survived for over a year after surgery. In this group, five patients received radiotherapy based on the severity of the growing mass, localization or postoperative recurrence, but all of them developed relapse, one of which (T80') transformed into a malignant glioblastoma. Their survival times were between 16 and 77 months. Of the non-irradiated grade II tumors, three also recurred; T33 and TC416 after 48 and 33 months, with survival over 6 years and 40 months, respectively, whereas time to relapse and survival for T86/B were much lower (14 and 16 months) after surgery. Notably, this tumor (T86/B) with the shortest survival, along with T80' giving rise to

a grade IV recurrence, showed the highest ErbB1 – integrin β1 heteroassociation rates within the grade II group (see Fig. 31A).

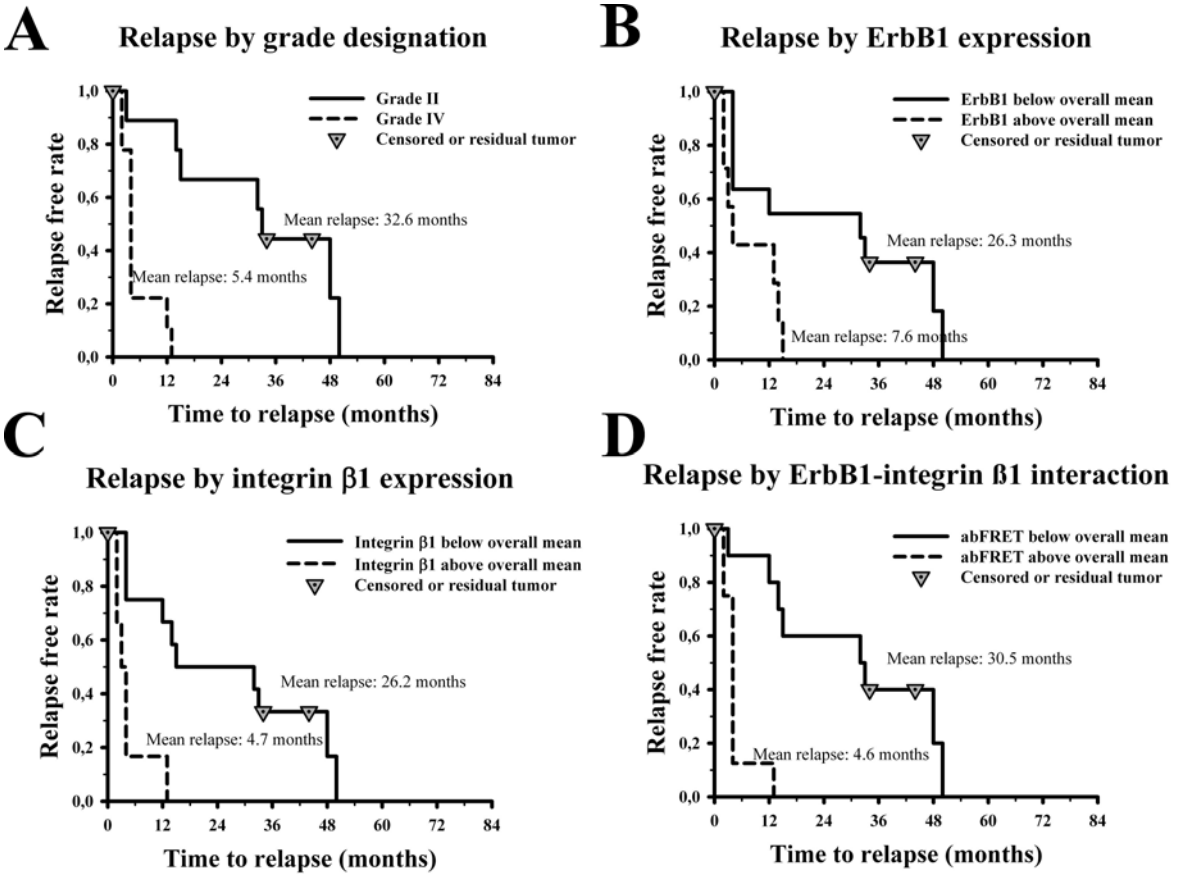

Figure 33. Prognostic significance of ErbB1, integrin β1 expression levels and that of the degree of their heteroassociation in the progression-free survival of patients with astrocytic tumors.

The progression-free survivals by grade designation (grade II and IV tumors) was determined by the Kaplan-Meier method **(A)**. The time-to-relapse periods of patients with tumors showing ErbB1 (**B**), integrin β1 (**C**) expression levels and abFRET efficiency states (**D**) below (▬) or above (▬ ▬) the overall mean, respectively, were also compared. Statistical comparison of the indicated patient-groups was estimated by the log-rank test followed by *post-hoc* Holm-Sidak procedures. Significance values are given as *p* values ($p<0.001$, $p=0.014$, $p=0.004$ and $p<0.001$ for grade, ErbB1, integrin β1 and the ErbB1 – integrin β1 heteroassociation, respectively).

Radiotherapy was administered to all patients with grade IV tumors, but all of them developed recurrence; seven patients within 6 months, and two (T71, T74) after 12-13 months. In the case of T10/B, only a biopsy could be managed. Overall, survival was 4-16 months after surgery, but diminished below only 6 months after a relaps occured. The highest ErbB1 and integrin β1 expression levels, and ErbB1 – integrin β1 heteroassociation were detected in tumors of patients, who developed the earliest recurrence (2 months, T53 and T82) and showed the shortest survival (4 months). Furthermore, the lowest ErbB1 – integrin β1

heteroassociation was observed in the case T71 (developing multiple recurrences, resected 3 times and irradiated after every surgical intervention), representing a patient with an exceptionally longer survival (40 months) compared to the rest of this cohort.

We accomplished the statistical survey of clinical data by performing Kaplan-Meier analysis. Overall and progression-free survival of grade II versus grade IV groups, as well as groups formed by splitting the pooled samples into below versus above the overall mean expression level of ErbB1, integrin β1 and their mean heteroassociation state were compared. ErbB1 - integrin β1 heteroassociation appeared to be as reliable determinant of survival as the histopathological grading ($p<0.001$ for both), whereas ErbB1 and integrin β1 levels showed less, but still significant differences ($p=0.014$, $p=0.004$) (Fig. 32). A similar trend was ascertainable for progression-free survivals, with $p<0.001$ for grade, integrin β1 expression and heteroassociation, and with $p=0.014$ for ErbB1 expression (Fig. 33).

7. DISCUSSION

Vast amount of literary data have so far corroborated that dynamic interactions of membrane proteins are responsible for the disturbed regulation of signal transduction processes in malignant tumors. Given the substantial role of certain growth factor receptors in the background of tumorous transformations, novel therapeutic regimens tend to include anti-cancer agents that target these proteins and their downstream signaling routes. In this aspect, members of the ErbB tyrosine kinase family were extensively studied and reported to contribute to the development of several types of tumors. The administration of inhibitors targeting ErbB signaling has now also come to a clinical phase, however, resistance to therapy occurs quite frequently, thereby hampering treatment success.

Since ErbB2 overexpression was shown to appear on the cell surface of malignant tumor cells, contrary to health tissue, blocking the signal transduction of this molecule seemed to be a reasonable and readily achievable path of prospective chemotherapeutic approaches. After intensive research on this topic, the humanized inhibitory monoclonal antibody, trastuzumab, against ErbB2 was approved for clinical application by the FDA in 1998. Although clinical outcome of patients with ErbB2 positive breast cancer has remarkably improved by the introduction and clinical use of this specific ErbB2 targeting modality, the therapeutic break-through is still incomplete because development of resistance can be observed in a great number of cases, even among initial responders. Comprehensive investigations revealed a broad spectrum of resistance mechanisms responsible for the failure of trastuzumab therapy, and it has been suggested that heterodimerization tendency of ErbB molecules with other cell membrane species can affect their association patterns leading to diverse downstream events that sustain the mitogenic potential (see sections 2.4.2, 3.1.3 and 3.2.3). However, despite the large number of studies on the role of ErbB proteins in cancer, mechanism of trastuzumab resistance remained still obscure.

As recent evidence supports the functional cooperation of cell adhesion integrin molecules and ErbB family members, we aimed to characterize the molecular interactions of ErbB2 and integrin β1 molecules and compare the functional significance of their interplay in trastuzumab sensitive and resistant cell lines.

Flow cytometric screening of the expression level of ErbB receptors and integrins revealed that trastuzumab resistance was associated with a lower ErbB2 expression that was accompanied by a higher integrin β1 expression on the cell surface both in breast and gastric cancer cell lines (Table I). The other members of the ErbB family (ErbB1, ErbB3 and ErbB4)

and the investigated integrin molecules (β3 and α6) did not show significant differences in their expression level neither on breast cancer nor on gastric cancer cell lines differing in their trastuzumab resistance. The reciprocal relationship of the ErbB2 and integrin β1 expression, however, suggested that there may be a regulatory mechanism in the background of trastuzumab resistance concerning these molecular species. To reveal the possible interactions of ErbB2 and integrin β1 molecules, the first experiments were conducted to unveil their closer association by measuring their colocalization in the membrane at the resolution of the optical (confocal) microscope. The assumption was triggered by literature data on the modulating effect of integrins in the signal transduction properties of growth factor receptors [96]. Detecting the distribution of lipid rafts was also included with the colocalization measurements, because they are well known to function as signal transmission platforms harboring various kinds of transmembrane receptors [31, 92]. Characterization of these membrane microdomains depends on the spatial, temporal and chemical resolution of the methods used to detect them, thus different approaches can provide distinct results [221]. In our experiments, we used CTX-B that binds to the GM1 component of lipid rafts and induces co-migration of GPI-anchored proteins by crosslinking them [222]. Thereby, the tenacity of raft-association of the colocalized signaling proteins ErbB2 and integrin β1 could also be checked in the crosslinking setup.

The results revealed an almost complete colocalization between ErbB2 and integrin β1 molecules on quiescent cells compared to the positive control (Table II). Raft associating tendency of ErbB2 and integrin β1 proteins was also underlined, however, we observed a remarkable difference between the breast and gastric cancer cell lines in this respect, and regardless of trastuzumab resistance; colocalization of ErbB2 and integrin β1 molecules to lipid rafts were markedly lower on breast cancer cells than those on gastric adenocarcinoma cell lines (Fig. 14). Crosslinking of lipid rafts or integrin β1 significantly decreased the colocalization between the crosslinked and the other two species, whereas the cross-correlation values of the remainders, i.e. not crosslinked, abided undisturbed. In addition, trastuzumab treatment brought intriguing findings. The colocalization of both ErbB2 and integrin β1 proteins to lipid rafts decreased significantly on the breast cancer cell lines, but contrary, no such a tendency could be observed on the gastric cancer cell lines. Moreover, trastuzumab treatment did not distract the association of ErbB2 and integrin β1 molecules on neither breast cancer nor gastric cancer cell lines regardless of trastuzumab resistance.

These results allowed for a partial explanation, but also called for the more detailed investigation of the ErbB2 - integrin β1 heteroassociation. On the one hand, different

molecular properties of tumors of different origin can critically affect the responsiveness of cells to distinct treatments, which possibly involves the modulating effect of other neighboring molecules to otherwise strong molecular associations (sustained association of ErbB2 and integrin β1 after CTX-B induced crosslinking of lipid rafts). On the other hand, the association of ErbB2 and integrin β1 molecules seems to be dynamically modifiable regarding both their heteroassociation, based on the disintegration of ErbB2 - integrin β1 association upon integrin β1 crosslinking, and their raft associating tendency, based on their co-migration from lipid rafts after trastuzumab treatment.

Along this deductive line, we intended to analyze the closer molecular interactions of ErbB2 and integrin β1 molecules by FCET measurements with a view to the possible interfering effect of the ErbB1 receptors in the trastuzumab resistance of breast cancer cells. In general, homoassociation of ErbB2 was significantly higher on the trastuzumab sensitive cell lines (both breast cancer SK-BR-3 and gastric cancer N87), whereas the extent of ErbB2 - integrin β1 heteroassociation displayed a remarkable increase on the trastuzumab resistant JIMT-1 breast cancer cells that expressed an extremely high number of integrin β1 molecules in the membrane (Table I and III). Notably, the ErbB1 homoassociation and ErbB1 - ErbB2 heteroassociation were considerably higher on the trastuzumab sensitive SK-BR-3 cell line, despite the relatively low and similar ErbB1 expression profile of both the trastuzumab sensitive (SK-BR-3) and resistant (JIMT-1) cells. In contrast, the ErbB1 - integrin β1 heteroassociation rate did not show any significant difference, however, turned out to be prominently high on both the investigated lines regardless of the meaningfully differing integrin β1 expression levels that was also worthy of further consideration (Table IV). We also aimed at disclosing the alterations of molecular interactions involving ErbB1 by FCET measurements after treatment with EGF, trastuzumab or heregulin. Based on the results, EGF-induced ErbB1 activation led to an elevated heteroassociation tendency of the ErbB1 receptor, but the treatments - summing up - did not bring unexpected results and did not reveal discernible differences between the association state of ErbB1 on the sensitive SK-BR-3 and the resistant JIMT-1 breast cancer cell lines (Table IV).

Next, to untangle cell function related changes in the activation of ErbB2 receptors, we performed Western blot analysis on ErbB2 and phosphorylated ErbB2 proteins after treatment with trastuzumab and/or integrin β1 crosslinking on trastuzumab sensitive SK-BR-3 and resistant JIMT-1 cell lines. Treatment with trastuzumab induced the phosphorylation of ErbB2 on both cell lines. Notably, crosslinking of integrin β1 molecules caused a slight increase in ErbB2 tyrosine phosphorylation in SK-BR-3 cells, however, no additional increase

in the trastuzumab-induced ErbB2 phosphorylation could be observed on either SK-BR-3 or JIMT-1 cell line in spite of the extreme high integrin β1 expression level on the latter (Fig. 16). The lack of effect of integrin β1 crosslinking on the trastuzumab-induced ErbB2 phosphorylation could probably be accounted for by the spatial separation of the molecules after integrin β1 crosslinking. Therefore, ErbB2 was out of the reach of integrin β1 molecules, however, the stimulatory $\beta1_A$ and the inhibitory $\beta1_C$ splice variants of the integrin β1 molecule were not distinguishable, since the anti-integrin β1 antibodies used in our experiments bind to the extracellular part of the molecule [56, 223]. These results suggested that despite a weak functional interaction between the ErbB2 and integrin β1 molecules, trastuzumab-induced changes in the activation state of ErbB2 receptors are not necessarily altered even by high integrin levels.

Taken together, these data proved a raft associating tendency for both ErbB2 and integrin β1 proteins, further supporting the role of lipid rafts as signal transduction platforms, however, these transmembrane proteins seemed to be less tightly raft-bound than GPI-anchored proteins and to be more likely loosely attached to the periphery of lipid raft domains. In addition, crosslinking experiments, extended with FCET results, proved ErbB2 and integrin β1 proteins molecularly associated with each other, but their interaction was found to be relatively weak, and could be dynamically modified. Trastuzumab resistance could not be explained solely by the lower ErbB2 or the higher integrin β1 expression levels of the resistant cells, and the difference in expression levels did not alter the trastuzumab-induced ErbB2 activation. Thus, although a strong correlation between trastuzumab resistance and high integrin β1 expression could not possibly be established on the basis of our studies, we may speculate that a high expression level of integrin β1 molecules alters the signal transduction properties of cancer cells, thereby increasing their metastatic potential and presenting an alternative pathway for the activation of the MAPK and Akt pathways.

Nevertheless, our results corroborated the involvement of integrins in growth factor receptor-mediated signaling and implied that the functional state of protein interactions cannot be assessed by detecting exclusively their expression levels nor by determining their mutual interference "*in flagrante delicto*" as membrane proteins compete with each other for a limited number of association partners that may change over time in the evolution of malignancy.

Thus, disclosure of dynamic interactions of membrane proteins would vastly enhance our knowledge on signaling events, which thereby probably diverge multitudinously and eventually affect cells' fate in a versatile way. Therefore, we developed, and demonstrated the applicability of a method, tsFRET, to measure the relationship between the association states

of two molecule-pairs of three arbitrarily chosen molecular species. Previously, several new approaches have already been introduced for analyzing the interactions of up to three molecules in solution at the single molecule level, such as the pulsed interleaved excitation (PIE) method [224], the three-color alternating-laser excitation (3c-ALEX) method [225], simultaneous fluorescence decay time measurements [226], multiparameter single-molecule fluorescence spectroscopy (SMFS) [227] and confocal multicolor single-molecule spectroscopy [228]. However, our method enabled the analysis of adherent cellular systems under such circumstances, where background from autofluorescence or higher density of labels would have impeded single molecule spectroscopy.

The tsFRET approach involves abFRET and dbFRET measurements on the same sample consecutively, using three appropriately chosen fluorophores, e.g. XFITC (D1), Cy3/Alexa555 (A1≡D2), and Cy5 (A2). In this case, the abFRET method can sequentially be followed by the dbFRET procedure, because the excitation wavelengths (543 nm for D2 and 633 nm for A2) used in abFRET do not excite D1 and the spectral overlaps between the emission spectra of A1≡D2 and the absorption spectrum of D1 are negligible. Based on the spectral properties, normalized fluorescence intensities, overlap integrals and normalized FRET efficiencies, the Alexa555-Cy5 pair was proved more reasonable for abFRET experiments and was used further on instead of the conventional Cy3-Cy5 pair [229].

The expediency of the tsFRET method was tested in a triple-labeled model system using three non-competing monoclonal antibodies binding to the same ErbB2 molecule. In this experimental setup, the FRET values represented intramolecular, and hence constant, separation distances between the fluorophores of both FRET pairs. The consecutive application of dbFRET after abFRET did not significantly alter the FRET values compared to those measured conventionally on double-labeled cells, and the lack of correlation between the dbFRET and abFRET values pixel-by-pixel was also in accordance with expectations regarding these intramolecular distances. These findings, and the narrow gaussian distribution of both dbFRET and abFRET values implied that the relationship of two molecular interactions sharing a common species can be reliably measured by the tsFRET method.

After confirming its applicability, we wished to use the tsFRET approach for assessing the coincident homo- and heteroassociation states of ErbB2 and integrin β1 molecules, in order to analyze the potential interfering influence of integrin β1 on ErbB2 homoassociation behind the trastuzumab responsiveness of the cells. As for recent data, suggesting the masking effect of certain large cell surface sialomucins to the trastuzumab-binding epitopes of ErbB2 [148, 149], we aimed at screening the expression level of CD44 on the investigated cell lines.

As initial flow cytometric experiments on receptor expression disclosed extremely high level of CD44 on trastuzumab resistant cell lines, in addition to the confirmation of lower ErbB2 and higher integrin β1 levels, extended experiments were performed and included the exploration of the modulating effect of CD44 on the association profile of ErbB2.

CD44 is a membane glycoprotein - existing in numerous splice variant isoforms - which recognizes hyaluronic-acid and other ECM molecules (such as osteopontin, collagens or matrix-metalloproteases), and indeed, can also interact with growth factor receptors via heparane-sulfate conjugation as well as binding and presenting certain heparin binding growth factors (e.g. EGF) for growth factor receptors - even on a neighboring cell, as it was shown earlier [230]. Following its discovery in 1980 [231], monoclonal antibodies - radiolabeled or DM1 mertansine conjugates - against the CD44v6 isoform have also reached clinical phase [232].

After the characterization of the expression profiles, we determined the association states of ErbB2, integrin β1 and CD44 molecules of the investigated cell lines by FCET measurements. The ErbB2 homoassociation turned out to be high on both trastuzumab sensitive cell lines (SK-BR-3 and N87), where saliently high ErbB2 expression was associated with depressed expression of integrin β1 and CD44, both heteroassociating with ErbB2. Furthermore, the ErbB2 – integrin β1, ErbB2 – CD44 and integrin β1 – CD44 heteroassociations were modestly high on the resistant JIMT-1 cells that showed extremely high levels of integrin β1 and CD44. The similarly resistant MKN-7 cells, however, displayed weak ErbB2 – CD44 and integrin β1 – CD44 heteroassociation, though still high, nevertheless markedly lower integrin β1 and CD44 expressions levels could be detected. These findings again substantiated that molecular behaviour, and hence treatment sensitivity to molecular targeting, of tumors can be strongly influenced by their origin and/or differing expression profiles, i.e. overexpressed molecules seem to compete with each other for finding association partners, perturbing this way their mutual interactions.

Therefore, we used the tsFRET method to map the inter-dependence of the associations of ErbB2, integrin β1 and CD44 proteins, since this method was previously proved to be an expedient approach to investigate the relationship between association states of different molecular species. According to the contour plots and the trendlines generated from dbFRET and abFRET values, we observed a clear anti-correlation between ErbB2 – integrin β1 heteroassociation and ErbB2 homoassociation on trastuzumab sensitive SK-BR-3 and N87 cells, whereas a modest positive correlation between ErbB2 – integrin β1 and integrin β1 – CD44 heteroassociation could be discerned on trastuzumab resistant MKN-7 gastric cancer

cells. The similarly resistant JIMT-1 breast cancer cells, however, exhibited no clear correlation regarding ErbB2 – integrin β1 and integrin β1 – CD44 heteroassociation, which is best explained by the extremely high integrin β1 and CD44 expression levels on this cell line, and that ErbB2, expressed at a much lower level, could interfere only with a small portion of integrin β1 and CD44 molecules leaving the association state of the majority of them undisturbed.

Moreover, FRET values on the same molecular interactions obtained by different measurement approaches (FCET, dbFRET and abFRET) were markedly differing in several relations (Table V and VI), which raised the need for further, detailed analysis and explanation of the results. That is, when comparing intramolecular FRET values that are likely unaffected by cytoskeletal organizing forces, FCET gave higher values than those measured by dbFRET, which were, in turn, still higher than those gained by the abFRET method. However, intriguingly, dbFRET values of ErbB2 – integrin β1 heteroassociation were significantly higher on most cells (except JIMT-1) than those from FCET measurements, whereas FCET results were in agreement with microscopic ones for ErbB2 homoassociation. On the one hand, the discrepancy between FCET and the microscopic FRET results can be explained by the pronounced sensitivity of photobleaching methods to environmental factors such as the local concentration of fluorochromes and oxygen [233]. Furthermore, the considerable overestimation by dbFRET compared to abFRET can be related to the different weighting of the methods [234], and to the fact that the dbFRET method requires a reference donor photobleaching decay time measured in the absence of the acceptor. However, the integrin β1 – CD44 heteroassociation state was similarly higher on MKN-7 cells by using either dbFRET or abFRET, as compared with that gained by the FCET method, implying that the overestimating effect of dbFRET is not solely responsible for the divergence of the results. Thereby, the well known tendency of membrane receptors to gather in signaling platforms - especially cell adhesion molecules in focal adhesion complexes - raises the issue whether their cell membrane distribution affects the results achieved by different investigation methods. This particularly emerges in the case of interpreting FCET and microscopic FRET results, as the former represents FRET efficiency values from whole cells and necessitates trypsinizing them, whereas the latter shows the membrane distribution of FRET efficiency values, but generally in a horizontal optical section.

That is why we wished to further investigate whether the trypsinization and the membrane distribution of molecules along the 'z' axis (from the bottom to the top of the cell) affect the results achieved by the different FRET approaches. According to our results,

trypsinized and cyto-centrifuged cells in microscopy gave very low FRET values in contrast to adherent cells. In addition, the distribution of FRET between ErbB2 and integrin β1 along the 'z' axis demonstrated that higher FRET efficiency values were observed in the membrane apposed to the glass surface than towards the top of the cell (Fig. 21). Considering that the microscopic FRET measurements were performed on adherent cells, and images were taken usually of the attached bottom layer of the cells, the higher expression level and probably increased activation state of integrin β1 and CD44 at these focal adhesion points could strongly affect their interactions, which were, in turn, disrupted when cells were trypsinized for FCET measurements.

Finally, it has to be emphasized that a pair of high FRET values, measured between pairwise combinations of three molecules in the tsFRET experimental setup, does not imply the presence of a trimer, because both pairwise dimers can separately exist in a single pixel at the resolution of the microscope. The tsFRET approach, thus, yields information about the correlation of the heteroassociations and not about a definite trimer formation of three investigated molecules in a single pixel, whose size is determined by the resolving power of the microscope. Therefore, the tsFRET method supplements, but not supplants the triple-FRET method [235] and can be used to reveal cross-associations and mutual interference of molecular interactions on a pixel-by-pixel basis.

In conclusion, according to the results of our tsFRET experiments, it may be assumed that the homoassociation state of ErbB2 is dynamically modulated by its interaction with integrin β1, and it is also tempting to speculate that the heteroassociation and activation of cell adhesion molecules can enhance the activity of survival pathways during disease progression that can boost proliferation and may give rise to the development of metastasizing ability.

Along similar lines, increasing evidence has been provided on the interaction of certain growth factor receptors and cell adhesion molecules, i.e. ErbB1 and integrin β1, in the background of radioresistance of brain tumors. Coherent with these observations, integrin β1 mediated PI-3K / Akt-PKB signaling was also shown to be critically involved in glioma cell adhesion and prolonged cell survival, and integrin β1 inhibitors have already been proved to be potentially promising radiosensitizers for glioblastoma *in vitro* (see section 3.2.2.). Accordingly, huge research efforts are ongoing to address more efficacious combined therapeutic strategies in the treatment of invasive astrocytomas. However, despite ever-broadening therapeutic options, prognosis of patients with high grade astrocytic tumors still remains tremendously unfavorable. Perifocal relapses ususally emerge from unresectably scattered tumor cells that have migrated to the surrounding intact brain tissue.

Molecular data have thus far indicated that integrins (i.e. integrin αV and β1) contribute to the more accelerated, and hence more infiltrative, migration of higher grade astrocytic tumor cells, which could be completely diminished by blocking integrin αV and β1 with specific monoclonal antibodies [236]. This functional role of integrin αV and β1 correlated well with our results, as initial screen on several members of the integrin family disclosed the pronounced expression of integrin αV and β1 in U251 astrocytoma subclones (Fig. 22). Moreover, inhibition of integrin αVβ3 signaling with the RGD mimetic peptide cilengitide has now reached the clinical phase [189]. However, the beneficial effects were more conceivably accounted for by the direct suppressing effects on endothelial cells and tumor vascularization [188], which were, in turn, also aligned with our results that integrin β3 was expressed at an utterly low level in U251 subclones (Fig. 22).

Indeed, the term "cell adhesion mediated therapy resistance" of glioblastoma cells is now steadily evolving to describe the potential role of survival pathways originating from cell-cell or cell-ECM interactions [237]. The theory is also substantiated by the different clinical behavior of infiltratively growing primary brain tumors and locally well confinable, isolated metastases of originally infiltrative tumors of different origin (e.g. breast cancer) (see Fig. 34).

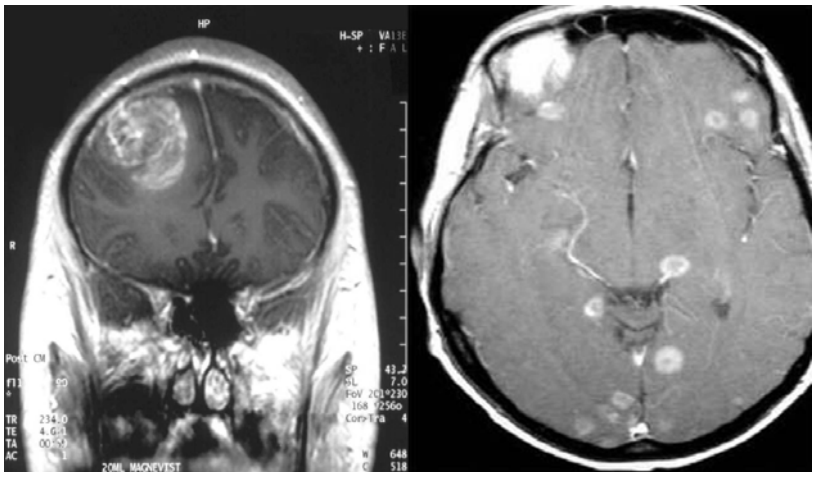

Figure 34. CT scans of a grade IV glioma (*left*) and intracranial metastases of a primarily invasive breast cancer (*right*) are shown. Notably, the locally infiltrative growth of a grade IV astrocytoma leads to pronounced mid-line dislocation, while the multiplex metastases of a primarily infiltrative breast cancer are well confined.

In addition, targeting downstream signaling of ErbB1 and integrin proteins has also been found to augment the anti-tumor and anti-angiogenic effects of radiotherapy [238-241]. However, the results have been achieved *in vitro* and *in xenograft* model experiments at the most, but the expression profiles and molecular associations of ErbB1 and integrin β1 molecules may differ on individual human glioblastoma tumors *in situ*, which may prejudice treatment and patient outcome. After its first description on non-human primate tissues [242],

the use of steadily improved FRET techniques has widely spread out over the recent years, becoming more and more prevalent in the characteriziation of molecular interactions even in fresh frozen or fixed human tissues [107, 108, 243, 244]. FRET imaging was also proved to be expedient in evaluating associations between cell surface receptors and ECM proteins in 2D or 3D cultures and tissues [245].

As our initial screen proved integrin β1 overexpressed in U251 astrocytoma subclones with extra chr7 fragments, we wished to analyze the molecular interactions and signaling outcomes of ErbB1 and integrin β1 molecules behind the radioresistance, and to further investigate their possible role in clinical samples *in situ* that may warrant the application of certain single or combined therapeutic modalities in selected tumors.

Interestingly, previously documented decreasing radiosensitivity parallel with increasing ErbB1 overexpression [204] was accompanied by increasing integrin β1 expression levels in U251 chr7 transferred subclones. Alongside with ErbB1, the PMS2, MAD1 and FAM126A proteins are also coded on chr7 that may be responsible and can contribute to developing radioresistance via repairing mismatch DNS after radioinjury, controlling mitotic assembly, and balancing the tumor-suppressing effect of the β-catenin pathway, respectively. However, integrin β1 is not coded on chr7, so, its overexpression may be initiated by a regulatory pathway activated by ErbB1 signaling. To confine the results to the clear effect of ErbB1 overexpression on radiation resistance, that is, to differentiate from the regulatory effects of other genes coded on chr7 and to verify ErbB1 induced integrin β1 upregulation, erbB1 gene-transfected U251 subclones were generated, exhibiting increased (E1L), and highly increased (E1H) ErbB1 expression.

In this cellular model system, ErbB1 overexpression was also accompanied by increased integrin β1 expression, and with increased radioresistance, as well. Interestingly, integrin β1 expression did not increase beyond a certain level regardless of how much ectopic ErbB1 was in the cell membrane. The difference of parameters α and β in the linear-quadratic model implicated that survival of cells was dependent mainly on the integrin β1 expression level, whereas additional surplus ErbB1 promoted colony forming capability, which was rendered unnecessary by paracrine signals of denser cultures. Accordingly, the subpopulation (E1H/H) carrying highly increased amounts of ErbB1 gradually disappeared (E1H/H → E1H/L drift), indicating that extreme ErbB1 overexpression did not carry a selection advantage, when the culture was passaged *en mass*. Thus, it appears that surplus ErbB1 contributes primarily to colony forming ability even if it does not represent a proliferative advantage in regular cell cultures.

Next, we intended to analyze the downstream signaling evoked by excess ErbB1 and integrin β1. We set out to quantitate the changes in the PI-3K/Akt pathway that is known to induce the STAT and NF-kappa-β transformation pathways [78], and has received much attention because of its negative regulation by PTEN, which most commonly suffers loss-of-function mutations in glioblastomas [68]. This was further substantiated by more recent data that proposed the modulating effect of radiation-induced Akt activation behind the radioresistance of human glioblastoma cells [246]. We observed an increased basal Akt phosphorylation and augmented output from the PI-3K/Akt pathway parallel with increasing radioresistance of the U251 transfectants. Furthermore, this decreased radiosensitivity could be reverted by inhibiting PI-3K with wortmannin that also strengthened the assumption on the involvement of this pro-survival pathway in the background of developing radioresistance.

Further on, we aimed at characterizing the molecular interactions of ErbB1 and integrin β1 that could stand behind the downstream signaling changes and concomitant increased radioresistance. We observed an anti-correlation between ErbB1 homoassociation, higher in parental U251, and ErbB1 - integrin β1 heteroassociation, more prevalent in the transfectant subclones by FCET measurements. As a control, FRET was also measured in the opposite, integrin-β1 – ErbB1, direction by reversing the donor-acceptor labeling, and similar tendency was observed as previously (2%, 3%, 4% and 18%), which excluded the dependency on stochiometry and the possibility of a simple random mass effect.

These findings, however, yielded information at the level of population average and under trypsinized conditions, but formerly we have already shown that the distribution of molecular interaction, especially in focal adhesion complexes, can vastly depend upon the adherence of cells to the environment. Therefore, tsFRET experiments were conducted to reveal the mutual relationship of ErbB1 homoassociation and ErbB1 - integrin β1 heteroassociation on the submicron scale of membrane compartments. The results suggested that excess integrin β1 preferentially clusters with ErbB1, competitively diminishing the extent of interaction in ErbB1 homoclusters, i.e. integrin β1 recruited ErbB1 to form heterodimers at the price of the disruption of ErbB1 homoclusters. The thereby evolving ErbB1 – integrin β1 heteroassociation then can induce versatile downstream signaling events that involves FAK, ILK, the bridging molecule PINCH, the Nck2 adaptor protein or GSK-3β related to adhesion and migration upregulated by integrin signaling [98]. Accordingly, the ILK / GSK-3β mediated canonical β-catenin / Tcf-4 pathway was proved to be exceptionally not only upregulated in astrocytomas but to directly regulate Akt2 gene expression and thereby promoting glioma progression [82]. Moreover, ongoing preclinical studies now tend

to address small-molecule PI-3K-related pathway inhibitors (NVP-BEZ235, LY294002, enzastaurin) that suggest a potential to sensitize chemotherapy-induced apoptosis via disrupting the PI-3K / Akt / mTOR / GSK-3β signaling routes [70].

In order to corroborate our in vitro findings and eventually to explore their possible relevance in comparison with clinical data, we determined the ErbB1 and integrin β1 expression on intraoperative fresh frozen tissue sections, which were overall higher in grade IV than in grade II tumors both for ErbB1 and for integrin β1 (Fig. 29). In addition, with a view to expected clinical implications, we have adapted the abFRET method to quantitate the actual extent of interaction between ErbB1 and integrin β1 in fresh frozen intraoperative astrocytoma samples. This approach shifted the information content from mere expression levels to a quasi-functional realm, and afforded the advantage of monitoring a reasonably stable molecular conformation relevant to an active signaling pathway. Comparing sets of grade II and grade IV tumors revealed that ErbB1 - integrin β1 heteroassociation was more prominent in grade IV tumors than in grade II, and served to classify tumor grade equally well as the complex histopathological diagnosis. Interestingly, we could also conclude that increased integrin β1 expression levels and stronger ErbB1 - integrin β1 associations were more important in determining grade and outcome than high ErbB1 levels, since survival time and time-to-relapse inversely correlated with the FRET results gained by *in situ* measurements. Additionally, there were extreme cases that diverged from the overall prognosis within both grade II and grade IV groups, and, although the small number of occurrences is not amenable to statistical analysis, stronger ErbB1 - integrin β1 interactions within each group predicted worse prognosis, and vice versa.

On the basis of these results, elevated integrin β1 expression, and especially a high degree of ErbB1 – integrin β1 heteroassociation in astrocytic tumors could predict ineffective response to ionizing radiation and an unfavorable survival outlook, which could potentially be overcome by inhibiting the function of overexpressed proteins or their interaction and the downstream output converging on the PI-3K/Akt pathway. Therefore, determining integrin β1 expression and ErbB1 – integrin β1 heteroassociation in newly diagnosed astrocytoma tumors, and/or quantitating the activation of relevant downstream effectors such as PI-3K, Akt or GSK-3β could allow for stratification into prognostically divergent patient subgroups and selection of appropriate therapeutic modalities [111].

8. CONCLUSIONS

Facing malignant tumors stands still in an outpost position of modern medicine, since the progressively growing, infiltrating and metastasizing nature of malignancies rapidly and severely spoils the affected healthy frame, depreciates short and long-time life quality and often presents challenging difficulties for assigning adequate treatment strategies despite broadening and increasingly available diagnostic and therapeutic modalities. The focus is highlighted on the chemo- and radiosensitivity of tumor cells, as virtual incurability of malignancies can be derived from evolving resistance to treatment attempts. In the recent years, growing evidence has highlighted the contribution of growth factor receptors and cell adhesion molecules to the downstream signaling alterations leading to uncontrollable cell proliferation and migration, thereby defining and restating the theory of cell adhesion mediated therapy resistance.

Along this line, we set out to investigate the molecular interactions of ErbB receptor tyrosine kinase proteins and integrin molecules to shed light on their possible interfering, correlative roles behind trastuzumab resistance of breast cancers and radioresistance of astrocytomas. To study the contingent mutual interplay of neighboring receptors, we have implemented a method, termed two-sided FRET (tsFRET), for the investigation of the relationship of associations of two molecule pairs of three arbitrarily chosen molecular species. For the evaluation of individual differences in inter-molecular relations in clinical samples, we also established a method for quantitatively assessing *in situ* molecular interactions by confocal microscopic abFRET measurements on intraoperative fresh frozen tissue sections.

According to our results, it is tempting to speculate that the homoassociation state of ErbB2 is dynamically modulated by the interaction with integrin β1 on breast cancer cells *in vitro*, although a strong correlation between trastuzumab resistance and high integrin β1 expression cannot possibly be established based on our studies. It may, however, be assumed that a high expression level of integrin β1 alters the signal transduction properties of breast cancer cells, thereby presenting an alternative pathway for the activation of the MAPK and PI-3K / Akt pathways and giving rise to the development of metastasizing ability.

Since our experiments confirmed existing and dynamically modifiable interactions between the ErbB and integrin β1 molecules on breast and gastric cancer cell lines and our protein level screen on astrocytoma cells *in vitro* proved integrin β1 overexpressed besides ErbB1, we set out to assess their possible interaction in the background of gliomagenesis.

Two cellular model systems showing expression profiles similar to low and high grade astrocytoma tumors have been generated, and we showed that increased ErbB1 expression was consequently followed by the presence of excess integrin β1 in the membrane. On these U251 NCI subclones, decreasing radiosensitivity correlated with increasing ErbB1 and integrin β1 expression levels, and also with decreasing ErbB1 homoassociation and increasing ErbB1 – integrin β1 heteroassociation rates. Radioresistance could be explained by the increased basal Akt phosphorylation, and augmented output from the PI-3K / Akt pathway upon EGF stimulation in the sublines with higher ErbB1 and integrin β1 expression and could be reverted by inhibiting PI-3K. The enhanced ErbB1 - integrin β1 interaction was also detectable in grade IV versus grade II astrocytoma fresh frozen sections and appeared to be an efficient predictor of patient survival and disease relaps. The abFRET procedure in confocal microscopy was proved to be a useful, cell function-related diagnostic method in assessing *in situ* ErbB1 – integrin β1 heteroassociation, which implies the potential exploitation of similar investigations on clinical glioblastoma samples, and may allow for discernment of prognostically diverse patient subgroups warranting the application of certain single or combined therapeutic modalities.

Altogether, our results suggest that the functional relationship between ErbB1 and integrin β1 molecules may play an important role in tumor progression and in the development of therapy resistance. Consequential shift of signaling from ErbB1 homoassociation to ErbB1 – integrin β1 heteroassociation and towards the activation of the PI-3K / Akt pathway may result in increased therapy resistance that can be potentially overcome by the inhibition of PI-3K. Thus, the clinically relevant ErbB1 – integrin β1 heteroassociation may be used both as a target of predictive diagnostics and of molecular therapy.

9. SUMMARY

Along the objectives on the investigation of ErbB - integrin molecular interactions in breast cancer, we can draw the following conclusions addressing the questions:

- trastuzumab resistant cell lines showed lower ErbB2, but higher integrin β1 expression
- ErbB2 and integrin β1, both, colocalized with lipid rafts
- integrin β1 cross-linking did not affect trastuzumab induced ErbB2 phosphorylation
- ErbB2 - integrin β1 heteroassociation negatively correlated with ErbB2 homoassociation in respect to trastuzumab resistance.

For assessing multimolecular interactions, we successfully established a new method, termed two-sided FRET. Application of tsFRET brought further evidence on the modifying effect of cell adhesion molecules to growth factor receptor signaling, as:

- tsFRET was proved to be applicable for measuring the relationship between the association states of two molecule-pairs of three arbitrarily chosen molecular species
- clear anti-correlation was found between the degree of ErbB2 homoassociation and ErbB2 - integrin β1 heteroassociation on trastuzumab sensitive cells
- modestly positive correlation could be discerned between ErbB2 - integrin β1 and integrin β1 - CD44 heteroassociation levels on trastuzumab resistant cells.

To study the importance of recent *in vitro* and *xenograft* findings on ErbB - integrin interactions in gliomagenesis, we successfully implemented abFRET on frozen sections of clinical astrocytoma *in situ* with a potential view on its clinical applicability. According to our results, we can make the following statements:

- grade IV glioma showed higher integrin β1 expression parallel with ErbB1 overexpression
- degree of ErbB1-integrin β1 heteroassociation was elevated and correlated negatively with that of ErbB1 homoassociation in high ErbB1 expresser U251 E1H/H
- degree of ErbB1-integrin β1 heteroassociation was also elevated in grade IV tumors *in situ*
- *in situ* results and activation of the PI-3K/Akt pathway was corroborated by results from cellular model systems showing expression profiles similar to low/high grade astrocytomas
- ErbB1 - integrin β1 interaction appeared to be an efficient predictor of patient survival and may be used as a target of predictive diagnostics and also of molecular therapy.

10. ACKNOWLEDGMENTS

Foremost, I would like to thank my advisors *Professor János Szöllősi* and *Álmos Klekner* for supporting me over the years and providing me the opportunity to finish my thesis.

I will always remember with grateful respect the late *Professor György Csécsei*, who conducted my first "footsteps" in the medical science, but unfortunately could not live to be here with us at the finish of our work.

I wish to express the most sincere gratitude to *Professor György Vereb* for the insightful discussions that have driven me along the way and helping me in every aspect of my work.

I pay great honour to *Professor Kálmán Nagy*, who always gave me enough time to do my scientific work besides my clinical duty, whose advisement led me on the way and helped to get over difficulties, and without whose selfless support this work could have not been done.

I am also very grateful to the *members of our research group*: Zsolt Fazekas, Zsolt Sebestyén, Péter Nagy, Tamás Lajtos, Maria-Magdalena Mocanu, Elza Friedlander, Barbara Zsebik, Gábor Horváth, Ákos Fábián, Márk Barok, László Ujlaky-Nagy, Zsuzsanna Pályiné Krekk, to Andrea Dóczy-Bodnár and Gergely Szentesi. I acknowledge the help of Mária Kern and Ms. Gabriella Őri, Ms. Tünde Terdik and Ms. Hajnalka Toldi in the technical assistance, and the help of the staff of the Departments of Biophysics and Cell Biology and Neurosurgery at the University of Debrecen, and also that of the Children Health Care Center at the Borsod County and University Hospital.

I owe a lot to *my wife* for providing this loving athmosphere, patiently encouraging me, and enduring till the end over assurgent "time tunnels and traps".

I am grateful to *my family* for giving me the opportunity to accomplish my plans.

Experimental work was performed by the support of the TÁMOP-4.2.2.A-11/1/KONV-2012-0025 project and the Baross Gábor Program (REG-EA-09-1-2009-0010). The doctoral training program was supported by the TÁMOP-4.2.2/B-10/1-2010-0024 project. The projects are co-financed by the European Union and the European Social Fund.

11. REFERENCES

1. International Agency for Research on Cancer, I., *The GLOBOCAN Project.* http://globocan.iarc.fr, 2008.
2. Jemal, A., et al., *Global cancer statistics.* CA Cancer J Clin, 2011. **61**(2): p. 69-90.
3. United Nations, D.o.E.a.S.A., Population Division, *World Population Prospects: The 2008 Revision, Highlights, Working Paper No. ESA/P/WP.210.* 2009.
4. National Cancer Institute, *Surveillance, Epidemiology and End Results (SEER) Database*, 1973-2010. p. Surveillance, Epidemiology and End Results (SEER) Database.
5. Wrensch, M., et al., *Environmental risk factors for primary malignant brain tumors: a review.* J Neurooncol, 1993. **17**(1): p. 47-64.
6. Cohen, S., *Isolation of a mouse submaxillary gland protein accelerating incisor eruption and eyelid opening in the new-born animal.* J Biol Chem, 1962. **237**: p. 1555-62.
7. Cohen, S., *The stimulation of epidermal proliferation by a specific protein (EGF).* Dev Biol, 1965. **12**(3): p. 394-407.
8. Carpenter, G., et al., *Characterization of the binding of 125-I-labeled epidermal growth factor to human fibroblasts.* J Biol Chem, 1975. **250**(11): p. 4297-304.
9. Gorden, P., et al., *Epidermal growth factor: morphological demonstration of binding, internalization, and lysosomal association in human fibroblasts.* Proc Natl Acad Sci U S A, 1978. **75**(10): p. 5025-9.
10. Ushiro, H. and S. Cohen, *Identification of phosphotyrosine as a product of epidermal growth factor-activated protein kinase in A-431 cell membranes.* J Biol Chem, 1980. **255**(18): p. 8363-5.
11. Carpenter, G., L. King, Jr., and S. Cohen, *Epidermal growth factor stimulates phosphorylation in membrane preparations in vitro.* Nature, 1978. **276**(5686): p. 409-10.
12. Saule, S., et al., *Characterization of the oncogene (erb) of avian erythroblastosis virus and its cellular progenitor.* J Virol, 1981. **38**(2): p. 409-19.
13. Downward, J., et al., *Close similarity of epidermal growth factor receptor and v-erb-B oncogene protein sequences.* Nature, 1984. **307**(5951): p. 521-7.
14. de Larco, J.E. and G.J. Todaro, *Epithelioid and fibroblastic rat kidney cell clones: epidermal growth factor (EGF) receptors and the effect of mouse sarcoma virus transformation.* J Cell Physiol, 1978. **94**(3): p. 335-42.
15. Zhang, H., et al., *ErbB receptors: from oncogenes to targeted cancer therapies.* J Clin Invest, 2007. **117**(8): p. 2051-8.
16. Yarden, Y. and M.X. Sliwkowski, *Untangling the ErbB signalling network.* Nat Rev Mol Cell Biol, 2001. **2**(2): p. 127-37.
17. Slamon, D.J., et al., *Human breast cancer: correlation of relapse and survival with amplification of the HER-2/neu oncogene.* Science, 1987. **235**(4785): p. 177-82.
18. Alroy, I. and Y. Yarden, *The ErbB signaling network in embryogenesis and oncogenesis: signal diversification through combinatorial ligand-receptor interactions.* FEBS Lett, 1997. **410**(1): p. 83-6.
19. Yamamoto, T., et al., *Similarity of protein encoded by the human c-erb-B-2 gene to epidermal growth factor receptor.* Nature, 1986. **319**(6050): p. 230-4.
20. Schechter, A.L., et al., *The neu oncogene: an erb-B-related gene encoding a 185,000-Mr tumour antigen.* Nature, 1984. **312**(5994): p. 513-6.
21. Plowman, G.D., et al., *Ligand-specific activation of HER4/p180erbB4, a fourth member of the epidermal growth factor receptor family.* Proc Natl Acad Sci U S A, 1993. **90**(5): p. 1746-50.
22. Kraus, M.H., et al., *Isolation and characterization of ERBB3, a third member of the ERBB/epidermal growth factor receptor family: evidence for overexpression in a subset of human mammary tumors.* Proc Natl Acad Sci U S A, 1989. **86**(23): p. 9193-7.
23. Ward, C.W., P.A. Hoyne, and R.H. Flegg, *Insulin and epidermal growth factor receptors contain the cysteine repeat motif found in the tumor necrosis factor receptor.* Proteins, 1995. **22**(2): p. 141-53.
24. Schlessinger, J., *The epidermal growth factor receptor as a multifunctional allosteric protein.* Biochemistry, 1988. **27**(9): p. 3119-23.
25. Burgess, A.W., et al., *An open-and-shut case? Recent insights into the activation of EGF/ErbB receptors.* Mol Cell, 2003. **12**(3): p. 541-52.
26. Citri, A. and Y. Yarden, *EGF-ERBB signalling: towards the systems level.* Nat Rev Mol Cell Biol, 2006. **7**(7): p. 505-16.
27. Citri, A., K.B. Skaria, and Y. Yarden, *The deaf and the dumb: the biology of ErbB-2 and ErbB-3.* Exp Cell Res, 2003. **284**(1): p. 54-65.
28. Nagy, P., et al., *Complexity of signal transduction mediated by ErbB2: clues to the potential of receptor-targeted cancer therapy.* Pathol Oncol Res, 1999. **5**(4): p. 255-71.
29. Vereb, G., Jr., et al., *Signaling revealed by mapping molecular interactions: implications for ErbB-targeted cancer immunotherapies.* Clinical and Applied Immunology Reviews, 2002. **2**: p. 169-186.
30. Nagy, P., et al., *Activation-dependent clustering of the erbB2 receptor tyrosine kinase detected by scanning near-field optical microscopy.* J Cell Sci, 1999. **112**(Pt 11): p. 1733-41.
31. Nagy, P., et al., *Lipid rafts and the local density of ErbB proteins influence the biological role of homo- and heteroassociations of ErbB2.* J Cell Sci, 2002. **115**(22): p. 4251-4262.
32. Zajchowski, L.D. and S.M. Robbins, *Lipid rafts and little caves. Compartmentalized signalling in membrane microdomains.* European Journal of Biochemistry, 2002. **269**(3): p. 737-52.

33. Yarden, Y. and J. Schlessinger, *Self-phosphorylation of epidermal growth factor receptor: evidence for a model of intermolecular allosteric activation.* Biochemistry, 1987. **26**(5): p. 1434-42.
34. Gadella, T.W., Jr. and T.M. Jovin, *Oligomerization of epidermal growth factor receptors on A431 cells studied by time-resolved fluorescence imaging microscopy. A stereochemical model for tyrosine kinase receptor activation.* J Cell Biol, 1995. **129**(6): p. 1543-58.
35. Brakebusch, C., et al., *Integrins in invasive growth.* J Clin Invest, 2002. **109**(8): p. 999-1006.
36. Basson, M.D., *An intracellular signal pathway that regulates cancer cell adhesion in response to extracellular forces.* Cancer Res, 2008. **68**(1): p. 2-4.
37. Guo, W. and F.G. Giancotti, *Integrin signalling during tumour progression.* Nat Rev Mol Cell Biol, 2004. **5**(10): p. 816-26.
38. Fujita, S., et al., *Alteration of expression in integrin beta 1-subunit correlates with invasion and metastasis in colorectal cancer.* Cancer Lett, 1995. **91**(1): p. 145-9.
39. Albelda, S.M., *Role of integrins and other cell adhesion molecules in tumor progression and metastasis.* Lab Invest, 1993. **68**(1): p. 4-17.
40. Leptin, M., R. Aebersold, and M. Wilcox, *Drosophila position-specific antigens resemble the vertebrate fibronectin-receptor family.* Embo J, 1987. **6**(4): p. 1037-43.
41. Hemler, M.E., J.G. Jacobson, and J.L. Strominger, *Biochemical characterization of VLA-1 and VLA-2. Cell surface heterodimers on activated T cells.* J Biol Chem, 1985. **260**(28): p. 15246-52.
42. Parise, L.V. and D.R. Phillips, *Fibronectin-binding properties of the purified platelet glycoprotein IIb-IIIa complex.* J Biol Chem, 1986. **261**(30): p. 14011-7.
43. Hynes, R.O., *The emergence of integrins: a personal and historical perspective.* Matrix Biol, 2004. **23**(6): p. 333-40.
44. Johnson, M.S., et al., *Integrins during evolution: evolutionary trees and model organisms.* Biochim Biophys Acta, 2009. **1788**(4): p. 779-89.
45. Hynes, R.O., *Integrins: bidirectional, allosteric signaling machines.* Cell, 2002. **110**(6): p. 673-87.
46. Humphries, M.J., E.J. Symonds, and A.P. Mould, *Mapping functional residues onto integrin crystal structures.* Curr Opin Struct Biol, 2003. **13**(2): p. 236-43.
47. Askari, J.A., et al., *Linking integrin conformation to function.* J Cell Sci, 2009. **122**(Pt 2): p. 165-70.
48. Barczyk, M., S. Carracedo, and D. Gullberg, *Integrins.* Cell Tissue Res, 2010. **339**(1): p. 269-80.
49. Wang, J. and T.A. Springer, *Structural specializations of immunoglobulin superfamily members for adhesion to integrins and viruses.* Immunol Rev, 1998. **163**: p. 197-215.
50. Komoriya, A., et al., *The minimal essential sequence for a major cell type-specific adhesion site (CS1) within the alternatively spliced type III connecting segment domain of fibronectin is leucine-aspartic acid-valine.* J Biol Chem, 1991. **266**(23): p. 15075-9.
51. Clements, J.M., et al., *Identification of a key integrin-binding sequence in VCAM-1 homologous to the LDV active site in fibronectin.* J Cell Sci, 1994. **107 (Pt 8)**: p. 2127-35.
52. Lee, J.W. and R. Juliano, *Mitogenic signal transduction by integrin- and growth factor receptor-mediated pathways.* Mol Cells, 2004. **17**(2): p. 188-202.
53. Armulik, A., *Splice variants of human beta 1 integrins: origin, biosynthesis and functions.* Front Biosci, 2002. **7**: p. d219-27.
54. Fornaro, M. and L.R. Languino, *Alternatively spliced variants: a new view of the integrin cytoplasmic domain.* Matrix Biol, 1997. **16**(4): p. 185-93.
55. Fornaro, M., et al., *Differential role of beta(1C) and beta(1A) integrin cytoplasmic variants in modulating focal adhesion kinase, protein kinase B/AKT, and Ras/Mitogen-activated protein kinase pathways.* Mol Biol Cell, 2000. **11**(7): p. 2235-49.
56. Goel, H.L., et al., *Selective modulation of type 1 insulin-like growth factor receptor signaling and functions by beta1 integrins.* J Cell Biol, 2004. **166**(3): p. 407-18.
57. Giancotti, F.G. and E. Ruoslahti, *Integrin signaling.* Science, 1999. **285**(5430): p. 1028-32.
58. Brar, P.K., et al., *Laminin alpha-1, alpha-3, and alpha-5 chain expression in human prepubertal [correction of prepubetal] benign prostate glands and adult benign and malignant prostate glands.* Prostate, 2003. **55**(1): p. 65-70.
59. Fornaro, M., T. Manes, and L.R. Languino, *Integrins and prostate cancer metastases.* Cancer Metastasis Rev, 2001. **20**(3-4): p. 321-31.
60. Jensen, U.B., S. Lowell, and F.M. Watt, *The spatial relationship between stem cells and their progeny in the basal layer of human epidermis: a new view based on whole-mount labelling and lineage analysis.* Development, 1999. **126**(11): p. 2409-18.
61. Gomperts, B.D., I.M. Kramer, and P.E.R. Tatham, *Signal Transduction*2003, London, San Diego: Elsevier Academic Press. 325-327.
62. Kennedy, S.G., et al., *The PI 3-kinase/Akt signaling pathway delivers an anti-apoptotic signal.* Genes Dev, 1997. **11**(6): p. 701-13.
63. Ekstrand, A.J., et al., *Functional characterization of an EGF receptor with a truncated extracellular domain expressed in glioblastomas with EGFR gene amplification.* Oncogene, 1994. **9**(8): p. 2313-20.
64. Guha, A., et al., *Expression of PDGF and PDGF receptors in human astrocytoma operation specimens supports the existence of an autocrine loop.* Int J Cancer, 1995. **60**(2): p. 168-73.
65. Liebmann, C., *Regulation of MAP kinase activity by peptide receptor signalling pathway: paradigms of multiplicity.* Cell Signal, 2001. **13**(11): p. 777-85.

66. Vivanco, I. and C.L. Sawyers, *The phosphatidylinositol 3-Kinase AKT pathway in human cancer.* Nat Rev Cancer, 2002. **2**(7): p. 489-501.
67. Di Cristofano, A. and P.P. Pandolfi, *The multiple roles of PTEN in tumor suppression.* Cell, 2000. **100**(4): p. 387-90.
68. Cantley, L.C. and B.G. Neel, *New insights into tumor suppression: PTEN suppresses tumor formation by restraining the phosphoinositide 3-kinase/AKT pathway.* Proc Natl Acad Sci U S A, 1999. **96**(8): p. 4240-5.
69. Nahta, R., et al., *Mechanisms of disease: understanding resistance to HER2-targeted therapy in human breast cancer.* Nat Clin Pract Oncol, 2006. **3**(5): p. 269-80.
70. Wick, W., et al., *Pathway inhibition: emerging molecular targets for treating glioblastoma.* Neuro Oncol, 2011. **13**(6): p. 566-79.
71. Patterson, R.L., et al., *Phospholipase C-gamma: diverse roles in receptor-mediated calcium signaling.* Trends Biochem Sci, 2005. **30**(12): p. 688-97.
72. Griner, E.M. and M.G. Kazanietz, *Protein kinase C and other diacylglycerol effectors in cancer.* Nat Rev Cancer, 2007. **7**(4): p. 281-94.
73. Bromberg, J. and J.E. Darnell, Jr., *The role of STATs in transcriptional control and their impact on cellular function.* Oncogene, 2000. **19**(21): p. 2468-73.
74. Haura, E.B., J. Turkson, and R. Jove, *Mechanisms of disease: Insights into the emerging role of signal transducers and activators of transcription in cancer.* Nat Clin Pract Oncol, 2005. **2**(6): p. 315-24.
75. Grandis, J.R., et al., *Constitutive activation of Stat3 signaling abrogates apoptosis in squamous cell carcinogenesis in vivo.* Proc Natl Acad Sci U S A, 2000. **97**(8): p. 4227-32.
76. Frame, M.C., *Newest findings on the oldest oncogene; how activated src does it.* J Cell Sci, 2004. **117**(Pt 7): p. 989-98.
77. Hiscox, S., et al., *Elevated Src activity promotes cellular invasion and motility in tamoxifen resistant breast cancer cells.* Breast Cancer Res Treat, 2006. **97**(3): p. 263-74.
78. Kapoor, G.S., et al., *Distinct domains in the SHP-2 phosphatase differentially regulate epidermal growth factor receptor/NF-kappaB activation through Gab1 in glioblastoma cells.* Mol Cell Biol, 2004. **24**(2): p. 823-36.
79. Brunet, A., et al., *Akt promotes cell survival by phosphorylating and inhibiting a Forkhead transcription factor.* Cell, 1999. **96**(6): p. 857-68.
80. Downward, J., *Mechanisms and consequences of activation of protein kinase B/Akt.* Curr Opin Cell Biol, 1998. **10**(2): p. 262-7.
81. Riemenschneider, M.J., et al., *In situ analysis of integrin and growth factor receptor signaling pathways in human glioblastomas suggests overlapping relationships with focal adhesion kinase activation.* Am J Pathol, 2005. **167**(5): p. 1379-87.
82. Zhang, J., et al., *High beta-catenin/Tcf-4 activity confers glioma progression via direct regulation of AKT2 gene expression.* Neuro Oncol, 2011. **13**(6): p. 600-9.
83. Tzahar, E., et al., *A hierarchical network of interreceptor interactions determines signal transduction by Neu differentiation factor/neuregulin and epidermal growth factor.* Mol Cell Biol, 1996. **16**(10): p. 5276-87.
84. Lenferink, A.E., et al., *Differential endocytic routing of homo- and hetero-dimeric ErbB tyrosine kinases confers signaling superiority to receptor heterodimers.* Embo J, 1998. **17**(12): p. 3385-97.
85. Graus-Porta, D., et al., *ErbB-2, the preferred heterodimerization partner of all ErbB receptors, is a mediator of lateral signaling.* Embo J, 1997. **16**(7): p. 1647-55.
86. Gamett, D.C., et al., *Secondary dimerization between members of the epidermal growth factor receptor family.* J Biol Chem, 1997. **272**(18): p. 12052-6.
87. Harari, D. and Y. Yarden, *Molecular mechanisms underlying ErbB2/HER2 action in breast cancer.* Oncogene, 2000. **19**(53): p. 6102-14.
88. Waterman, H., et al., *The C-terminus of the kinase-defective neuregulin receptor ErbB-3 confers mitogenic superiority and dictates endocytic routing.* Embo J, 1999. **18**(12): p. 3348-58.
89. B.W. van der Meer, G.C.I.a.S.-Y.C., *Resonance Energy Transfer: Theory and Data.* Wiley - VCH Publishers, Inc., New York, 1994.
90. Sebestyen, Z., et al., *Long wavelength fluorophores and cell-by-cell correction for autofluorescence significantly improves the accuracy of flow cytometric energy transfer measurements on a dual-laser benchtop flow cytometer.* Cytometry, 2002. **48**(3): p. 124-35.
91. Szollosi, J., et al., *Supramolecular complexes of MHC class I, MHC class II, CD20, and tetraspan molecules (CD53, CD81, and CD82) at the surface of a B cell line JY.* J Immunol, 1996. **157**(7): p. 2939-46.
92. Leitinger, B. and N. Hogg, *The involvement of lipid rafts in the regulation of integrin function.* J Cell Sci, 2002. **115**(Pt 5): p. 963-72.
93. Falcioni, R., et al., *Alpha 6 beta 4 and alpha 6 beta 1 integrins associate with ErbB-2 in human carcinoma cell lines.* Exp Cell Res, 1997. **236**(1): p. 76-85.
94. Katz, M., et al., *A reciprocal tensin-3-cten switch mediates EGF-driven mammary cell migration.* Nat Cell Biol, 2007. **9**(8): p. 961-9.
95. Adelsman, M.A., J.B. McCarthy, and Y. Shimizu, *Stimulation of beta1-integrin function by epidermal growth factor and heregulin-beta has distinct requirements for erbB2 but a similar dependence on phosphoinositide 3-OH kinase.* Mol Biol Cell, 1999. **10**(9): p. 2861-78.
96. Miyamoto, S., et al., *Integrins can collaborate with growth factors for phosphorylation of receptor tyrosine kinases and MAP kinase activation: roles of integrin aggregation and occupancy of receptors.* J Cell Biol, 1996. **135**(6 Pt 1): p. 1633-42.

97. Moro, L., et al., *Integrin-induced epidermal growth factor (EGF) receptor activation requires c-Src and p130Cas and leads to phosphorylation of specific EGF receptor tyrosines.* J Biol Chem, 2002. **277**(11): p. 9405-14.
98. Hehlgans, S., M. Haase, and N. Cordes, *Signalling via integrins: implications for cell survival and anticancer strategies.* Biochim Biophys Acta, 2007. **1775**(1): p. 163-80.
99. Stommel, J.M., et al., *Coactivation of receptor tyrosine kinases affects the response of tumor cells to targeted therapies.* Science, 2007. **318**(5848): p. 287-90.
100. Förster, T., *Energiewanderung und Fluoreszenz.* Naturwissenschaften, 1946. **6**: p. 166-175.
101. Szollosi, J., et al., *Fluorescence energy transfer measurements on cell surfaces: a critical comparison of steady-state fluorimetric and flow cytometric methods.* Cytometry, 1984. **5**(2): p. 210-216.
102. Szollosi, J., et al., *Fluorescence energy transfer and membrane potential measurements monitor dynamic properties of cell membranes: a critical review.* Prog Biophys Mol Biol, 1987. **49**(2-3): p. 65-87.
103. Szollosi, J., et al., *Applications of fluorescence resonance energy transfer for mapping biological membranes.* J Biotechnol, 2002. **82**(3): p. 251-66.
104. Szollosi, J., S. Damjanovich, and L. Matyus, *Application of fluorescence resonance energy transfer in the clinical laboratory: routine and research.* Cytometry, 1998. **34**(4): p. 159-79.
105. Jares-Erijman, E.A. and T.M. Jovin, *FRET imaging.* Nat Biotechnol, 2003. **21**(11): p. 1387-95.
106. Vereb, G., C.K. Meyer, and T.M. Jovin, *Novel microscope-based approaches for the investigation of protein - protein interactions in signal transduction*, in *Interacting protein domains, their role in signal and energy transduction. NATO ASI series*, L.M.G. Heilmeyer Jr, Editor 1997, Springer-Verlag: New York. p. 49-52.
107. Mills, J.D., et al., *Illuminating protein interactions in tissue using confocal and two-photon excitation fluorescent resonance energy transfer microscopy.* J Biomed Opt, 2003. **8**(3): p. 347-56.
108. Schmid, J.A. and A. Birbach, *Fluorescent proteins and fluorescence resonance energy transfer (FRET) as tools in signaling research.* Thromb Haemost, 2007. **97**(3): p. 378-84.
109. Kong, A., et al., *Prognostic value of an activation state marker for epidermal growth factor receptor in tissue microarrays of head and neck cancer.* Cancer Res, 2006. **66**(5): p. 2834-43.
110. Konig, P., et al., *FRET-CLSM and double-labeling indirect immunofluorescence to detect close association of proteins in tissue sections.* Lab Invest, 2006. **86**(8): p. 853-64.
111. Sawyers, C.L., *Cancer: mixing cocktails.* Nature, 2007. **449**(7165): p. 993-6.
112. Slamon, D.J., et al., *Studies of the HER-2/neu proto-oncogene in human breast and ovarian cancer.* Science, 1989. **244**(4905): p. 707-12.
113. Menard, S., et al., *Biologic and therapeutic role of HER2 in cancer.* Oncogene, 2003. **22**(42): p. 6570-8.
114. Prost, S., et al., *Association of c-erbB2-gene amplification with poor prognosis in non-inflammatory breast carcinomas but not in carcinomas of the inflammatory type.* Int J Cancer, 1994. **58**(6): p. 763-8.
115. Latta, E.K., et al., *The role of HER2/neu overexpression/amplification in the progression of ductal carcinoma in situ to invasive carcinoma of the breast.* Mod Pathol, 2002. **15**(12): p. 1318-25.
116. Lakhani, R.S., Ellis. I.O., Schnitt, S.J., Hoon, P.H., van de Vijver, M.J., *WHO Classification of Tumours of the Breast, Fourth Edition.* IARC WHO Classification of Tumours, No 4, 2011. **in press, expected in July 2012**.
117. van der Groep, P., E. van der Wall, and P.J. van Diest, *Pathology of hereditary breast cancer.* Cell Oncol (Dordr), 2011. **34**(2): p. 71-88.
118. Guarneri, V., et al., *Anti-HER2 neoadjuvant and adjuvant therapies in HER2 positive breast cancer.* Cancer Treat Rev, 2010. **36 Suppl 3**: p. S62-6.
119. von Minckwitz, G., et al., *Impact of treatment characteristics on response of different breast cancer phenotypes: pooled analysis of the German neo-adjuvant chemotherapy trials.* Breast Cancer Res Treat, 2011. **125**(1): p. 145-56.
120. Clavarezza, M. and M. Venturini, *Adjuvant chemotherapy for the treatment of HER2-positive early breast cancer.* Oncology, 2009. **77 Suppl 1**: p. 14-7.
121. Honig, A., et al., *State of the art of neoadjuvant chemotherapy in breast cancer: rationale, results and recent developments.* Ger Med Sci, 2005. **3**: p. Doc08.
122. Mohsin, S.K., et al., *Neoadjuvant trastuzumab induces apoptosis in primary breast cancers.* J Clin Oncol, 2005. **23**(11): p. 2460-8.
123. von Minckwitz, G., et al., *Integrating bevacizumab, everolimus, and lapatinib into current neoadjuvant chemotherapy regimen for primary breast cancer. Safety results of the GeparQuinto trial.* Ann Oncol, 2011. **22**(2): p. 301-6.
124. Wong, K.K., et al., *A phase I study with neratinib (HKI-272), an irreversible pan ErbB receptor tyrosine kinase inhibitor, in patients with solid tumors.* Clin Cancer Res, 2009. **15**(7): p. 2552-8.
125. Perez, E.A. and J.P. Spano, *Current and emerging targeted therapies for metastatic breast cancer.* Cancer, 2011.
126. Eichhorn, P.J., et al., *Phosphatidylinositol 3-kinase hyperactivation results in lapatinib resistance that is reversed by the mTOR/phosphatidylinositol 3-kinase inhibitor NVP-BEZ235.* Cancer Res, 2008. **68**(22): p. 9221-30.
127. Neckers, L. and P. Workman, *Hsp90 molecular chaperone inhibitors: are we there yet?* Clin Cancer Res, 2012. **18**(1): p. 64-76.
128. Baselga, J., et al., *Phase II trial of pertuzumab and trastuzumab in patients with human epidermal growth factor receptor 2-positive metastatic breast cancer that progressed during prior trastuzumab therapy.* J Clin Oncol, 2010. **28**(7): p. 1138-44.
129. Kiewe, P. and E. Thiel, *Ertumaxomab: a trifunctional antibody for breast cancer treatment.* Expert Opin Investig Drugs, 2008. **17**(10): p. 1553-8.
130. Junttila, T.T., et al., *Superior in vivo efficacy of afucosylated trastuzumab in the treatment of HER2-amplified breast cancer.* Cancer Res, 2010. **70**(11): p. 4481-9.

131. Sarup, J.C., et al., *Characterization of an anti-p185HER2 monoclonal antibody that stimulates receptor function and inhibits tumor cell growth.* Growth Regul, 1991. **1**(2): p. 72-82.
132. Sliwkowski, M.X., et al., *Nonclinical studies addressing the mechanism of action of trastuzumab (Herceptin).* Semin Oncol, 1999. **26**(4 Suppl 12): p. 60-70.
133. Baselga, J., et al., *Mechanism of action of trastuzumab and scientific update.* Semin Oncol, 2001. **28**(5 Suppl 16): p. 4-11.
134. Klapper, L.N., et al., *Tumor-inhibitory antibodies to HER-2/ErbB-2 may act by recruiting c-Cbl and enhancing ubiquitination of HER-2.* Cancer Res, 2000. **60**(13): p. 3384-8.
135. Austin, C.D., et al., *Endocytosis and sorting of ErbB2 and the site of action of cancer therapeutics trastuzumab and geldanamycin.* Mol Biol Cell, 2004. **15**(12): p. 5268-82.
136. Colomer, R., et al., *Circulating HER2 extracellular domain and resistance to chemotherapy in advanced breast cancer.* Clin Cancer Res, 2000. **6**(6): p. 2356-62.
137. Molina, M.A., et al., *Trastuzumab (herceptin), a humanized anti-Her2 receptor monoclonal antibody, inhibits basal and activated Her2 ectodomain cleavage in breast cancer cells.* Cancer Res, 2001. **61**(12): p. 4744-9.
138. Nagata, Y., et al., *PTEN activation contributes to tumor inhibition by trastuzumab, and loss of PTEN predicts trastuzumab resistance in patients.* Cancer Cell, 2004. **6**(2): p. 117-27.
139. Le, X.F., F. Pruefer, and R.C. Bast, Jr., *HER2-targeting antibodies modulate the cyclin-dependent kinase inhibitor p27Kip1 via multiple signaling pathways.* Cell Cycle, 2005. **4**(1): p. 87-95.
140. Niu, G. and W.B. Carter, *Human epidermal growth factor receptor 2 regulates angiopoietin-2 expression in breast cancer via AKT and mitogen-activated protein kinase pathways.* Cancer Res, 2007. **67**(4): p. 1487-93.
141. Wen, X.F., et al., *HER2 signaling modulates the equilibrium between pro- and antiangiogenic factors via distinct pathways: implications for HER2-targeted antibody therapy.* Oncogene, 2006. **25**(52): p. 6986-96.
142. Motoyama, A.B., N.E. Hynes, and H.A. Lane, *The efficacy of ErbB receptor-targeted anticancer therapeutics is influenced by the availability of epidermal growth factor-related peptides.* Cancer Res, 2002. **62**(11): p. 3151-8.
143. Lu, Y., X. Zi, and M. Pollak, *Molecular mechanisms underlying IGF-I-induced attenuation of the growth-inhibitory activity of trastuzumab (Herceptin) on SKBR3 breast cancer cells.* Int J Cancer, 2004. **108**(3): p. 334-41.
144. Lu, Y., et al., *Overexpression of ErbB2 receptor inhibits IGF-I-induced Shc-MAPK signaling pathway in breast cancer cells.* Biochem Biophys Res Commun, 2004. **313**(3): p. 709-15.
145. Carraway, K.L., et al., *ErbB2 and its ligand Muc4 (sialomucin complex) in rat lacrimal gland.* Adv Exp Med Biol, 2002. **506**(Pt A): p. 289-95.
146. Barok, M., et al., *Trastuzumab causes antibody-dependent cellular cytotoxicity-mediated growth inhibition of submacroscopic JIMT-1 breast cancer xenografts despite intrinsic drug resistance.* Mol Cancer Ther, 2007. **6**(7): p. 2065-72.
147. Tanner, M., et al., *Characterization of a novel cell line established from a patient with Herceptin-resistant breast cancer.* Mol Cancer Ther, 2004. **3**(12): p. 1585-92.
148. Price-Schiavi, S.A., et al., *Rat Muc4 (sialomucin complex) reduces binding of anti-ErbB2 antibodies to tumor cell surfaces, a potential mechanism for herceptin resistance.* Int J Cancer, 2002. **99**(6): p. 783-91.
149. Nagy, P., et al., *Decreased accessibility and lack of activation of ErbB2 in JIMT-1, a herceptin-resistant, MUC4-expressing breast cancer cell line.* Cancer Res, 2005. **65**(2): p. 473-82.
150. Kozloski, G.A., C.A. Carraway, and K.L. Carraway, *Mechanistic and signaling analysis of Muc4-ErbB2 signaling module: new insights into the mechanism of ligand-independent ErbB2 activity.* J Cell Physiol, 2010. **224**(3): p. 649-57.
151. Workman, H.C., C. Sweeney, and K.L. Carraway, 3rd, *The membrane mucin Muc4 inhibits apoptosis induced by multiple insults via ErbB2-dependent and ErbB2-independent mechanisms.* Cancer Res, 2009. **69**(7): p. 2845-52.
152. Barok, M., et al., *Trastuzumab decreases the number of circulating and disseminated tumor cells despite trastuzumab resistance of the primary tumor.* Cancer Lett, 2008. **260**(1-2): p. 198-208.
153. Nahta, R. and F.J. Esteva, *HER2 therapy: molecular mechanisms of trastuzumab resistance.* Breast Cancer Res, 2006. **8**(6): p. 215.
154. Nahta, R., et al., *P27(kip1) down-regulation is associated with trastuzumab resistance in breast cancer cells.* Cancer Res, 2004. **64**(11): p. 3981-6.
155. Isakoff, S.J., et al., *Breast cancer-associated PIK3CA mutations are oncogenic in mammary epithelial cells.* Cancer Res, 2005. **65**(23): p. 10992-1000.
156. Kataoka, Y., et al., *Association between gain-of-function mutations in PIK3CA and resistance to HER2-targeted agents in HER2-amplified breast cancer cell lines.* Ann Oncol, 2010. **21**(2): p. 255-62.
157. Musolino, A., et al., *Immunoglobulin G fragment C receptor polymorphisms and clinical efficacy of trastuzumab-based therapy in patients with HER-2/neu-positive metastatic breast cancer.* J Clin Oncol, 2008. **26**(11): p. 1789-96.
158. Li, X., et al., *Brk/PTK6 sustains activated EGFR signaling through inhibiting EGFR degradation and transactivating EGFR.* Oncogene, 2012.
159. Motoyama, A.B. and N.E. Hynes, *BAD: a good therapeutic target?* Breast Cancer Res, 2003. **5**(1): p. 27-30.
160. Disis, M.L., et al., *Concurrent trastuzumab and HER2/neu-specific vaccination in patients with metastatic breast cancer.* J Clin Oncol, 2009. **27**(28): p. 4685-92.
161. Cardoso, F., et al., *Resistance to trastuzumab: a necessary evil or a temporary challenge?* Clin Breast Cancer, 2002. **3**(4): p. 247-57; discussion 258-9.
162. Jones, K.L. and A.U. Buzdar, *Evolving novel anti-HER2 strategies.* Lancet Oncol, 2009. **10**(12): p. 1179-87.
163. Mukohara, T., *Mechanisms of resistance to anti-human epidermal growth factor receptor 2 agents in breast cancer.* Cancer Sci, 2011. **102**(1): p. 1-8.

164. Frederick, L., et al., *Diversity and frequency of epidermal growth factor receptor mutations in human glioblastomas.* Cancer Res, 2000. **60**(5): p. 1383-7.
165. Central Brain Tumor Registry of the United States, *CBTRUS (2005-2006). Primary Brain Tumors in the United States 1998-2002.*, 2006: 3333 West 47th St. Chicago, IL 60632.
166. National Comprehensive Cancer Network, *Central Nervous System Cancers Practice Guidelines in Oncology*, 2005: Jenkitown, PA.
167. Louis, D.N., Ohgaki, H., Wiestler, O.D., Cavenee, W.K., *WHO Classification of Tumours of the Central Nervous System, Fourth Edition.* IARC WHO Classification of Tumours, No 1, 2007.
168. Galli, R., et al., *Isolation and characterization of tumorigenic, stem-like neural precursors from human glioblastoma.* Cancer Res, 2004. **64**(19): p. 7011-21.
169. Huhn, S.L., et al., *Identification of phenotypic neural stem cells in a pediatric astroblastoma.* J Neurosurg, 2005. **103**(5 Suppl): p. 446-50.
170. Yuan, X., et al., *Isolation of cancer stem cells from adult glioblastoma multiforme.* Oncogene, 2004. **23**(58): p. 9392-400.
171. Clarke, M.F., et al., *Cancer stem cells--perspectives on current status and future directions: AACR Workshop on cancer stem cells.* Cancer Res, 2006. **66**(19): p. 9339-44.
172. Hemmati, H.D., et al., *Cancerous stem cells can arise from pediatric brain tumors.* Proc Natl Acad Sci U S A, 2003. **100**(25): p. 15178-83.
173. Singh, S.K., et al., *Identification of human brain tumour initiating cells.* Nature, 2004. **432**(7015): p. 396-401.
174. Gerweck, L.E., et al., *Tumor cell radiosensitivity is a major determinant of tumor response to radiation.* Cancer Res, 2006. **66**(17): p. 8352-5.
175. Hambardzumyan, D., M. Squatrito, and E.C. Holland, *Radiation resistance and stem-like cells in brain tumors.* Cancer Cell, 2006. **10**(6): p. 454-6.
176. Bernstein M and Berger MS, *Neuro-Oncology: The Essentials*2008, New York: Thieme Medical Publishers, Inc. 32-33.
177. Weller, M., et al., *MGMT promoter methylation in malignant gliomas: ready for personalized medicine?* Nat Rev Neurol, 2010. **6**(1): p. 39-51.
178. Yan, H., et al., *IDH1 and IDH2 mutations in gliomas.* N Engl J Med, 2009. **360**(8): p. 765-73.
179. Sartor, C.I., *Epidermal growth factor family receptors and inhibitors: radiation response modulators.* Semin Radiat Oncol, 2003. **13**(1): p. 22-30.
180. Stupp, R., et al., *Chemoradiotherapy in malignant glioma: standard of care and future directions.* J Clin Oncol, 2007. **25**(26): p. 4127-36.
181. Stupp, R. and F. Roila, *Malignant glioma: ESMO clinical recommendations for diagnosis, treatment and follow-up.* Ann Oncol, 2009. **20 Suppl 4**: p. 126-8.
182. van den Bent, M.J., et al., *Adjuvant procarbazine, lomustine, and vincristine improves progression-free survival but not overall survival in newly diagnosed anaplastic oligodendrogliomas and oligoastrocytomas: a randomized European Organisation for Research and Treatment of Cancer phase III trial.* J Clin Oncol, 2006. **24**(18): p. 2715-22.
183. Wick, W., et al., *NOA-04 randomized phase III trial of sequential radiochemotherapy of anaplastic glioma with procarbazine, lomustine, and vincristine or temozolomide.* J Clin Oncol, 2009. **27**(35): p. 5874-80.
184. Westphal, M., et al., *Gliadel wafer in initial surgery for malignant glioma: long-term follow-up of a multicenter controlled trial.* Acta Neurochir (Wien), 2006. **148**(3): p. 269-75; discussion 275.
185. van den Bent, M.J., et al., *Randomized phase II trial of erlotinib versus temozolomide or carmustine in recurrent glioblastoma: EORTC brain tumor group study 26034.* J Clin Oncol, 2009. **27**(8): p. 1268-74.
186. Raymond, E., et al., *Phase II study of imatinib in patients with recurrent gliomas of various histologies: a European Organisation for Research and Treatment of Cancer Brain Tumor Group Study.* J Clin Oncol, 2008. **26**(28): p. 4659-65.
187. Friedman, H.S., et al., *Bevacizumab alone and in combination with irinotecan in recurrent glioblastoma.* J Clin Oncol, 2009. **27**(28): p. 4733-40.
188. Mikkelsen, T., et al., *Radiation sensitization of glioblastoma by cilengitide has unanticipated schedule-dependency.* Int J Cancer, 2009. **124**(11): p. 2719-27.
189. Nabors, L.B., et al., *Phase I and correlative biology study of cilengitide in patients with recurrent malignant glioma.* J Clin Oncol, 2007. **25**(13): p. 1651-7.
190. National Comprehensive Cancer Network, *Central Nervous System Cancers v.2.2009, Clinical Practice Guidelines in Oncology*, 2009: Jenkitown, PA.
191. Bao, S., et al., *Glioma stem cells promote radioresistance by preferential activation of the DNA damage response.* Nature, 2006. **444**(7120): p. 756-60.
192. O'Rourke, D.M., et al., *Conversion of a radioresistant phenotype to a more sensitive one by disabling erbB receptor signaling in human cancer cells.* Proc Natl Acad Sci U S A, 1998. **95**(18): p. 10842-7.
193. Schmidt-Ullrich, R.K., et al., *ERBB receptor tyrosine kinases and cellular radiation responses.* Oncogene, 2003. **22**(37): p. 5855-65.
194. Bowers, G., et al., *The relative role of ErbB1-4 receptor tyrosine kinases in radiation signal transduction responses of human carcinoma cells.* Oncogene, 2001. **20**(11): p. 1388-97.
195. Schmidt-Ullrich, R.K., et al., *Signal transduction and cellular radiation responses.* Radiat Res, 2000. **153**(3): p. 245-57.
196. Kao, G.D., et al., *Inhibition of phosphatidylinositol-3-OH kinase/Akt signaling impairs DNA repair in glioblastoma cells following ionizing radiation.* J Biol Chem, 2007. **282**(29): p. 21206-12.

197. Park, C.M., et al., *Ionizing radiation enhances matrix metalloproteinase-2 secretion and invasion of glioma cells through Src/epidermal growth factor receptor-mediated p38/Akt and phosphatidylinositol 3-kinase/Akt signaling pathways.* Cancer Res, 2006. **66**(17): p. 8511-9.
198. Bonner, J.A., et al., *Radiotherapy plus cetuximab for squamous-cell carcinoma of the head and neck.* N Engl J Med, 2006. **354**(6): p. 567-78.
199. Murat, A., et al., *Stem cell-related "self-renewal" signature and high epidermal growth factor receptor expression associated with resistance to concomitant chemoradiotherapy in glioblastoma.* J Clin Oncol, 2008. **26**(18): p. 3015-24.
200. Cordes, N., et al., *beta1-integrin-mediated signaling essentially contributes to cell survival after radiation-induced genotoxic injury.* Oncogene, 2006. **25**(9): p. 1378-90.
201. Cordes, N. and C.C. Park, *beta1 integrin as a molecular therapeutic target.* Int J Radiat Biol, 2007. **83**(11-12): p. 753-60.
202. Park, C.C., et al., *Beta1 integrin inhibition dramatically enhances radiotherapy efficacy in human breast cancer xenografts.* Cancer Res, 2008. **68**(11): p. 4398-405.
203. Bullard, D.E., et al., *Growth and chemotherapeutic response in athymic mice of tumors arising from human glioma-derived cell lines.* J Neuropathol Exp Neurol, 1981. **40**(4): p. 410-27.
204. Misra, A., et al., *Chromosome transfer experiments link regions on chromosome 7 to radiation resistance in human glioblastoma multiforme.* Genes Chromosomes Cancer, 2006. **45**(1): p. 20-30.
205. Misra, A., et al., *Array comparative genomic hybridization identifies genetic subgroups in grade 4 human astrocytoma.* Clin Cancer Res, 2005. **11**(8): p. 2907-18.
206. Brock, R., et al., *Rapid characterization of green fluorescent protein fusion proteins on the molecular and cellular level by fluorescence correlation microscopy.* Proc Natl Acad Sci U S A, 1999. **96**(18): p. 10123-8.
207. Szentesi, G., et al., *Computer program for determining fluorescence resonance energy transfer efficiency from flow cytometric data on a cell-by-cell basis.* Comput Methods Programs Biomed, 2004. **75**(3): p. 201-11.
208. Vereb, G., Jr., et al., *Cholesterol-dependent clustering of IL-2Ralpha and its colocalization with HLA and CD48 on T lymphoma cells suggest their functional association with lipid rafts.* Proc Natl Acad Sci U S A, 2000. **97**(11): p. 6013-8.
209. Bastiaens, P.I.H., et al., *Imaging the intracellular trafficking and state of the AB_5 quaternary structure of cholera toxin.* EMBO J., 1996. **15**(16): p. 4246-4253.
210. Vereb, G., J. Matko, and J. Szollosi, *Cytometry of fluorescence resonance energy transfer.* Methods Cell Biol, 2004. **75**: p. 105-52.
211. R. Van Balen, D.K., T. K. Ten Kate, B. Mosterd, and A. W. M. Smeulders, *SciIImage: a multi-layered environment for use and development of image processing software. Experimental environments for computer vision & image processing, ed. H.I.C.a.J.L. Crowley.* World Scientific Publishing Co. Pte. Ltd., 1994: p. 107-126.
212. Roszik, J., J. Szollosi, and G. Vereb, *AccPbFRET: an ImageJ plugin for semi-automatic, fully corrected analysis of acceptor photobleaching FRET images.* BMC Bioinformatics, 2008. **9**: p. 346.
213. Dean, P., et al., *Proposed standard for image cytometry data files.* Cytometry, 1990. **11**(5): p. 561-9.
214. Jovin, T.M. and D.J. Arndt-Jovin, *Luminescence digital imaging microscopy.* Annu Rev Biophys Biophys Chem, 1989. **18**: p. 271-308.
215. Szentesi, G., et al., *Computer program for analyzing donor photobleaching FRET image series.* Cytometry A, 2005. **67**(2): p. 119-28.
216. Nagy, P., et al., *EGF-induced redistribution of erbB2 on breast tumor cells: flow and image cytometric energy transfer measurements.* Cytometry, 1998. **32**(2): p. 120-31.
217. Gronowski, A.M. and P.J. Bertics, *Modulation of epidermal growth factor receptor interaction with the detergent-insoluble cytoskeleton and its effects on receptor tyrosine kinase activity.* Endocrinology, 1995. **136**(5): p. 2198-205.
218. Bagossi, P., et al., *Molecular modeling of nearly full-length ErbB2 receptor.* Biophys J, 2005. **88**(2): p. 1354-63.
219. Zsebik, B., et al., *Hsp90 inhibitor 17-AAG reduces ErbB2 levels and inhibits proliferation of the trastuzumab resistant breast tumor cell line JIMT-1.* Immunol Lett, 2006. **104**(1-2): p. 146-55.
220. Sandfort, V., U. Koch, and N. Cordes, *Cell adhesion-mediated radioresistance revisited.* Int J Radiat Biol, 2007. **83**(11-12): p. 727-32.
221. Edidin, M., *Shrinking patches and slippery rafts: scales of domains in the plasma membrane.* Trends Cell Biol, 2001. **11**(12): p. 492-6.
222. Harder, T., et al., *Lipid domain structure of the plasma membrane revealed by patching of membrane components.* J Cell Biol, 1998. **141**(4): p. 929-42.
223. Moro, L., et al., *Integrins induce activation of EGF receptor: role in MAP kinase induction and adhesion-dependent cell survival.* Embo J, 1998. **17**(22): p. 6622-32.
224. Muller, B.K., et al., *Pulsed interleaved excitation.* Biophys J, 2005. **89**(5): p. 3508-22.
225. Lee, N.K., et al., *Three-color alternating-laser excitation of single molecules: monitoring multiple interactions and distances.* Biophys J, 2007. **92**(1): p. 303-12.
226. Rothwell, P.J., et al., *Multiparameter single-molecule fluorescence spectroscopy reveals heterogeneity of HIV-1 reverse transcriptase:primer/template complexes.* Proc Natl Acad Sci U S A, 2003. **100**(4): p. 1655-60.
227. Heilemann, M., et al., *Dissecting and reducing the heterogeneity of excited-state energy transport in DNA-based photonic wires.* J Am Chem Soc, 2006. **128**(51): p. 16864-75.
228. Ross, J., et al., *Multicolor single-molecule spectroscopy with alternating laser excitation for the investigation of interactions and dynamics.* J Phys Chem B, 2007. **111**(2): p. 321-6.

229. Horvath, G., et al., *Selecting the right fluorophores and flow cytometer for fluorescence resonance energy transfer measurements.* Cytometry A, 2005. **65**(2): p. 148-57.
230. Heider, K.H., et al., *CD44v6: a target for antibody-based cancer therapy.* Cancer Immunol Immunother, 2004. **53**(7): p. 567-79.
231. Dalchau, R., J. Kirkley, and J.W. Fabre, *Monoclonal antibody to a human leukocyte-specific membrane glycoprotein probably homologous to the leukocyte-common (L-C) antigen of the rat.* Eur J Immunol, 1980. **10**(10): p. 737-44.
232. Gurtner, K., et al., *Combined treatment of the immunoconjugate bivatuzumab mertansine and fractionated irradiation improves local tumour control in vivo.* Radiother Oncol, 2012. **102**(3): p. 444-9.
233. Song, L., et al., *Photobleaching kinetics of fluorescein in quantitative fluorescence microscopy.* Biophys J, 1995. **68**(6): p. 2588-600.
234. Nagy, P., et al., *Intensity-based energy transfer measurements in digital imaging microscopy.* Eur.Biophys.J., 1998. **27**(4): p. 377-389.
235. Galperin, E., V.V. Verkhusha, and A. Sorkin, *Three-chromophore FRET microscopy to analyze multiprotein interactions in living cells.* Nat Methods, 2004. **1**(3): p. 209-17.
236. Friedlander, D.R., et al., *Migration of brain tumor cells on extracellular matrix proteins in vitro correlates with tumor type and grade and involves alphaV and beta1 integrins.* Cancer Res, 1996. **56**(8): p. 1939-47.
237. Westhoff, M.A., et al., *Identification of a novel switch in the dominant forms of cell adhesion-mediated drug resistance in glioblastoma cells.* Oncogene, 2008. **27**(39): p. 5169-81.
238. Abdollahi, A., et al., *Inhibition of alpha(v)beta3 integrin survival signaling enhances antiangiogenic and antitumor effects of radiotherapy.* Clin Cancer Res, 2005. **11**(17): p. 6270-9.
239. Eller, J.L., et al., *Anti-epidermal growth factor receptor monoclonal antibody cetuximab augments radiation effects in glioblastoma multiforme in vitro and in vivo.* Neurosurgery, 2005. **56**(1): p. 155-62; discussion 162.
240. Lu, K.V., et al., *Fyn and SRC are effectors of oncogenic epidermal growth factor receptor signaling in glioblastoma patients.* Cancer Res, 2009. **69**(17): p. 6889-98.
241. Razis, E., et al., *Phase II study of neoadjuvant imatinib in glioblastoma: evaluation of clinical and molecular effects of the treatment.* Clin Cancer Res, 2009. **15**(19): p. 6258-66.
242. Lobashevsky, A.L., X.L. Jiang, and J.M. Thomas, *Allele-specific in situ analysis of microchimerism by fluorescence resonance energy transfer (FRET) in nonhuman primate tissues.* Hum Immunol, 2002. **63**(2): p. 108-20.
243. Chen, Y., J.D. Mills, and A. Periasamy, *Protein localization in living cells and tissues using FRET and FLIM.* Differentiation, 2003. **71**(9-10): p. 528-41.
244. Xu, X., et al., *Imaging protein interactions with bioluminescence resonance energy transfer (BRET) in plant and mammalian cells and tissues.* Proc Natl Acad Sci U S A, 2007. **104**(24): p. 10264-9.
245. Kong, H.J., T. Boontheekul, and D.J. Mooney, *Quantifying the relation between adhesion ligand-receptor bond formation and cell phenotype.* Proc Natl Acad Sci U S A, 2006. **103**(49): p. 18534-9.
246. Li, H.F., J.S. Kim, and T. Waldman, *Radiation-induced Akt activation modulates radioresistance in human glioblastoma cells.* Radiat Oncol, 2009. **4**: p. 43.

APPENDIX

UNIVERSITY AND NATIONAL LIBRARY UNIVERSITY OF DEBRECEN
KENÉZY LIFE SCIENCES LIBRARY

Register Number: DEENKÉTK/104/2013.
Item Number:
Subject: Ph.D. List of Publications

Candidate: Miklós Petrás

Neptun ID: ELUGCO

Doctoral School: Doctoral School of Molecular Medicine

List of publications related to the dissertation

1. **Petrás, M.**, Lajtos, T., Friedländer, E., Klekner, Á., Pintye, É., Feuerstein, B.G., Szöllősi, J., jr. Vereb, G.: Molecular interactions of ErbB1 (EGFR) and integrin-beta1 in astrocytoma frozen sections predict clinical outcome and correlate with Akt mediated in vitro radioresistance.
Neuro-Oncology. "accepted by publisher", 2013.
IF:5.723 (2011)

2. **Petrás, M.**, Hutóczki, G., Varga, I., jr. Vereb, G., Szöllősi, J., Bognár, L., Ruszthi, P., Kenyeres, A., Tóth, J., Hanzély, Z., Scholtz, B., Klekner, Á.: Különböző eredetű malignus agydaganatok invazivitásának panelszerű vizsgálata.
Magyar Onkológia. 53 (3), 253-258, 2009.
DOI: http://dx.doi.org/10.1556/MOnkol.53.2009.3.3

3. Fazekas, Z., **Petrás, M.**, Fábián, Á., Pályi-Krekk, Z., Nagy, P., Damjanovich, S., jr. Vereb, G., Szöllősi, J.: Two-sided fluorescence resonance energy transfer for assessing molecular interactions of up to three distinct species in confocal microscopy.
Cytom. Part A. 73 (3), 209-219, 2008.
DOI: http://dx.doi.org/10.1002/cyto.a.20489
IF:3.259

4. **Petrás, M.**, Lajtos, T., Pintye, É., Feuerstein, B.G., Szöllősi, J., jr. Vereb, G.: Significance of Epidermal Growth Factor Receptor in the Radiation Resistance of Glioblastoma Tumors.
In: Radiation Damage In Biomolecular Systems : Proceedings of the 5th International Conference (RADAM 2008). Ed.: by Károly Tőkési, Béla Sulik, American Institute of Physics, Melville (New York), 204-217, 2008.
DOI: http://dx.doi.org/10.1063/1.3058983

H-4032 Debrecen, Egyetem tér 1. e-mail: publikaciok@lib.unideb.hu

5. Mocanu, M., Fazekas, Z., **Petrás, M.**, Nagy, P., Sebestyén, Z., Isola, J., Timár, J., Park, J.W., jr. Vereb, G., Szöllősi, J.: Associations of ErbB2, beta1-integrin and lipid rafts on Herceptin (Trastuzumab) resistant and sensitive tumor cell lines.
Cancer Lett. 227 (2), 201-212, 2005.
DOI: http://dx.doi.org/10.1016/j.canlet.2005.01.028
IF:3.049

List of other publications

6. Varga, I., Hutóczki, G., **Petrás, M.**, Scholtz, B., Miko, E., Kenyeres, A., Tóth, J., Zahuczky, G., Bognár, L., Hanzély, Z., Klekner, Á.: Expression of Invasion-Related Extracellular Matrix Molecules in Human Glioblastoma Versus Intracerebral Lung Adenocarcinoma Metastasis.
Cent. Eur. Neurosurg. 71 (04), 173-180, 2010.
DOI: http://dx.doi.org/10.1055/s-0030-1249698
IF:0.472

7. Horváth, G., **Petrás, M.**, Szentesi, G., Fábián, Á., Park, J.W., jr. Vereb, G., Szöllősi, J.: Selecting the right fluorophores and flow cytometer for fluorescence resonance energy transfer measurements.
Cytometry A. 65A (2), 148-157, 2005.
DOI: http://dx.doi.org/10.1002/cyto.a.20142
IF:2.115

Total IF: 14.618

Total IF (publications related to the dissertation): 12.031

The Candidate's publication data submitted to the Publication Database of the University of Debrecen have been validated by Kenezy Life Sciences Library on the basis of Web of Science, Scopus and Journal Citation Report (Impact Factor) databases.

14 March, 2013